

AN ABSTRACT OF THE THESIS OF

DeQian Wang for the degree of

Doctor of Philosophy in Mechanical Engineering

Presented on December 6, 1990

Title: Thermophysical Properties and Temperature Response of Surimi --

Measurement and Modeling

Abstract approved by: _____

Redacted for Privacy
Dr. Edward R. Kolbe

Redacted for Privacy

Dr. Lorin R. Davis

Freezing is one of the important technologies for preservation of foods. In this project, using surimi as a food model, thermophysical properties of frozen foods were evaluated and the freezing process was simulated using a finite element package.

To measure temperature-dependent thermal conductivity, a line-source probe system was used. Effects of test conditions and sample history were investigated. Thermal conductivity of Alaska pollock (Theragra chalcogramma) surimi having 0, 4, 6, 8, and 12% cryoprotectant levels was measured in the range of -40 to 30° C. Other thermal properties were analyzed using differential scanning calorimetry (DSC) at the same cryoprotectant concentrations and in the same temperature range. Each dynamically corrected DSC thermogram was used to determine initial freezing point, unfreezable water (bound water), apparent specific heat, enthalpy and unfrozen water weight fraction.

When water content of the sample is controlled, thermophysical properties of surimi have a relatively weak dependence upon cryoprotectant level in the unfrozen and fully frozen (-40° C) ranges. However, the initial freezing

point and the properties just below this point were significantly affected.

From measured data, the Schwartzberg thermal property models for frozen foods were investigated. The models agreed well with experimental data. However, possibility for further improvement is demonstrated by using DSC analysis. This research additionally demonstrated the great potential of DSC for measuring and modeling frozen food thermal properties.

Using the derived property models, a commercial PC-based finite element package was used to simulate the process of freezing a food block in a plate freezer. The capability of the program to handle temperature-dependent thermal properties and time-dependent boundary conditions enabled a simulation which accounted for measured changes in thermal properties, ambient temperatures and overall heat transfer coefficient. Predicted temperature history agreed well with measured data. Sensitivities of important model parameters, which were varied within their experimental error range, were also investigated using a factorial experimental design method. The result showed that in decreasing order of influencing freezing time prediction, attention should be given to apparent specific heat, block thickness, overall heat transfer coefficient, ambient temperature, thermal conductivity, and density.

**Thermophysical Properties and Temperature Response of Surimi--
Measurement and Modeling**

By

DeQian Wang

A THESIS

submitted to

Oregon State University

in partial fulfillment of
the requirements for the
degree of

Doctor of Philosophy

Completed December 6, 1990

Commencement June 1991

APPROVED:

Redacted for Privacy

Associate Professor of Bioresource Engineering in charge of major

Redacted for Privacy

Professor of Mechanical Engineering in charge of major

Redacted for Privacy

Head of Department of Mechanical Engineering

Redacted for Privacy

Dean of Graduate School

Date thesis is presented December 6, 1990

Typed by DeQain Wang for DeQian Wang

ACKNOWLEDGMENTS

I would like to thank Charles Crapo, Fishery Industrial Technology Center in Kodiak, Alaska; Kermit Reppond, National Marine Fisheries Service in Kodiak, Alaska; and Harold Barnett and Roy Porter, National Fisheries Service in Seattle, Washington, for their assistance in procuring samples and implementing experiments.

This work is the result of research sponsored by Oregon Sea Grant and I would like to express a special acknowledgment here with thanks.

I express my heartfelt appreciation to all faculty, staff and graduate students in the Bioresource Engineering Department lead by Dr. Andrew Hashimoto, for their family-type support since I came to the U.S.

I would like to thank my committee members, Drs. Lorin Davis, Gordon Reistad and Edward Piepmeier, for their guidance, time and consideration.

Special thank to Dr. Marshall English and Dr. Joseph McGuire, for not only their guidance, but also their friendship.

There is no way that can express my gratitude to my major advisor, Dr. Edward Kolbe, for his excellent guidance with almost everything that occurred to me and my family in the past six and half years. What I have learned from him is far beyond what I have described in this thesis. His influence in western philosophy, culture and values is at least equally important to me.

Finally, to my wife Yan and my son Nye, I love you.

COPYRIGHT ACKNOWLEDGMENTS

This dissertation consists of the following three manuscripts. The author thanks the publishers for permission to reproduce these articles.

Wang, D. Q. and Kolbe, E. 1990. Thermal conductivity of surimi -- measurement and modeling. J. Food Science, 55(5):1217.

Wang, D. Q. and Kolbe, E. 1990. Thermal properties of surimi analyzed using DSC. J. Food Science, in press.

Wang, D. Q. and Kolbe, E. 1990. Analysis of food block freezing using a PC-based finite element package. J. Food Engineering, in review.

TABLE OF CONTENTS

CHAPTER 1. INTRODUCTION	1
CHAPTER 2. LITERATURE REVIEW	11
FREEZING MODELS	11
Analytical models	11
Numerical models	12
PC-based finite element package	13
THERMOPHYSICAL PROPERTIES	15
Thermophysical property models	15
Thermophysical property measurement	20
OTHER ASSOCIATED EXPERIMENTS	28
Determination of the overall heat transfer coefficient	28
Verification of freezing model	28
CHAPTER 3. THERMAL CONDUCTIVITY OF SURIMI --	
MEASUREMENT AND MODELING	30
ABSTRACT	30
INTRODUCTION	31
MATERIALS & METHODS	33
Materials	33
System development	34
Thermal conductivity measurement for surimi	37
RESULTS & DISCUSSION	39
System development	39

Thermal conductivity measurement for surimi	41
Model application	48
CONCLUSIONS	56
CHAPTER 4. THERMAL PROPERTIES OF SURIMI	
ANALYZED USING DSC	58
ABSTRACT	58
INTRODUCTION	59
MATERIALS & METHODS	63
Materials	63
DSC measurement	63
Initial freezing point	64
Apparent specific heat	64
Unfreezable water	67
Unfrozen water weight fraction	67
Enthalpy	69
RESULTS & DISCUSSION	69
DSC measurement	69
Initial freezing point	71
Apparent specific heat	73
Unfreezable water	77
Enthalpy	79
Unfrozen water weight fraction	82
Modeling	82

CONCLUSIONS	92
CHAPTER 5. ANALYSIS OF FOOD BLOCK FREEZING USING A PC-BASED FINITE ELEMENT PACKAGE	94
ABSTRACT	94
INTRODUCTION	95
THEORETICAL CONSIDERATIONS	97
EXPERIMENTAL PROCEDURES	103
Food samples	103
Temperature measurement	103
Overall heat transfer coefficient measurement	105
Sensitivity analysis of model parameters	106
RESULTS & DISCUSSION	109
ANSYS analysis	109
Sensitivity analysis	115
CONCLUSIONS	116
CHAPTER 6. SUMMARY AND RECOMMENDATIONS	118
BIBLIOGRAPHY	120

LIST OF FIGURES

Fig. 1.1. Freezing of foods (not in scale)	2
Fig. 1.2. Typical thermal conductivity for frozen foods	5
Fig. 1.3. Typical enthalpy for frozen foods	6
Fig. 1.4. Typical apparent specific heat for frozen foods	7
Fig. 2.1. A schematic representation of DSC cell (DuPont Instruments, 1988)	25
Fig. 2.2. A typical DSC thermogram	26
Fig. 3.1. Set-up of the k measurement system	35
Fig. 3.2. Thermal conductivity of surimi with 0% cryoprotectant concentration	43
Fig. 3.3. Thermal conductivity of surimi with 4% cryoprotectant concentration	44
Fig. 3.4. Thermal conductivity of surimi with 6% cryoprotectant concentration	45
Fig. 3.5. Thermal conductivity of surimi with 8% cryoprotectant concentration	46
Fig. 3.6. Thermal conductivity of surimi with 12% cryoprotectant concentration	47
Fig. 3.7. Plot of T_i vs cryoprotectant concentration	49
Fig. 3.8. Plot of B vs cryoprotectant concentration	51
Fig. 3.9. Plot of k'_f vs cryoprotectant concentration	52
Fig. 3.10. Comparison of predicted k values by the modified model	

(The k values at -70° C obtained by extrapolation).....	54
Fig. 3.11. Predicted k values at -70° C vs cryoprotectant concentration....	55
Fig. 4.1. A typical DSC thermogram of surimi sample	65
Fig. 4.2. Illustration of the correction and calculation	68
Fig. 4.3. Thermogram of surimi with different cryoprotectant levels	70
Fig. 4.4. Measured apparent specific heat of surimi	
with 0% cryoprotectant concentration	75
Fig. 4.5. Enthalpy of surimi with 8% cryoprotectant concentration	81
Fig. 4.6. Unfrozen water weight fraction of surimi	
with 8% cryoprotectant concentration	84
Fig. 4.7. Apparent specific heat of surimi	
with 8% cryoprotectant concentration	88
Fig. 4.8. Enlargement of the portion A in the Fig. 4.7.	89
Fig. 4.9. Thermal conductivity of surimi	
with 8% cryoprotectant concentration	91
Fig. 5.1. Grid and boundary conditions used	
in the finite element analysis	98
Fig. 5.2. Illustration of boundary conditions	100
Fig. 5.3. Experiment set-up and thermocouple locations	104
Fig. 5.4. Predicted temperature history	
compared with experimental data	110
Fig. 5.5. Measured variable ambient temperature	111

Fig. 5.6. A semi-log plot of time-temperature history of the aluminum block	112
Fig. 5.7. Variable overall heat transfer coefficient used in the ANSYS analysis	114

LIST OF TABLES

Table 3.1. Measured k values of surimi	42
Table 4.1. Initial freezing points	72
Table 4.2. Measured apparent specific heat of surimi	74
Table 4.3. Unfreezable water, latent heat of fusion and water activity of surimi	78
Table 4.4. Measured enthalpy of surimi	80
Table 4.5. Measured unfrozen water weight fraction of surimi	83
Table 4.6. Parameters in Equation 4.5	87
Table 5.1. Factors and levels in the experiment	107
Table 5.2. Layout and results of the sensitivity analysis	108

NOMENCLATURE

- a Thickness in product in Equation 2.1
- a' Constant in Equation 4.5
- b Unfreezable water in g water/g solids
- B Slope of a straight line in Equation 2.11 and 3.1
- b' Constant in Equation 4.5
- C Apparent specific heat in Equation 4.6 (Schwartzberg, 1977, 1983)
- C_f Apparent specific heat in fully frozen state
- C_p^* Uncorrected apparent specific heat in kJ/kg.C
- C_p Apparent specific heat in kJ/kg.C (Dynamic corrected value in Chapter 4)
- C_{PI} Specific heat (kJ/kg.C) of ice in Equation 2.3
- C_{PU} Specific heat (kJ/kg.C) of water in Equation 2.3
- C_{PS} Specific heat (kJ/kg.C) of product solids in Equation 2.3
- $C_p(T)$ Dynamic corrected C_p values in Equation 4.2
- $C_p^*(T)$ Uncorrected C_p values determined by raw data in Equation 4.2
- c Constant in Equation 2.3
- c' Constant in Equation 4.5
- D Thickness of packaging material in Equation 5.4
- d' Constant in Equation 4.5
- E DSC calibration constant (DuPont Instruments, 1988)
- h Heat transfer coefficient in W/m^2K

H Enthalpy in kJ/kg

H_L Latent heat of fusion in kJ/kg

ΔH_o Latent heat of fusion of ice at normal melting point

k Thermal conductivity in W/m.C

k_L Thermal conductivity (W/m.C) of continuous phase in food system

k_o Thermal conductivity in thawed state, in W/m.C

k_s Thermal conductivity (W/m.C) of discontinuous phase in food system

k Thermal conductivity (W/m.C) of fibrous food system in direction parallel to fibers

k Thermal conductivity (W/m.C) of fibrous food system in direction perpendicular to fibers

K'_f Intercept at T_i in Equation 3.1

L Thickness of the surimi block in mm

m Sample mass in g

M_s Mass of product solids

M_U Mass of unfrozen water in the frozen food system

M_I Mass of ice in the frozen food system

n_s Mass fraction of food solids in g solids/g total sample

n_w Unfrozen water weight fraction in g water/g total sample

n_{wo} Initial water content in g water/g total sample

n^2 Volume fraction for discontinuous phase in Equation 2.9, 2.10 and 2.11

P Constant in Equation 2.1

- Q Constant in Equation 2.1
- q' Power consumed by prob heater in W/m
- Δq Heat flow in W
- R Gas constant
- t Time
- t_1 Time since probe heater was energized in s
- t_2 Time since probe heater was energized in s
- t_f Freezing time in Equation 2.1
- T Temperature in ° C
- T_1 Temperature of probe thermocouple at t_1 in ° C
- T_2 Temperature of probe thermocouple at t_2 in ° C
- T_A Absolute temperature in ° K
- T_a Ambient temperature in ° C. For a plate freezer, it is in fact the temperature of refrigerant flowing in the plates and a step changed variable.
- T_i Initial freezing point in ° C
- T_o Freezing temperature of the pure water in ° C
- T_0 Initial temperature in ° C
- T_R Datum temperature of H determination, in ° C
- T_s Temperature on the surface in ° C
- U Overall heat transfer coefficient in W/m²K and a step changed variable for plate freezer.
- X_A Mole fraction of water in Equation 2.2

- x Rectangular coordinate
- y Rectangular coordinate
- z Rectangular coordinate
- α Thermal diffusivity in m^2/s
- β Heating rate in $^{\circ}\text{C}/\text{min}$
- γ Intermediate variable in Equation 2.1
- ρ Density of foods in kg/m^3
- τ Time constant in Equation 2.2 in second

Thermophysical Properties and Temperature Response of Surimi--Measurement and Modeling

CHAPTER 1. INTRODUCTION

As modern science has developed, interdisciplinary research has become more and more common and important. For example, in the ASME (American Society of Mechanical Engineers) 1990 winter annual meeting, the ASME Heat Transfer Division Committee on Heat Transfer in Manufacturing and Material Processing (K-15) sponsored a session on "Heat Transfer in Food and Polymer Processing."

In the food industry, many processes are oriented to heating and cooling. Heat transfer analysis is a powerful tool to optimize the processes and equipment design. In this thesis, I focused on the process of freezing foods.

Freezing has been a long time technology for preservation of foods. Food is a complex biological system, and therefore freezing food is a complex process. Since water is often a major part of food, phase change occurs. Fig. 1.1 shows a temperature-time curve for freezing foods compared to that of pure water. As indicated in the figure, the process can be divided into three stages (Hung, 1990):

1. **Precooling.** This reflects the reduction of product temperature from the initial temperature to the initial freezing point, which is the temperature

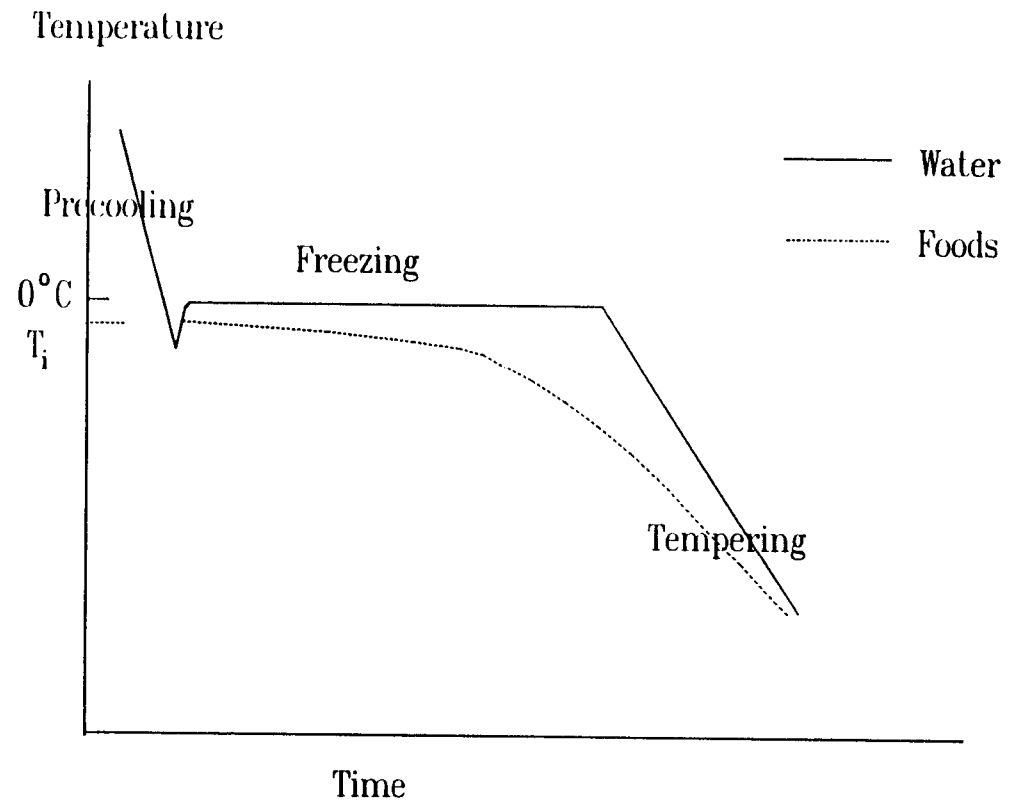


Fig.1.1 Freezing of foods (not in scale)

that ice crystallization begins. There is no change of phase in this stage and the removed heat is referred to as "sensible heat."

2. **Freezing.** This represents the crystallization of water in foods. The heat removed for this phase change is referred to as "latent heat of fusion." However, at a temperature marginally below the initial freezing point, a small amount of water first crystalize and consequently the concentration of solutes in the food increases and the freezing point further decreases. Thus, the phase change of foods occurs over a broad range of temperatures, unlike pure water that changes phase at a single temperature of 0° C. This phenomenon was characterized as "freezing point depression" (Heldman and Singh, 1981). In this stage, removal of heat involves both sensible heat and the latent heat of fusion.
3. **Tempering.** This begins when the removal of latent heat of fusion is negligible compared to sensible heat. This stage continues until the food reaches its final temperature.

Mathematically, a heat conduction equation can describe the freezing process as:

$$C_p(T)\rho(T)\frac{\partial T}{\partial t} - \frac{\partial}{\partial x}\left[k(T)\frac{\partial T}{\partial x}\right] + \frac{\partial}{\partial y}\left[k(T)\frac{\partial T}{\partial y}\right] + \frac{\partial}{\partial z}\left[k(z)\frac{\partial T}{\partial z}\right] \dots\dots\dots 1.1$$

with the initial condition (at $t \leq 0$):

$$T(t,x,y,z) = T_o \dots\dots\dots 1.2$$

and the third kind boundary condition (at $t > 0$) imposed on the outer boundaries:

$$U(T_a - T_s) = -k(T) \left[\frac{\partial T}{\partial x} + \frac{\partial T}{\partial y} + \frac{\partial T}{\partial z} \right] \dots \dots \dots 1.3$$

As indicated in Equation 1.1, the partial differential equation is nonlinear because thermal properties are a function of temperatures due to the freezing point depression. Obviously, descriptions of these temperature-dependent property data must be available to model the process.

Thermal properties of interest in this research are thermal conductivity, enthalpy and apparent specific heat. Thermal conductivity, k , indicates the ease with which heat will flow through the material, which is a solid-liquid mixture for foods. Enthalpy, H , is the energy content of the substance, relative to some low temperature datum, often selected as -40°C . Apparent specific heat, C_p , is the change in enthalpy with temperature, dH/DT . It includes both sensible heat and latent heat of fusion (Comini and Bonacina, 1974; Schwartzberg, 1977; and Chen, 1984). Fig. 1.2, 1.3, and 1.4 show expected forms of the functions describing the temperature-dependent thermal conductivity, enthalpy and apparent specific heat. Enthalpy does not appear in Equation 1.1, but it is a fundamental property to determine required heat loading for a refrigeration system. It is therefore included in this project. Density appears in Equation 1.1 but it is not included as part of this research project. Its change is negligible relative to other food thermal properties because it usually decreases only about 5 to 9% near the freezing temperature even for high moisture content foods

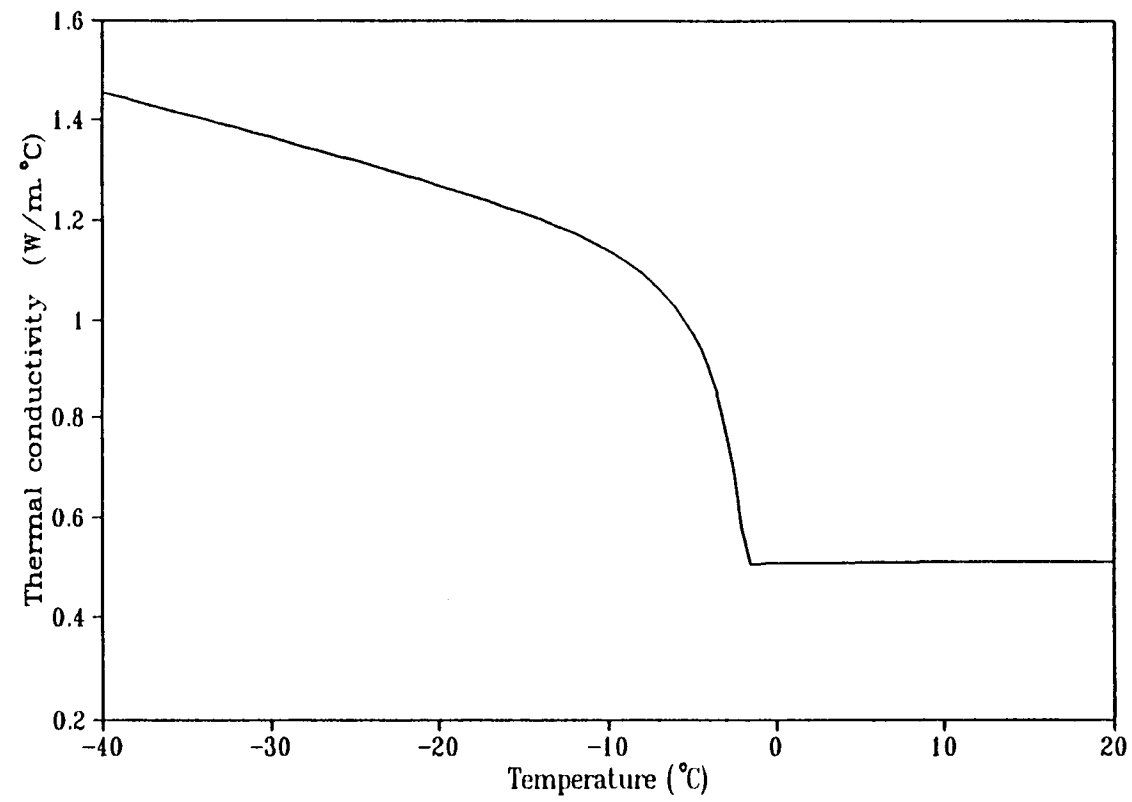


Fig. 1.2. Typical thermal conductivity for frozen foods

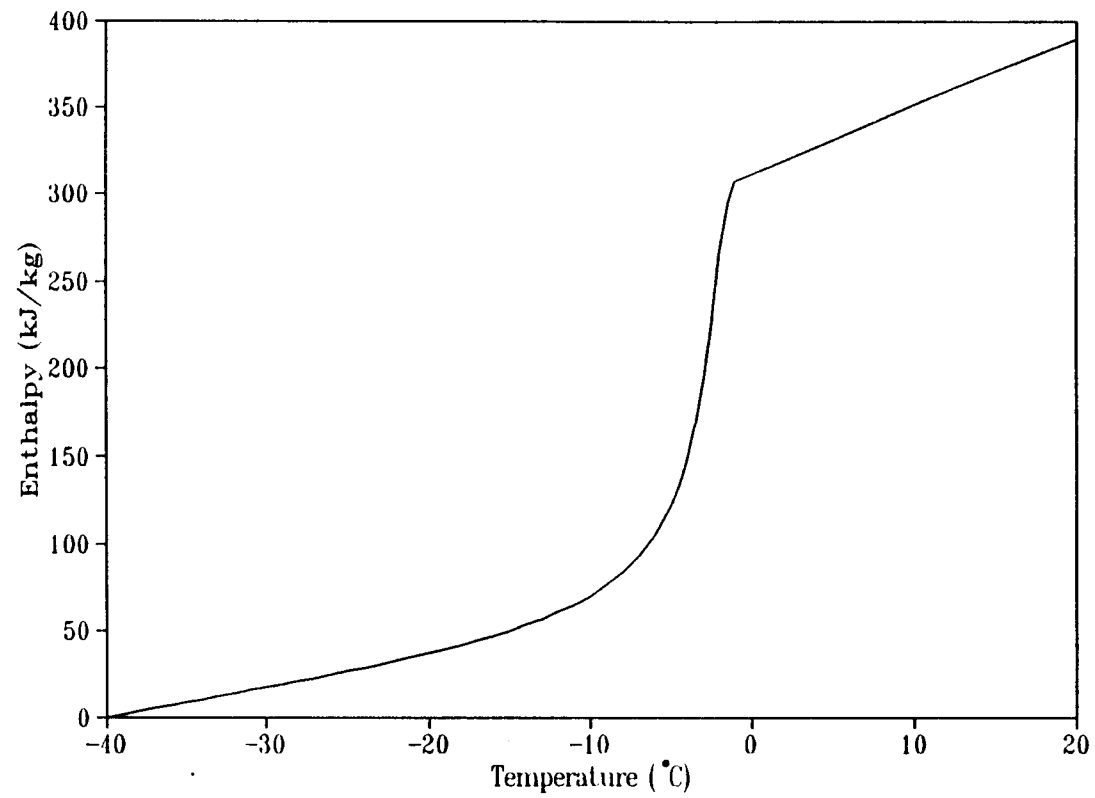


Fig. 1.3. Typical enthalpy for frozen foods

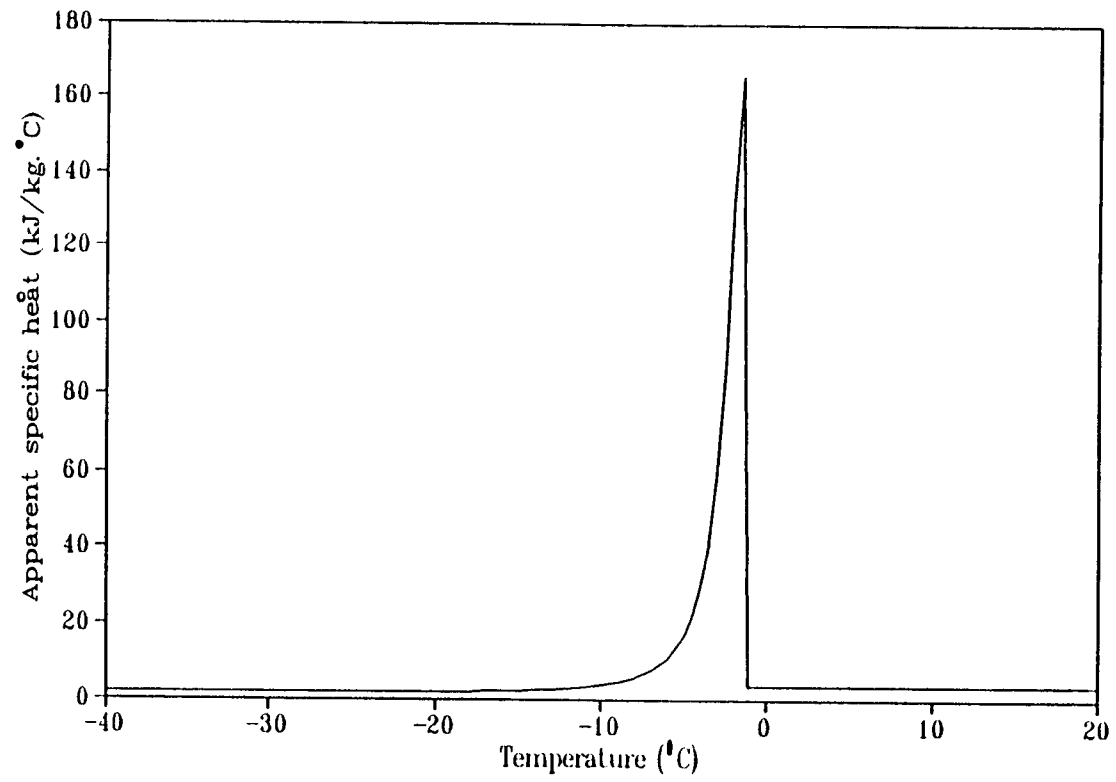


Fig. 1.4. Typical apparent specific heat for frozen foods

(Schwartzberg, 1977).

In equation 1.3, the overall heat transfer coefficient, U , is not a property of the food, but of the environment. It is the measure of heat being transferred between the foods and ambient and it includes food packaging effect on convection heat transfer. The value of U may present additional nonlinearities and complications in the freezing model. For example, it may be spatially-dependent in a blast freezer and time-dependent in a plate freezer.

Engineers are interested in studying freezing models because they need information to optimize the process and to design refrigeration systems. To optimize the process, we need to find an economical means to achieve a relatively faster freezing rate. This is desirable because it results in fine ice crystals and consequently better food quality. (This subject has been extensively studied by food scientists; a detailed review is available through Fennema et al., 1973; and Fennema, 1985). Another term related to freezing rate is "freezing time". It is the time required to lower the temperature of the food from its initial temperature to a given final temperature at its thermal center. The higher the freezing rate, the shorter the freezing time. The freezing time is also important to design the process and it can be predicted using Equations 1.1-1.3.

Equations 1.1-1.3 and associated thermophysical property data are also applicable to many other food processes. Examples are thawing foods, temperature changes in cold storage and transportation, among others. All of these processes and associated temperature changes have an important influence

on the final quality of the products.

In this thesis, a product called "surimi" is used as a food model to conduct the study. Surimi is an intermediate raw material made of washed minced fish meat and is used to make imitation seafoods such as crab legs and shrimp meat. Surimi has two major and important features. One is its gel-forming capacity that, upon heating, creates a desired texture for a variety of imitation seafoods. The other is its long-term stability in frozen storage due in part to the additional of cryoprotectants like sucrose and sorbitol (Sonu, 1986).

Surimi technology originally came from Japan. In recent years, Japan's exports of surimi-based products to the U.S. have been rising sharply. For example, exports of simulated crab meat to the U.S. have risen from about 2,600 tons in 1981 to 27,000 tons in 1984. An interesting point is that Japanese surimi production depends mostly on Alaska pollock taken from the U.S. waters (Sonu, 1986).

In recent years, the surimi-based food industry has rapidly developed in the U.S. However many phenomena in the process are still poorly understood. One example has been the temperature-dependence of thermal properties. An anti-denaturant, also called cryoprotectant, such as 4% sucrose and 4% sorbitol, is commonly added to stabilize surimi quality during cold storage. Boose and Keppeler (1967) reported that the concentration in a sugar solution exhibited a great influence on its thermal properties. Therefore, determination of thermal properties of surimi is even more complicated than that of other foods.

Plate freezers are generally used for freezing surimi blocks in industry. By bringing the surimi package into direct contact with freezer plates that are maintained at desired freezing temperature, rapid freezing can be achieved. Usually, the plate freezer is designed to make food package in direct contact with plates on two sides and to apply pressure increasing the surface heat transfer coefficient (Heldman and Singh, 1981).

Because of the unique characteristics of surimi, the availability of large fish resources off Oregon and the Pacific Northwest, and the intense national interest in surimi-based products, I conducted this research attempting to provide a better understanding of thermophysical properties of surimi and temperature response in its freezing process. However, the ultimate objectives were aimed at frozen foods in general:

1. Develop instrumentation and measure thermophysical properties of foods in freezing temperature range.
2. Evaluate existing thermophysical property models and explore possibility of improvement.
3. Simulate the freezing process, with the example of a surimi block in a plate freezer in this case, using the finite element method.

CHAPTER 2. LITERATURE REVIEW

Discussion in this chapter follows the order of Equations 1.1-1.3. First, different approaches to construct freezing models will be described. Second, methods to measure and model thermophysical properties are discussed. Third, techniques to estimate the overall heat transfer coefficient and to verify the freezing models are briefly introduced.

FREEZING MODELS

Freezing as a method of food preservation began at the turn of the century. The earliest freezing model was developed by Plank in 1913 (Hung, 1990). In recent decades, the freezing model has been extensively investigated, especially after modern computers and numerical modeling technologies became powerful tools in heat transfer analysis. As recently reviewed by Hung (1990) and Cleland et al. (1986), existing models may be divided into two major categories. One is "analytical models" that can be characterized as its assumption that the phase-change occurs at a single temperature. Another is "numerical models" that can simulate the phase-change taking place over a broad range of temperatures.

Analytical models

High nonlinearity of Equation 1.1 makes it impossible to be solved by an

analytical means. Hayakawa and Bakal (1973) considered an approximate analytical solution by applying the third kind of boundary condition (convective and radiative cooling or heating). Although it was analytical in nature, the complexity of calculation makes it impractical to use. Plank (cited by Heldman and Singh, 1981) developed a simple form solution, which has been extensively applied for about half century. The most general form of Plank's equation is:

$$t_F = \frac{\rho H_L}{T_i - T_a} \left[\frac{Pa}{h} + \frac{Qa^2}{k} \right] \dots\dots\dots 2.1$$

Where P and Q are constants that vary depending on the geometry of the object. The major limitations are assumptions that latent heat is removed at a single temperature, sensible heat is neglected, and thermophysical properties are constant over temperature. Since these are serious limitations, many researchers (Nagaoka et al., 1955; Hung and Thompson, 1983; Cleland and Earle, 1976, 1977, 1979, 1982, 1984) had tried to modify the Plank's equation. For example, Cleland and Earle (1976, 1977, 1979, 1982, 1984) empirically modified the geometric factors by regression analysis of experimental data. In a recent study, Wang and Kolbe (1987) found that their formulas were not only simple to apply, but more accurate than many other models.

Numerical models

As computers become more and more powerful, a numerical solution of Equation 1.1 has become a preferred method if one needs accurate solution.

The advantage is that it requires fewer assumptions on the physical process of freezing. The only concerns are the possible errors caused from imprecise thermophysical data, and numerical truncation and rounding (Cleland et al., 1986). By using a finite difference approach, Heldman and Gorby (1975), Hsieh et al. (1977), Succar and Hayakawa (1984), Bonacina and Comini (1971), Cleland and Earle (1977 and 1979), and many others, successfully simulated the process of freezing foods. By using a finite element method, Comini and Bonacina (1974), Hayakawa et al. (1983), Purwadaria and Heldman (1983), and others, also provided many good examples. In general, the finite element approach is more powerful than that using finite differences. The major reasons are that the finite element approach can easily handle irregular geometries, heterogeneous materials, and complex boundary conditions. In addition, a high order (quadratic or cubic rather than linear) approximation can be used to obtain more accurate results if necessary. Its disadvantage is that the computer storage requirements and run times are greater than those for finite difference (Cleland et al., 1986).

In any event, it appears that the numerical models are more accurate over the analytical ones because of more reasonable assumptions (Hung, 1990). They are therefore the more appropriate method to be applied in this thesis.

PC-based finite element package

Because of the unique characteristics of the food freezing process, many

researchers, especially those who were graduate students, have spent tremendous amount of time to develop computer programs, whether using the finite element or the finite difference approach. In many circumstances, the efforts even became the major part of their theses. In recent years, many commercial finite element packages, which are very powerful in handling nonlinearities, complex boundaries, irregular geometry, graphics and interfacing, have been marketed to aerospace and automotive industries. It is certainly significant if these packages can be used to simulate food freezing process. One of these packages is a PC-based program, ANSYS (Swanson Analysis System, Inc., Houston, PA). It allows using temperature-dependent thermal properties, thus allowing Equation 1.1 to be numerically solved. It is also able to handle complex boundary conditions. This is important because cooling media in plate freezers is a two-phase-flow refrigerant. This results in the overall heat transfer coefficient and ambient (refrigerant) temperature being time-dependent variables.

In Chapter 5, ANSYS was used to simulate the process of freezing a surimi block using measured temperature-dependent thermal properties, and time-dependent values of overall heat transfer coefficient and ambient temperature. Results showed that predicted temperature history agreed well with measured data. By applying the model, sensitivity of these parameters appearing in Equations 1.1-1.3 was investigated using a factorial experimental design method.

THERMOPHYSICAL PROPERTIES

Equation 1.1 suggests that freezing time prediction requires not only a model, but knowledge of the thermal properties as well. As computer and numerical modeling technologies have developed, precise solution of Equation 1.1 depends mainly on the quality of property data. Generally speaking, the methods to determine these temperature-dependent properties can be classified into two major groups: prediction and measurement.

Thermophysical property models

Due to difficulties in the measurement of thermophysical properties in frozen foods, models can provide reasonably accurate means of determination. Some researchers (Heldman, 1975; Heldman and Singh, 1986) believed that predicted results are as good as measured data and that therefore measurement is not necessary. Several researchers (Sweat, 1983; Succar, 1985; and Miles, 1983) have reviewed food thermophysical property models in great detail. All such literature indicated that existing models may be divided into three categories: regression (of empirical data), analytical and analytical-empirical.

Regression models are usually easy to develop and apply due to their simple forms, which are typically a function of temperature and moisture content. They are also relatively accurate because of their basis upon experimental data. Their disadvantages, however, are that they are usually

limited to certain conditions or foodstuffs, and often have no underlying physical meaning.

Analytical models are based on physical principles of the freezing process. For example, because of the four-fold difference between the thermal conductivities of water and ice, thermal conductivity of foods in the freezing zone strongly depends upon how the water changes its phase. Long (1955) proposed that the thermal conductivities of frozen foods could be predicted by the temperature-dependent unfrozen water fraction, which is the amount of unfrozen water which decreases with temperature during freezing. Lentz (1961) successfully predicted thermal conductivities of fish muscle, fats and gelatin gels by applying the Maxwell equation (1904). Heldman (1974) derived an equation to predict unfrozen water fractions by an expression of freezing point. Later, He developed a unique procedure to model all thermal properties appearing in Equation 1.1 (1982). The derivation can be described as following.

Based on chemical potential of the pure solute and the pure liquid, a freezing point depression equation can be derived by introducing molar free energies and enthalpy. It gives a mole fraction of water in the freezing product as a function of temperature as:

$$\frac{H_L}{R} \left[\frac{1}{T_o} - \frac{1}{T_A} \right] - \ln X_A \dots \dots \dots 2.2$$

Then, enthalpy of frozen foods could be predicted by the sum of the integrations of the heat content for each component (including product solids, unfrozen

water, and ice) over appropriate limits. Using -40°C as a datum at which $H=0$, it is:

$$H = M_S C_{PS} \int_{-40}^{T_i} dT + M_U C_{PU} \int_{-40}^{T_i} dT + \int_{-40}^{T_f} M_U(T) C_{PU}(T) dT \\ + M_U(T) L + \int_{-40}^{T_f} M_I(T) C_{PI}(T) dT \dots \dots \dots 2.3$$

And apparent specific heat is simply given as:

$$C_p(T) = \frac{dH}{dT} \dots \dots \dots 2.4$$

For thermal conductivity, Heldman suggested using the models developed by Kopelman (1966) which assumed food as a two-phase system (solids and liquid) having a fibrous structure. For heat flow parallel to the fibers:

$$k_{\parallel} = k_L \left[1 - N^2 \left(1 - \frac{k_S}{k_L} \right) \right] \dots \dots \dots 2.5$$

and for flow perpendicular to the fibers:

$$k_{\perp} = \frac{1 - Q}{1 - Q(1 - N)} \dots \dots \dots 2.6$$

Where

$$Q = \frac{N}{\left(1 - \frac{k_S}{k_L} \right)} \dots \dots \dots 2.7$$

Heldman also cited that, however, thermal properties predicted by his procedure

agreed well with tested data of fruits, vegetables and juices, but not for meats.

Succar (1985) reported that Heldman's procedure to determine thermal conductivity for meats could produce a variance of up to 24%. The reasons are: 1) the solutes in the food system become more concentrated and create non-ideal conditions which depart from ideal assumptions made in the derivation; and 2) unfreezable water (or bound water), which is the amount of water remaining unfrozen at -40° C (Fennema, 1985) is not considered. The advantage of these models, however, is that only two parameters--initial freezing point and moisture content of the unfrozen product--need to be measured and the measurements are easier than those for other thermal properties in the freezing temperature range.

Analytical-empirical models, which were developed by Schwartzberg (1976, 1977, 1985), are based on a similar theory but with additional consideration of the unfreezable water and empirical parameters. These models were derived by correlating thermodynamic activity of water and temperature; their final form became an unfrozen water fraction model as:

$$\frac{n_w - bn_s}{n_{wo} - bn_s} = \frac{T_o - T_i}{T_o - T} \dots\dots\dots 2.8$$

where b is unfreezable water. With this relationship, other thermal properties, which are functions of food components, can be described as functions of temperature. The apparent specific heat is:

$$C_p = C_f + \frac{(n_{wo} - bn_s)(T_o - T_i)\Delta H_o}{(T_o - T)^2} \dots\dots\dots 2.9$$

Based on this C_p expression, the enthalpy equation was then changed to the form:

$$H = (T - T_R) \left[C_f + \frac{(n_{wo} - bn_s)\Delta H_o}{T_o - T_R} \frac{T_o - T_i}{T_o - T} \right] \dots\dots\dots 2.10$$

Observing that frozen foods are two-phase systems, the thermal conductivity could be determined by interpolating between conductivity values in the thawed and fully frozen states as:

$$k = k_f + B(T_i - T) + (k_o - k_f) \left[\frac{T_o - T_i}{T_o - T} \right] \dots\dots\dots 2.11$$

The advantage of Schwartzberg's models is that accuracy can be improved by considering bound water and by using empirical parameters such as C_f , B , k_f and k_o . For example, a better agreement with measured data was reported by Succar and Hayakawa (1983). The disadvantage of these models is that they are restricted to foods for which empirical parameters are determined.

Because one of our objectives in this research is to measure thermal properties, it is therefore not difficult to determine the empirical parameters in Schwartzberg's models. With appreciation of their simple forms and accuracy, this research used Schwartzberg's models. In light of measured data, his models

were evaluated and the possibility of improvement was explored as described in Chapters 3 and 4.

Thermophysical property measurement

Regardless of what models are used, evaluation, improvement and sometimes development of these models still must depend on experimental data. The major difficulty in such measurements is the influence and state of water, especially in the temperature range slightly below the initial freezing point. In this section, I discuss not only the techniques to measure the thermal properties appearing in Equation 1.1, but also those properties associated with the thermal property models, such as unfreezable water, unfrozen water fraction, and initial freezing point.

Thermal conductivity can be measured using two different techniques: steady-state and transient.

A typical and widely used steady-state apparatus is the Guarded Hot Plate. It is a unidirectional heat flow method to measure thermal conductivity for dry homogenous specimens in slab form. The details of the technique are given by ASTM (1970). Several workers have reported the use of this method for foods; the accuracy of their results diminished if the samples contained appreciable amounts of moisture (Mohsenin, 1980). This is presumably due to the migration of moisture during the period before steady-state is reached.

For transient measurement, Sweat (1972, 1975, and 1983), Sastry and

Datta (1984) and Mohsenin (1980) reported the use of a line source probe as a sensor specifically developed for small food samples. The theory of this technique was developed by Ingersoll and Zobel (1954), Underwood and McTaggart (1960) and Nix et al. (1967) based upon the following observation: the temperature rise at any point in an infinite solid containing a suddenly initiated, constant-rate, line heat source, is a function of spatial position, time, thermal properties of the solid and source strength (Nix et al., 1967). The analytical solution of this transient heat transfer problem in cylindrical geometry is reported by Ingersoll and Zobel (1954) as:

$$T - T_{\infty} = \frac{q'}{2\pi k} \int_{\beta}^{\infty} \frac{e^{-x^2}}{x} dx \dots\dots\dots 2.12$$

where

$$\beta = \frac{r}{2\sqrt{\alpha t}} \dots\dots\dots 2.13$$

The solution may be expressed in terms of an infinite series as:

$$T - T_{\infty} = \frac{q'}{2\pi k} \left(-\frac{c}{2} - \ln \beta + \frac{\beta^2}{2 \cdot 1!} - \frac{\beta^4}{4 \cdot 2!} + \dots \right) \dots\dots\dots 2.14$$

If $\beta < 0.16$, which is valid in most cases, all but the first two terms of the series can be deleted with no more than a 1% error. Therefore, between times t_1 and t_2 , we have:

$$T_2 - T_1 = \frac{q'}{4\pi k} \ln \left(\frac{t_2}{t_1} \right) \dots\dots\dots 2.15$$

Then the thermal conductivity can be calculated as:

$$k = \frac{q'}{4\pi} \left[\frac{T_2 - T_1}{\ln(t_2 - t_1)} \right] \dots\dots\dots 2.16$$

During the test, a line heat source is inserted into a sample initially at a uniform temperature. The line source is then heated at a constant rate and the temperature adjacent to the line source is monitored. A plot of ln(time) vs. temperature is assumed to be linear and the thermal conductivity can be calculated by the slope as suggested in Equation 2.16.

Many researchers (Sweat and Haugh, 1974; Ramaswamy and Tung, 1981; Murakami and Okos, 1988) have measured thermal conductivity using this technique and reported that it was fast and simple. The disadvantage is that the nonlinearity of the ln(time)-temperature plot and excess temperature increase resulting from heating significantly influence the accuracy.

In Chapter 3, I described the development of a PC-controlled system and the measures to improve this technique by investigating a variety of experimental conditions. In light of measured data with respect to the different concentrations of cryoprotectant in surimi, thermal conductivity models were also evaluated.

Enthalpy and apparent specific heat are often measured using calorimeters, such as adiabatic calorimeters (Long, 1955; Hwang and Hayakawa, 1979), ice calorimeters (Disney, 1954; Haswell, 1954), electrically heated box calorimeter (Sastry and Datta, 1984) and Differential Scanning Calorimetry (DSC) (Mohsenin, 1980; Lund, 1983; McNaughton and Mortimer, 1983).

DSC is preferred in this project for the following reasons: it gives accurate results, needs a very small sample size and works rapidly and simply (McNaughton and Mortimer, 1975; and Lund, 1983); and it is not only suitable for measuring thermal properties appearing in Equation 1.1 but is also applicable to the study of other parameters associated with the thermal property models. These include initial freezing point, unfreezable water, and unfrozen water fractions (Roos, 1978 & 1986; McNaughton and Mortimer, 1975; and Lund, 1983).

Fig 2.1 is a schematic representation of a DuPont 910 DSC (DuPont instruments, Wilmington, DE). The sample and reference pans are placed on the platform of the thermoelectric (constantan) disc. As heat is transferred through the disc at a prescribed rate, the differential heat flow to the sample and reference can be calculated using the measured temperature difference over the chromal discs. Thus, differential heat input (dH/dt) as a function of temperature (or time because of constant rate of temperature rise) can be determined. An example DSC plot may look like Fig. 2.2. The displacement from the thermogram to the baseline is proportional to apparent specific heat at that temperature while the shaded area indicates the enthalpy of the reaction.

Unfreezable water (bound water) also can be measured using DSC (Ross, 1978 and Roos, 1986). First, the water content of the food needs to be determined. The sample is then cooled to -40°C or lower in the DSC cell. As the frozen sample is heated at a constant rate, fusion of ice is detected as a peak

area on the thermogram. Unfreezable water is simply the difference between the total water content and the amount of ice melted.

Unfrozen water fraction can be determined using DSC as the summation of unfreezable water and melted ice fraction at the temperatures of interest.

As a dynamic calorimeter, a disadvantage of DSC is that the thermogram is often distorted due to time "lag." Such distortions were found in reports of Roos (1986) and Ramaswamy and Tung (1981) and limited the DSC applicability in the study of frozen food properties. Investigating a similar problem for microcalorimetry applications in biophysical chemistry, some scientists (Randzio and Suurkuusk, 1980; Mayorga and Freire, 1987) developed a dynamic correction method to restore the thermogram.

In Chapter 4, The model was modified for DSC and applied to correct the thermogram obtained from the apparent specific heat measurement. In light of measured enthalpy, apparent specific heat, unfreezable water and unfrozen water fraction of surimi with different cryoprotectant concentrations, possibility to improve Schwartzberg's thermal property models was also exhibited.

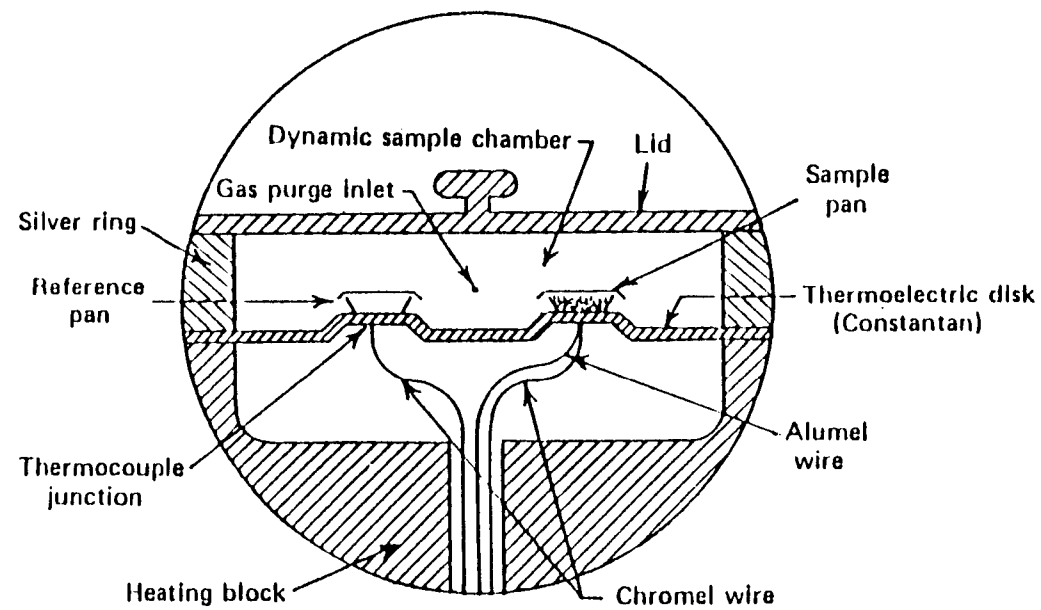


Fig. 2.1. A schematic representation of DSC cell (DuPont Instruments, 1988)

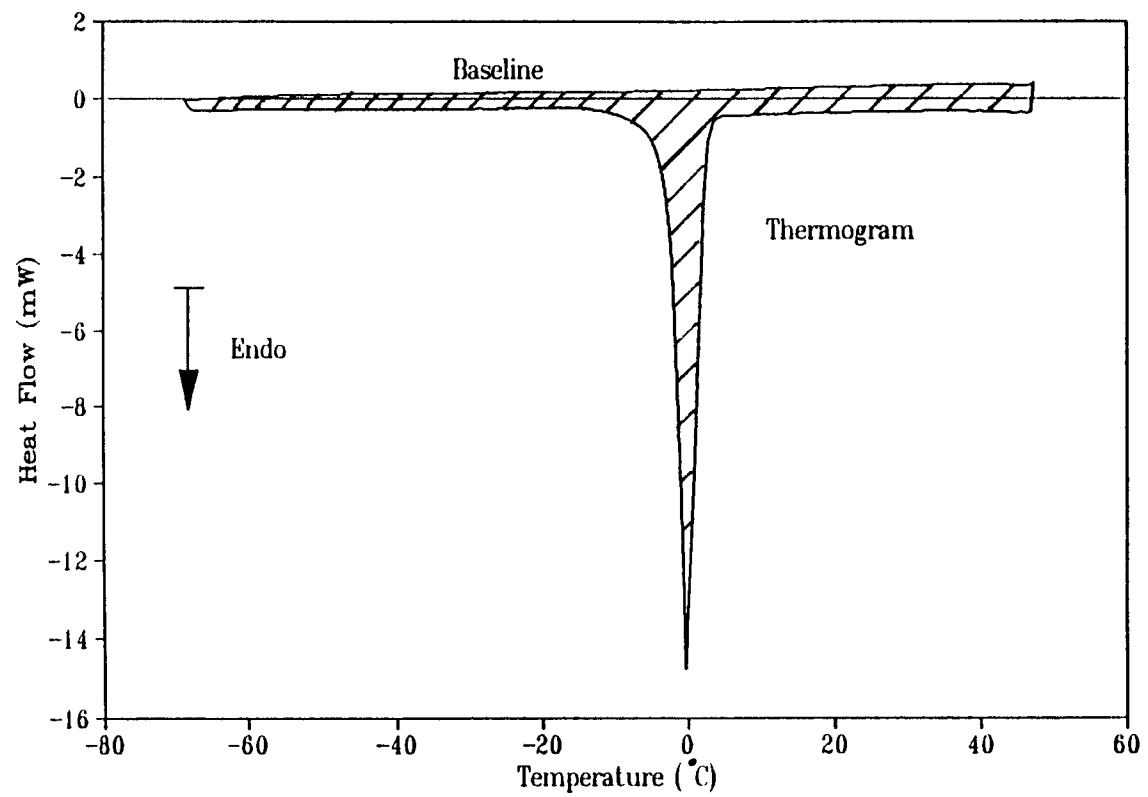


Fig. 2.2. A typical DSC thermogram

Initial freezing point of foods is lower than that of pure water because of additional solutes, either due to the initial chemical composition or due to ice fraction increase during freezing (Fennema et al., 1973). Obviously, it is necessary to measure the initial freezing point, because both the changes of phase and thermophysical properties begin at this temperature.

Fennema et al. (1973) reviewed two types of freezing point apparatuses that are in common use. One is a conventional cryoscope specified by ASTM (1955). The sample is cooled and stirred at a rate just sufficient to ensure uniformity in the fluid phase. The cooling rate should be moderately slow (on the order of 1° C/min) and temperature-time data is collected. The temperature is measured by a mercury-in-glass or platinum resistance thermometer. To induce crystallization, the tip of a cold rod may be immersed. The freezing point can be determined from the time-temperature curve after the correction for supercooling is made by an extrapolation method. Another apparatus, called a thermistor cryoscope, is similar to the previous one except a thermistor replaces the thermometer, and a vibrating wire is used to induce crystallization.

In this project, I measured the initial freezing points of surimi with different cryoprotectant concentrations, using two different means. In Chapter 3, the technique used was similar as that described by Fennema et al. (1973). In Chapter 4, DSC was used because its thermogram also shows the temperature that phase change begins.

OTHER ASSOCIATED EXPERIMENTS

Determination of the overall heat transfer coefficient

There are many empirical data and models available for the general determination of heat transfer coefficients. However, these data and models are often only accurate to within $\pm 30\%$ for general geometries and conditions (Kreith, 1963). In addition, I am interested in the "overall" heat transfer coefficient. For a plate freezer, the overall heat transfer coefficient depends upon a variety of factors such as surface condition, contact pressure and packaging material (Cowell and Namor, 1974). Many researchers (Cowell and Namor, 1974; Zuritz and Singh, 1985; Sastry et al., 1985, Wang and Kolbe, 1987) have successfully used aluminum or brass (for which internal heat conduction is known) to simulate a food package under practical industrial conditions. This classical lumped parameter method (Welty et al., 1984) should be applicable in this project.

In Chapter 5, I developed a PC-controlled apparatus to determine the overall heat transfer coefficient as a function of time for the plate freezer.

Verification of freezing model

Many researchers (Bonacina and Comini, 1973; Schwartzberg et al., 1977; Purwadaria and Heldman, 1983; and Zuritz and Singh, 1985) used measured temperature history of food at its thermal center to verify their freezing models.

There is no difficult to adopt this technique in this research and the application was successful as described in Chapter 5.

CHAPTER 3. THERMAL CONDUCTIVITY OF SURIMI-- MEASUREMENT AND MODELING

ABSTRACT

To measure temperature-dependent thermal conductivity of surimi, a line-source probe system was developed. Effects of test conditions and sample history were investigated. Thermal conductivity of Alaska pollock surimi having 0, 4, 6, 8, and 12% cryoprotectant levels was measured in the range of -40 to 30° C. Thermal conductivity of surimi has a relatively weak dependence upon cryoprotectant level when water content of the sample is controlled at 80.3%. From measured data, the Schwartzberg model and its modification were selected for future prediction. Three parameters in the model, T_i , B , and k'_f were found to have a linear variation with cryoprotectant concentration.

INTRODUCTION

Before food scientists and engineers can model, optimize and design processes and equipment, they must understand the thermal properties of foods. To simulate freezing and frozen storage is no longer the problem it once was; with the advent of modern computer and numerical methods, we can accurately solve nonlinear heat conduction equations. Consequently, the essential task for food engineers now is to improve the accuracy of predictions of temperature-dependent thermal properties. Among the many existing models for foods, those developed by Heldman (1982), Schwartzberg (1977, 1983) and Murakami et al. (1985) are the most favorable because of their sound theoretical background and the broad range of their potential applications. After comparing several existing models with published experimental data, Succar (1985) reported that Schwartzberg model showed the best agreement. For more accurate prediction, however, its modified form, developed by Succar and Hayakawa (1983), fit best.

In the case of a new food product, we need to measure its thermal properties before we can apply the models. This project focuses on the thermal conductivity, k , of surimi, an intermediate raw material in the frozen state, used to make seafood analogs. It is made of minced and washed fish meat with a range of cryoprotectant concentrations. Sucrose and sorbitol are commonly used as the cryoprotectant to stabilize surimi's quality during freezing and frozen storage.

For measuring the thermal conductivity of foods, the line-source probe

method is fast and simple and to require a relatively small sample (Sweat, 1985). It therefore was the preferred means for our study. To apply this method on foods in the temperature range below 0° C, two conditions must be met: linearity of the temperature vs. $\ln(\text{time})$ plot must be satisfied, and temperature increase after heating must be limited to assure measurement at the correct temperature and to minimize effect of latent heat of fusion. The relation between the two conditions has been discussed by Sweat (1976), but there is limited and conflicting published information on the influencing factors, such as power level, scanning rate and time. For linearity, Sweat and Haugh (1974) reported that $r^2 > 0.99$ was used; Ramaswamy and Tung (1981) used $r^2 > 0.8$; Murakami and Okos (1988) used $r^2 > 0.9$. For temperature increase, no specific value was given by Sweat and Haugh (1974), and Sastry (1987) recommended that for frozen foods, temperature increase be limited to 1.5° C. Murakami and Okos (1988), however, cited that the probe method is not applicable in cases where the time is short or the temperature change is less than 3° C. Therefore, it is appropriate to investigate how these factors affect a new system for which no standard experimental procedure exists.

Measuring the thermal properties of frozen foods requires an understanding of sample history (such as previous freezing and thawing conditions) and freezing rate during the experiment. For sample history, Poppendiek (1966) compared a sample of bovine liver that had been slowly frozen and thawed (freezing to a little below 0° C and slow thawing to room

temperature) with one that had been rapidly frozen and thawed (freezing to -196°C by liquid nitrogen and thawing in warm water). He reported that measured k values of the first sample was 10 to 20% greater than that of the second. Neither of the cases, however, are typical of rates encountered in the food industry. Although many researchers have observed that freezing rate will significantly influence ice crystallization (Reid, 1988), little information has been found in existing literature to describe how it affects k measurement.

The objectives of this research were (1) to develop an appropriate measurement system for frozen foods and to investigate the effects of various experimental conditions; (2) to examine the effects of sample history on measured k values and to measure the thermal conductivity of surimi having different levels of cryoprotectant; and (3) to select the most accurate model for future prediction.

MATERIALS & METHODS

Materials

Calibration materials. To calibrate the system, both glycerine and a gel of 0.5% agar and water were used.

Surimi samples. Surimi samples were Alaska pollock (Theragra chalcogramma) obtained from Western Alaska, Inc. of Kodiak, Alaska. Surimi was taken from the production line prior to the addition of cryoprotectants and air-shipped with gel-ice to Corvallis, Oregon. The water content of the surimi was 80.3%, measured by drying the sample in a vacuum oven at 105°C for 24

hours, with six replicates. The surimi was then mixed using a mortar and pestle to obtain five different levels of cryoprotectant, which consisted of half sucrose and half sorbitol (Lampila, 1988). Cryoprotectant concentrations were 0, 4, 6, 8, and 12% expressed as percent of total weight (8% is the typical commercial level). Water content of the mixture was controlled to 80.3% (wet basis). Each sample was then stored in a -80°C freezer after evacuating and sealing in three plastic frozen storage bags (to prevent moisture loss). Water content was checked after completion of experiments.

System development

Apparatus. Our k measurement apparatus configuration was based on the system described by Sweat (1976) and appears in Fig. 3.1. The line-source probes, purchased from V. E. Sweat (Texas A&M University), had a heater resistance of $223.1\ \Omega/\text{m}$. Sample holders were plastic tubes (5 cm X 3 cm diameter) made from film capsules and having both ends insulated. From previous tests with glycerine, there was no edge effect under the conditions of a routine test. Temperature was controlled in a Neslab LT-50DD bath having a temperature stability of $\pm 0.02^{\circ}\text{C}$. Both the multimeter and the DC power supply are Microntas (made for Radio Shack). The accuracy of the current measurement in the heater circuit (Fig. 3.1) was $\pm 0.1\ \text{mA}$. An additional switch (Fig. 3.1) was used to initiate heating in an effort to minimize time delay. A Campbell 21X datalogger (Logan, Utah) supported temperature-time

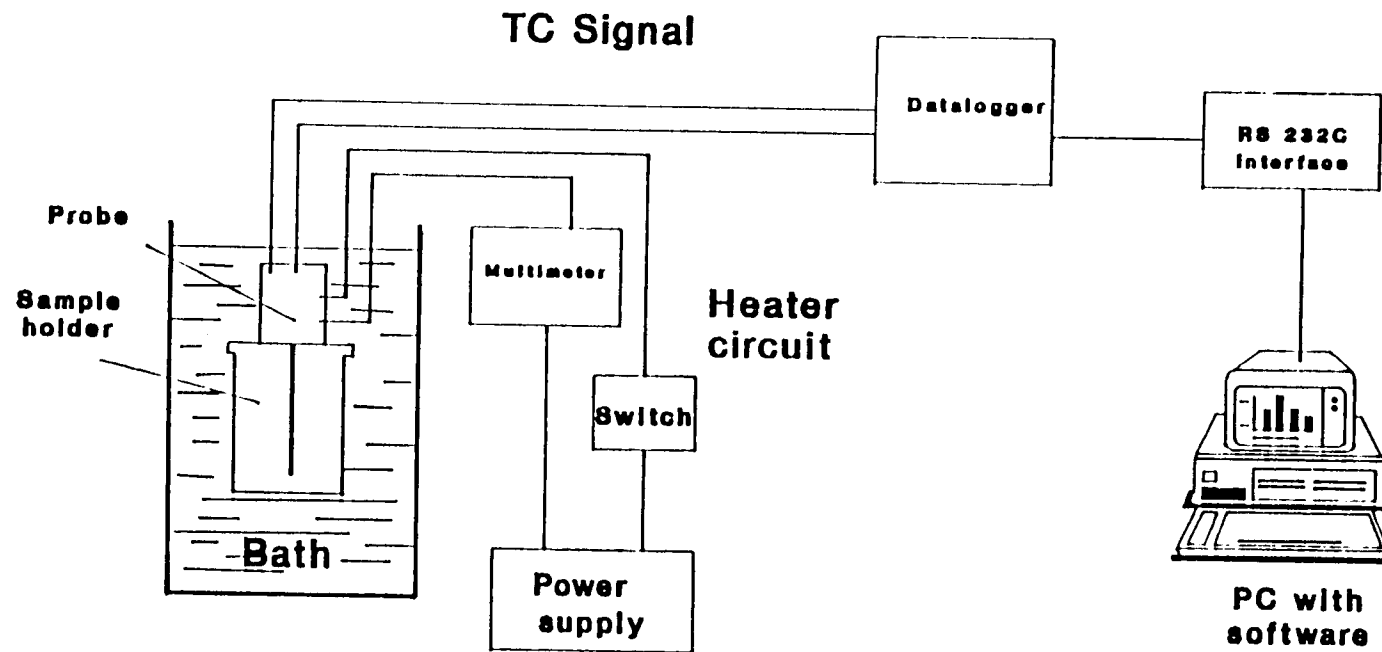


Fig. 3.1. Set-up of the k measurement system

measurement to a maximum scanning rate of 25 readings/sec. The datalogger was bi-directionally interfaced with a PC so measurement could be programmed. Analysis of data and calculation of thermal conductivity were done using Lotus 1-2-3 software.

Power level test. Effect of power level on the results of the line source probes was tested both on 0.5% agar and water gel, and on the surimi with 0% cryoprotectant level. For the sample of 0.5% agar and water gel, k values at two power levels (8.9 and 3.2 W/m) were measured at 30° C, while those at four power levels (8.9, 5.7, 3.2 and 1.4 W/m) were examined at -20° C. Six replicates were used for each level. For the sample of surimi, k measurement with various power levels (from 0.8 W/m to 8.9 W/m) was tested at temperatures of -15, -10, and -5° C. Four replicates were used for each measurement.

Scanning rate & time duration. To obtain satisfactory linearity of temperature vs $\ln(\text{time})$ plot and to limit temperature increase after heating, fast scanning rate and short time are necessary. Five levels of scanning rate, 20, 10, 1, 0.1 and 0.05 readings/sec, were examined while the duration for these five levels were 8, 16, 16, 100 and 200 sec, respectively. Thermal conductivity of four replicates for each level was measured at -10° C. The average of tested k values, standard deviation, and r^2 were recorded for analysis. The sample used was surimi with 6% cryoprotectant concentration.

Thermal conductivity measurement for surimi

Sample history effects. To examine the effects of previous freezing and thawing history on the measured k values, samples with 0% cryoprotectant level were tested with four different treatments: (1) fresh (unfrozen) sample just arrived; (2) sample rapidly frozen in a -37°C freezer, then thawed in a 30°C bath; (3) sample frozen in a -23°C freezer, then thawed in a 20°C bath; and (4) sample slowly frozen in a home freezer (-18°C), then thawed by ambient room air. Frozen storage time for all treatments was less than one week. Thermal conductivity at 30°C and -30°C were measured for each treated sample with four replicates.

To evaluate the effects of chilled storage time on k measurement, samples without cryoprotectant were tested at zero time (2 days post-catch), after 2 days in a refrigerator at 4°C , and after 6 days in a refrigerator at 4°C . Thermal conductivity values at 30°C and -30°C were measured with four replicates.

Thermal conductivity measurement for surimi. Thermal conductivity values of the pollock surimi having five different cryoprotectant levels were measured in the range -40 to 30°C . Samples were removed from the -80°C storage freezer and thawed in a 30°C bath. Probes were inserted in the samples which were placed in latex bags and immersed in the controlled temperature bath. From a variance analysis, four replicate samples were required for statistical significance. The samples were simultaneously cooled in the bath from 30°C , stopping at each temperature at which a k measurement

was to be taken. It often required over an hour to reach equilibrium, as detected by the center temperature reading. The k value was measured at 30, 20, 10, 0, -5, -10, -15, -20, -25, -30, -35 and -40° C. The scanning rate was 20 readings/sec for all experiments. The power levels used were 1.4 W/m at -5° C, 1.8 W/m at -10 and -15° C, and 7.2 W/m at the rest of temperatures. During the regression of temperature vs $\ln(\text{time})$, the procedure was standardized by (1) eliminating the first 1.5 of seconds data (30 data points), (2) using a duration of 8 sec, and (3) accepting k values measured only when $r^2 > 0.99$. To minimize the effect of the heat of fusion, however, the k measurement at -5° C differed from the others in three respects: (1) the earliest available linear data was used; (2) the duration was shortened to 2-3 sec; and (3) the r^2 value was lowered to 0.9.

Freezing rate effects. The samples were first slowly frozen in a -5° C bath. I also determined what would happen to the measured k values if a faster freezing rate were used. For this study, k values of two samples, cooled by different freezing rates, were measured at -30° C. One was frozen step by step as described before, while the other was directly and rapidly frozen at -30° C. The sample used was Pacific whiting surimi with 8% cryoprotectant level, made by the Seafoods Lab, Oregon State University, Astoria, Oregon. There were 4 replicates for each measurement.

Initial freezing point measurement. Application of numerical thermal property models requires measurement of the initial freezing point, T_i . Apparatus similar to that described by Fennema et al. (1973) was developed.

Thermocouples, calibrated at 0° C by an NBS-certified thermometer, were used. Pollock surimi with five different cryoprotectant levels were packed as before and submerged in a -8° C bath. Temperature-time data was recorded by the Campbell 21x datalogger. An electro-magnetic vibrator was employed to initialize ice crystallization when the temperature reached a point near the expected T_i value. There were 4 replicates for each cryoprotectant level. (The error was estimated at $\pm 0.1^\circ \text{C}$, limited mainly by the resolution of the NBS-certified thermometer.)

RESULTS & DISCUSSION

System development

The system was satisfactory for quick and simple k measurements with reasonable accuracy and reproducibility. During the experiments, calibration was checked against a 0.5% agar and water gel at 30° C nine times, each with 4 to 6 replicates. The mean k value of these nine runs was 0.623 W/mC, with standard deviation of 0.015 W/mC (2.4%). Error could be estimated as -0.8% when compared with an expected value of 0.628 W/mC (Sweat and Haugh, 1974). The system was also calibrated once against glycerine at 25° C with 5 replicates. The mean k value was 0.289 W/mC with standard deviation of 0.0045 W/mC (1.5%), and the expected value was 0.285 W/mC (Welty et al., 1984), indicating an error of +1.4%. Thus our system performance equalled or exceeded that reported by

Sweat and Haugh (1974), Ramaswamy and Tung (1981), and Murakami and Okos (1988).

The results of power level tests agreed well with those of Sweat (1976). In the unfrozen temperature range, there was no significant difference in measured k values when applying either 8.9 or 3.2 W/m power. A power level of 7.2 W/m was chosen for surimi measurements because the higher power levels gave higher r^2 values. Even though a greater temperature increase occurred in the high power case, it did not affect the accuracy very much since thermal conductivity of foods has a very low temperature dependence in the unfrozen temperature range.

In the frozen temperature range, for the same reason 7.2 W/m was again selected in the range -40 to -20° C. Thermal conductivity of foods is temperature dependent in this range, but the dependence is relatively weaker than that at temperatures slightly below T_i . A power level of 1.8 W/m was selected at temperatures of -15 to -10° C, and a level of 1.4 W/m was chosen at -5° C. A smaller power level was used at these temperatures because it would result in a smaller temperature increase, less heat of fusion, and consequently more reasonable k values.

For the effects of scanning rate and duration, k measurement at -10° C was selected because it was neither near T_i (which would cause more difficulty), nor near fully frozen range (which has a relatively weak temperature dependence). Results showed that as the scanning rate decreased, the departure

of measured k from expected values increased, as did the standard deviation. An opposite trend was found for the time and r^2 values.

Thermal conductivity measurement for surimi

Knowledge of the effect of sample history on k measurement is important to the food scientists and engineers for handling foods in frozen temperature range. This is especially true for seafoods because fresh samples are often not available. In this case, the result of the test on the effect of sample history indicated no significant difference for measured k values at 30 and -30° C. This conclusion was drawn from an ANOVA analysis with 95% confidence. The same conclusion was found for the effects of refrigerated storage time postmortem and of freezing rate during the experiments.

Measured k values of pollock surimi with five different cryoprotectant levels are given in Table 3.1. Data in the Table are the mean of four replicates, with maximum standard deviations less than 5.0% in the unfrozen range and less than 10.1% in the frozen range. These error results agree with the estimations reported by Sweat and Haugh (1974). Data are also plotted in Fig. 3.2 to 3.6 to describe subsequent model development. For the temperature ranges of -40 to -10° C and 0 to 30° C, data indicated no statistical difference between k values measured on samples having different cryoprotectant levels, using an ANOVA analysis with 95% confidence.

Table 3.1. Measured k value of surimi

Temp. ° C	Cryoprotectant Concentration									
	0%		4%		6%		8%		12%	
	$T_i = -0.35^\circ \text{ C}$		$T_i = -0.75^\circ \text{ C}$		$T_i = -1.01^\circ \text{ C}$		$T_i = -1.16^\circ \text{ C}$		$T_i = -1.63^\circ \text{ C}$	
	k W/mC	Std. Dev. %	k W/mC	Std. Dev. %	k W/mC	Std. Dev. %	k W/mC	Std. Dev. %	k W/mC	Std. Dev. %
-40	1.473	5.2	1.429	4.9	1.508	3.8	1.434	3.0	1.465	5.5
-35	1.425	2.1	1.390	2.0	1.434	3.5	1.404	1.6	1.422	4.1
-30	1.397	3.5	1.362	4.4	1.390	2.0	1.373	5.0	1.362	4.3
-25	1.333	3.6	1.274	6.4	1.373	3.7	1.352	5.0	1.349	6.4
-20	1.252	5.0	1.263	5.3	1.324	3.6	1.307	9.2	1.284	5.6
-15	1.227	9.5	1.192	4.4	1.252	3.4	1.260	4.6	1.276	5.8
-10	1.123	10.1	1.152	4.0	1.194	5.4	1.176	10.8	1.218	4.1
-5	1.031	8.8	1.023	7.4	1.056	3.7	1.181	2.3	1.230	5.0
T_i	0.504	1.6	0.465	9.4	0.477	4.1	0.492	3.4	0.489	5.8
10	0.487	2.5	0.484	5.0	0.489	2.4	0.509	3.0	0.505	4.9
20	0.521	0.4	0.472	4.0	0.509	1.2	0.516	3.2	0.498	5.0
30	0.516	2.2	0.508	2.0	0.506	4.2	0.527	3.4	0.508	3.2

1. Freezing points, T_i for each cryoprotectant level are also given in the table.

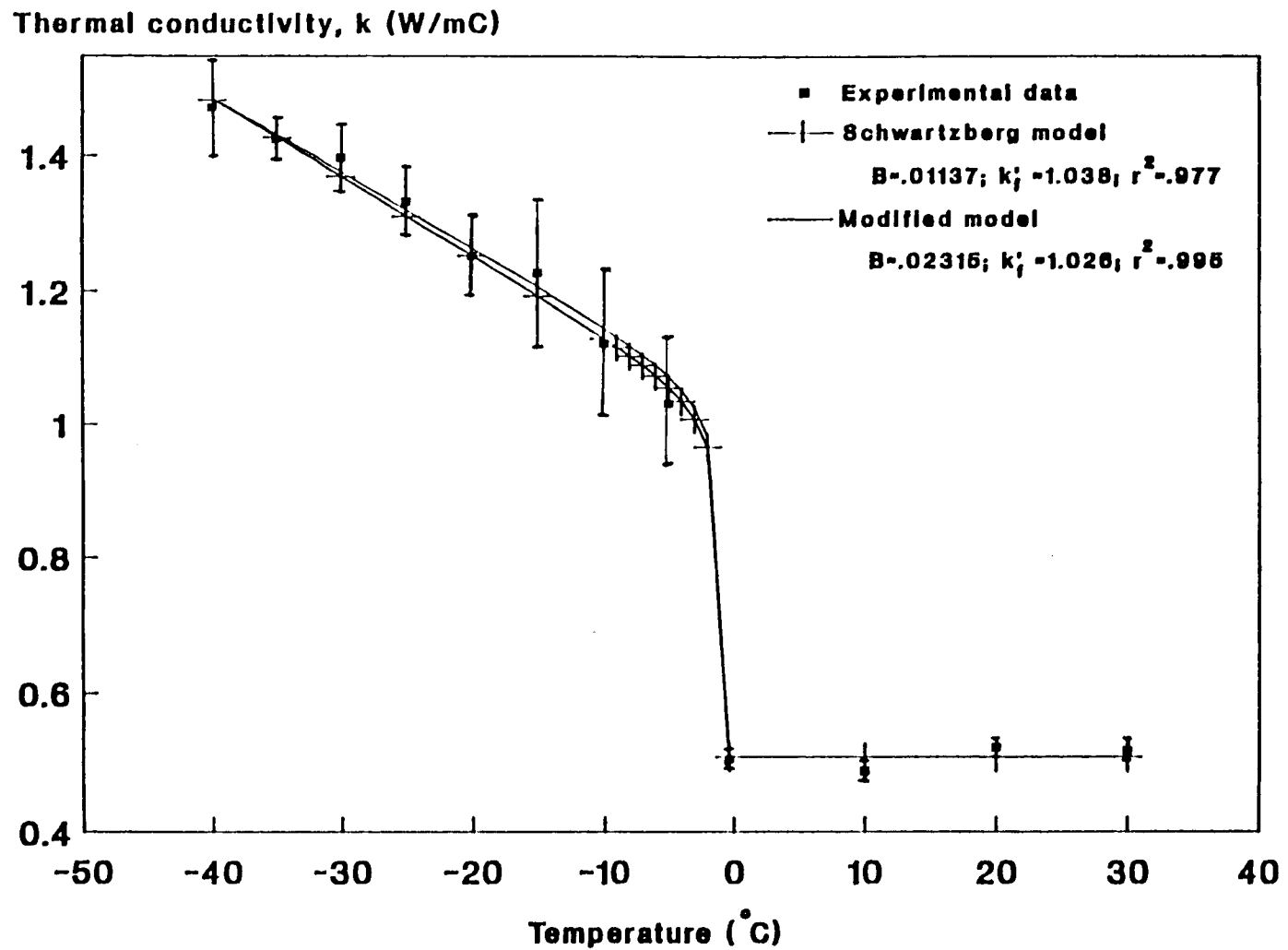


Fig. 3.2. Thermal conductivity of surimi with 0% cryoprotectant concentration

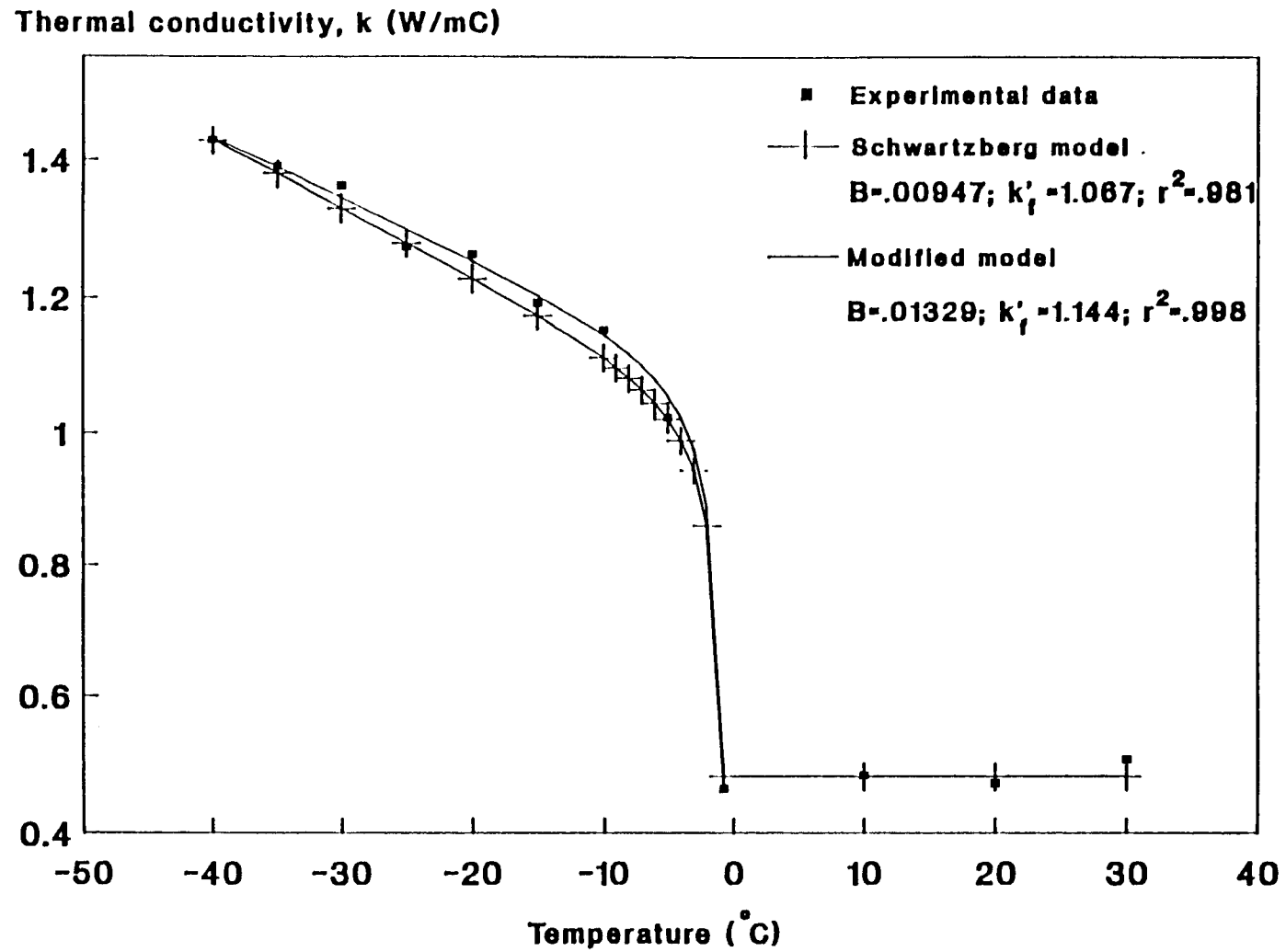


Fig. 3.3. Thermal conductivity of surimi with 4% cryoprotectant concentration

Thermal conductivity, k (W/mC)

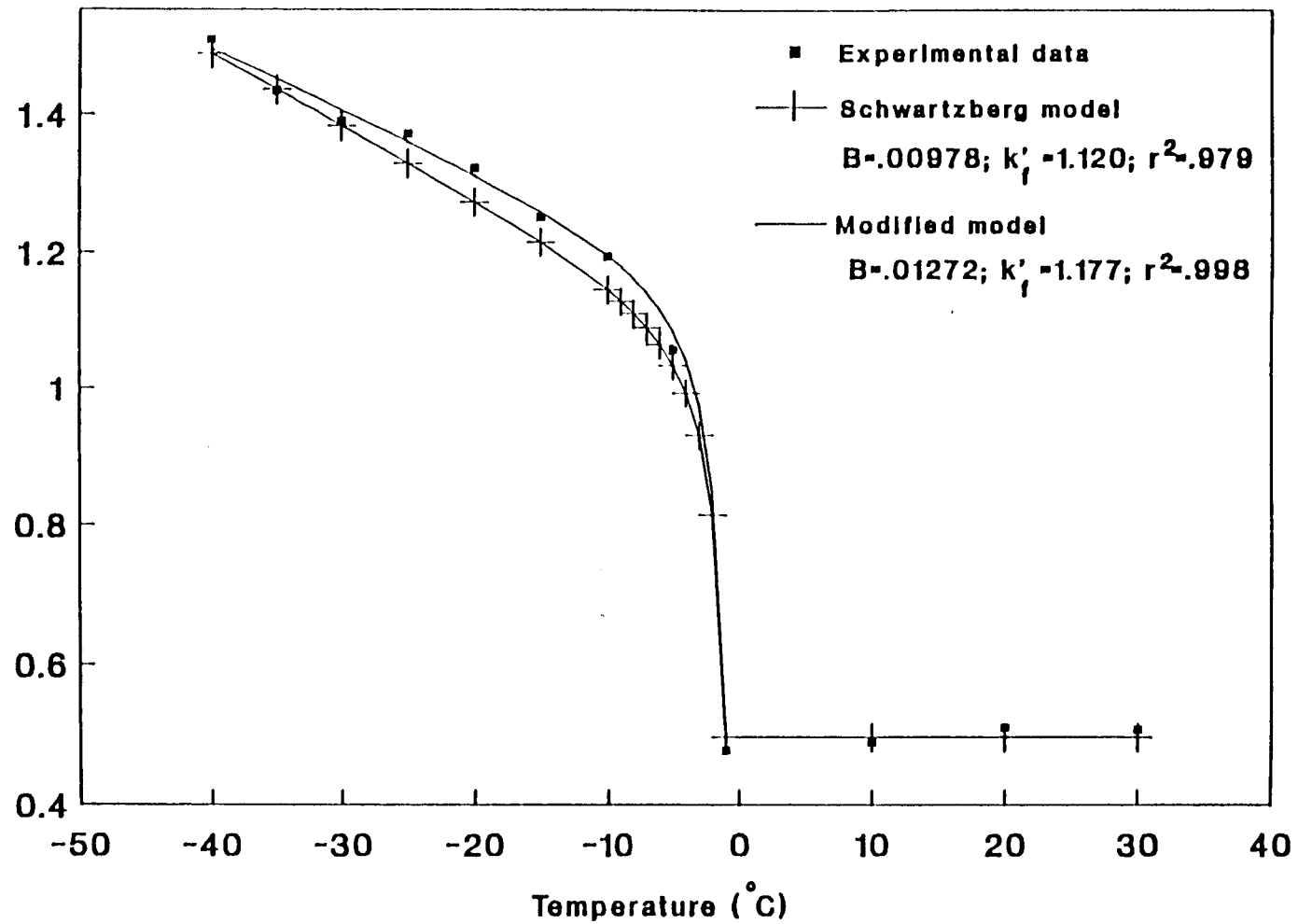


Fig. 3.4. Thermal conductivity of surimi with 6% cryoprotectant concentration

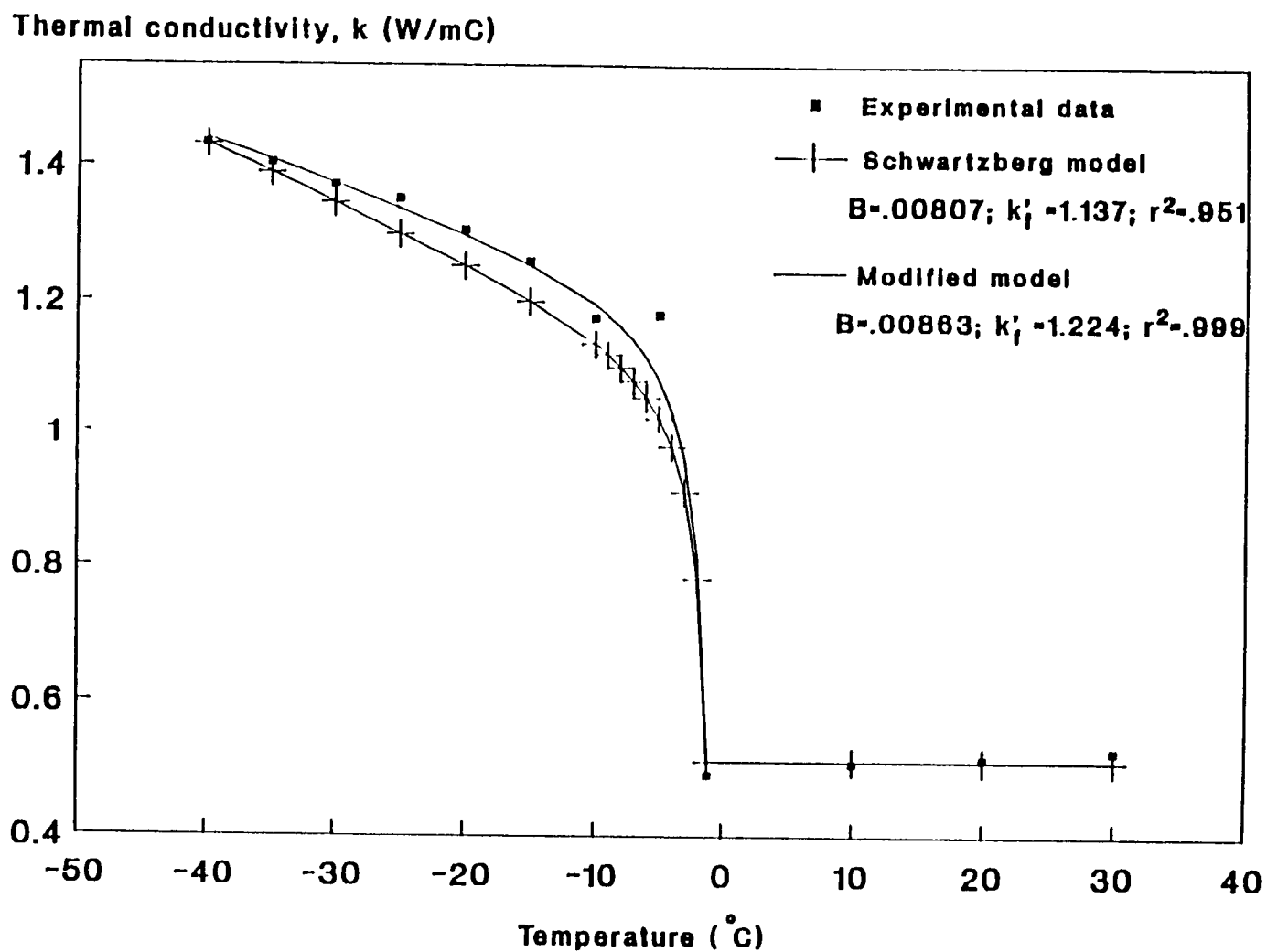


Fig. 3.5. Thermal conductivity of surimi with 8% cryoprotectant concentration

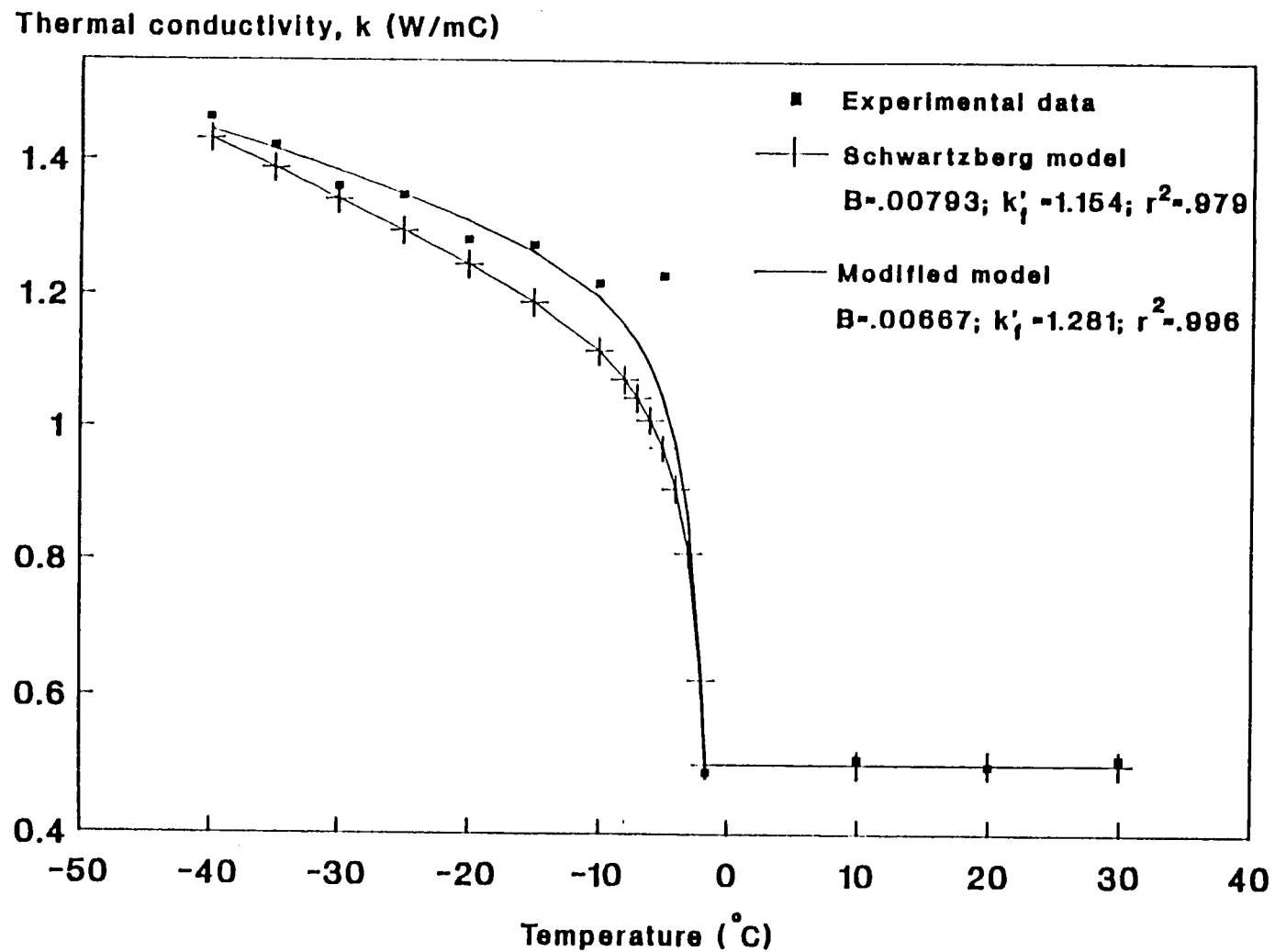


Fig. 3.6. Thermal conductivity of surimi with 12% cryoprotectant concentration

The initial freezing point, T_i , varied linearly with cryoprotectant levels, as shown in Table 3.1 and Fig. 3.7. The standard deviation of each measurement was less than 8.0%.

Model application

To select an appropriate model, four reported by Heldman (1982), Murakami et al. (1985), Schwartzberg (1977, 1983) and Succar and Hayakawa (1983), were investigated. The Murakami et al. model was not suitable to this project because detailed composition of the surimi is not commonly available. The Heldman model, as reported by Succar and Hayakawa (1983), was found to deviate somewhat from the tested data and, therefore, was not chosen in this research.

The Schwartzberg model (1977, 1983) for thermal conductivity agrees well with experimental data because all three parameters used by the model have to be obtained from experiments. The model is:

$$k = k'_f + B(T_i - T) + (k_o - k'_f) \left(\frac{T_o - T_i}{T_o - T} \right) \dots \dots \dots 3.1$$

where T is the temperature; T_i is the initial freezing point which has been discussed previously; T_o is the normal freezing temperature for pure water; k_o is the thermal conductivity in thawed state; B and k'_f are respectively the slope and intercept at T_i of a straight line representing the thermal conductivity values in the "fully frozen" zone. As shown in Fig. 3.2-3.6, the model agreed well for low

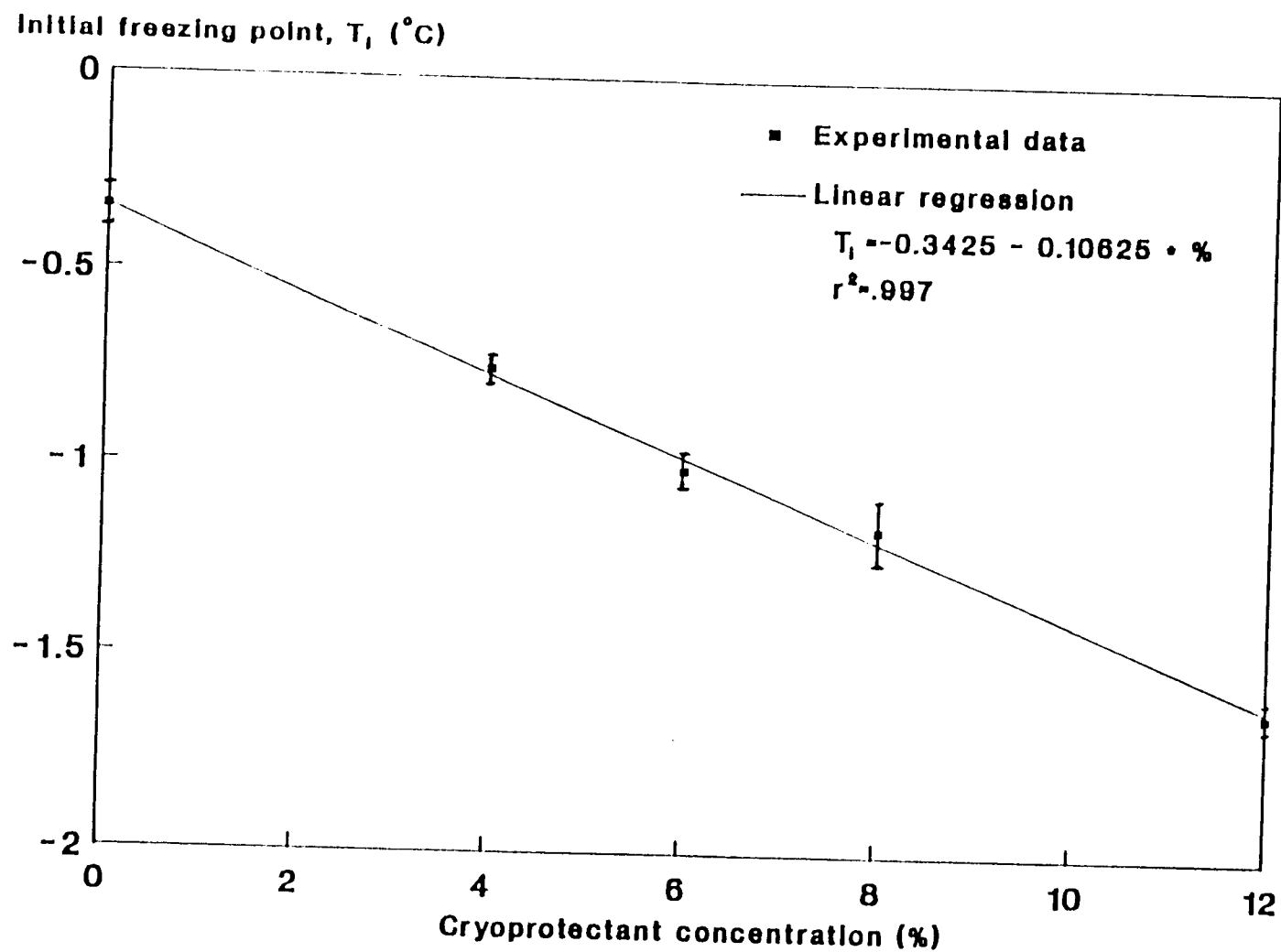


Fig. 3.7. Plot of T_i vs cryoprotectant concentration

cryoprotectant level samples. Agreement was not so good as cryoprotectant concentration increased. This is probably due to the fact that for high cryoprotectant concentrations, the ideal solution approximation used by the model is less valid.

Both parameters B and k'_f were found to have a linear relationship with cryoprotectant level, as shown in Fig. 3.8 and 3.9. For comparison, B and k'_f of pure ice are respectively 0.01177 W/mC^2 and 2.22 W/mC , calculated from data given by Dickerson (1969). Variations in T_i , B and k'_f need to be well-defined to more easily allow their use in models.

To obtain an improved fit, Succar and Hayakawa (1983) modified the Schwartzberg model by determining B and k'_f simultaneously through nonlinear parameter estimation. When this is done the two parameters no longer have their original physical meanings. Plots of this modified model are included in Fig. 3.2-3.6. Agreement became very good ($R^2 > 0.99$) because of the parameter estimation technique used. Values of B and k'_f determined by the modified model remain linear functions of cryoprotectant level, as shown in Fig. 3.8 and 3.9.

Although cryoprotectant level had no statistically significant effect in the range -40 to -10°C , k value in the range of temperatures slightly below T_i was a linear function of the cryoprotectant level. This is probably because T_i is a linear variation of the cryoprotectant concentration. The question arises why, in the range of -40 to -10°C , T_i , B and k'_f are linear functions of cryoprotectant level,

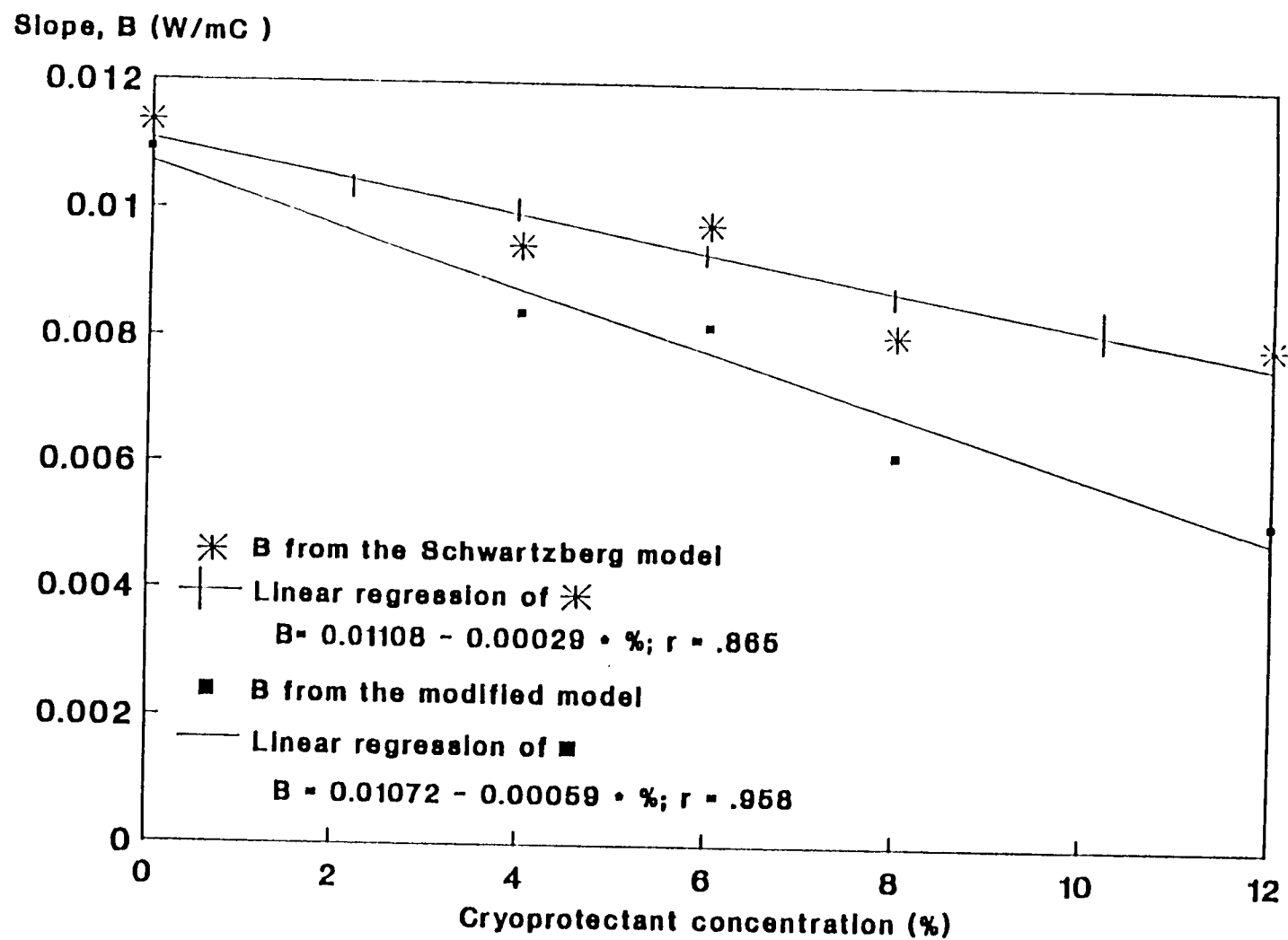


Fig. 3.8. Plot of B vs cryoprotectant concentration

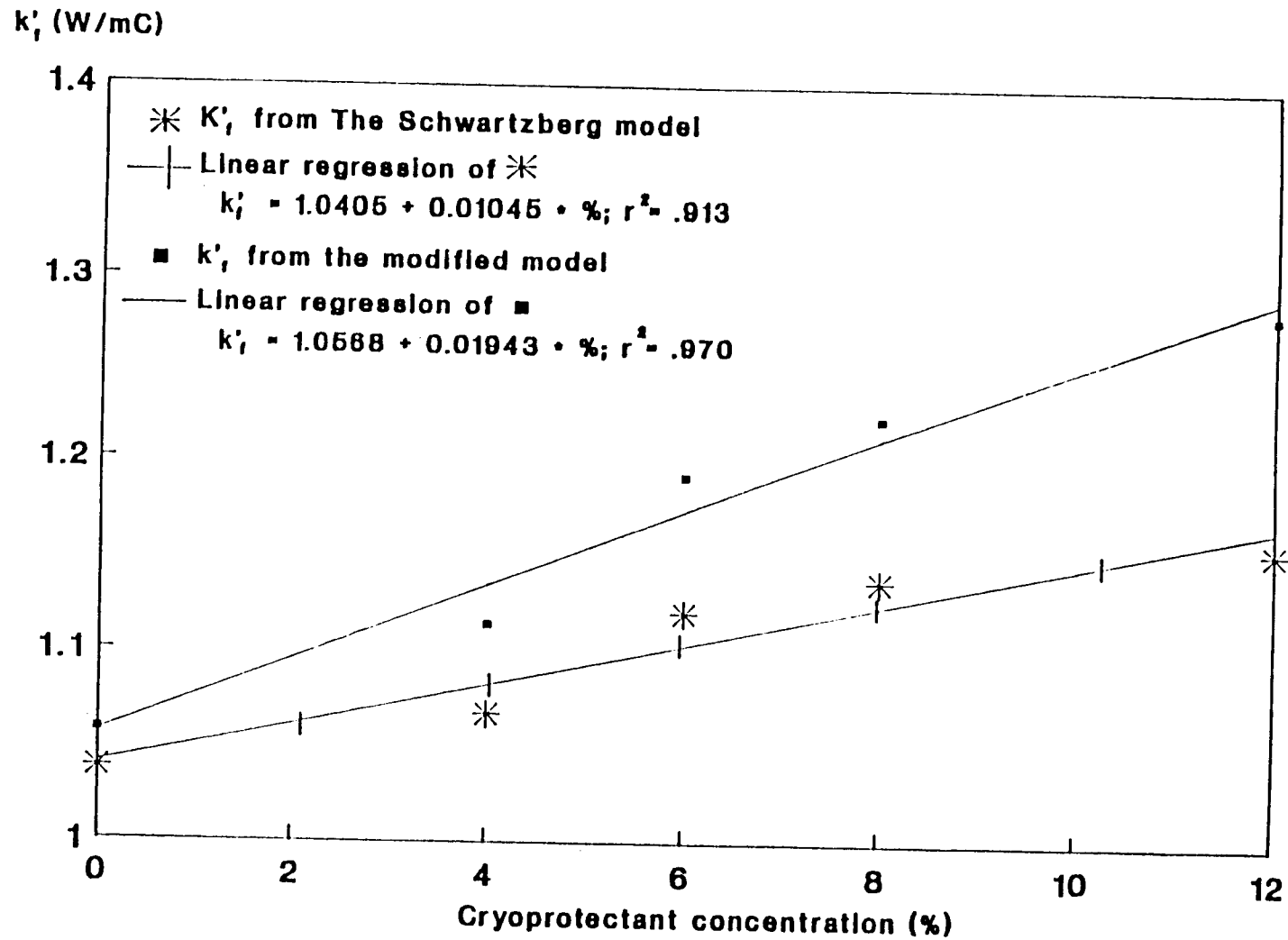


Fig. 3.9. Plot of k'_f vs cryoprotectant concentration

but k value is not. The five treatments described by the modified model, extended to -70°C are shown in Fig. 3.10. Though it is not clear how much validity one should give to such extrapolations, the predicted k values at -70°C (plotted in Fig. 3.11) were a linear function of cryoprotectant level. In results reported by Boose and Keppeler (1967), measured k value of sugar solutions was significantly affected by the sugar concentration. It may be appropriate to conclude thus, that k value of surimi has a relatively weak linear relationship with cryoprotectant level when water content is controlled.

Noted that in order to obtain reasonable measured k values at -5°C , the standard procedure of the regression had to be modified. Latent heat has a very strong influence on measurements at temperatures slightly below the initial freezing point. The line-source technique originally resulted from solution of a linear, transient, cylindrical heat conduction equation (Ingersoll et al., 1954). Linearity particularly implies that the thermal properties used in the equation were independent of temperature or time. This equation, and its further development by Nix et al. (1967), however, are no longer valid when applied to a food material undergoing a rapid phase change. This occurs in the temperature range between T_i and about -10°C , when both k and apparent specific heat (a sum of sensible heat and latent heat of fusion) vary strongly with temperature. As described by Schwartzberg (1977) and Heldman (1982), the sharp peak displayed by apparent specific heat just below the freezing point, will create a positive error in the value of k measured by the line-source method. In short,

Thermal conductivity, k (W/mC)

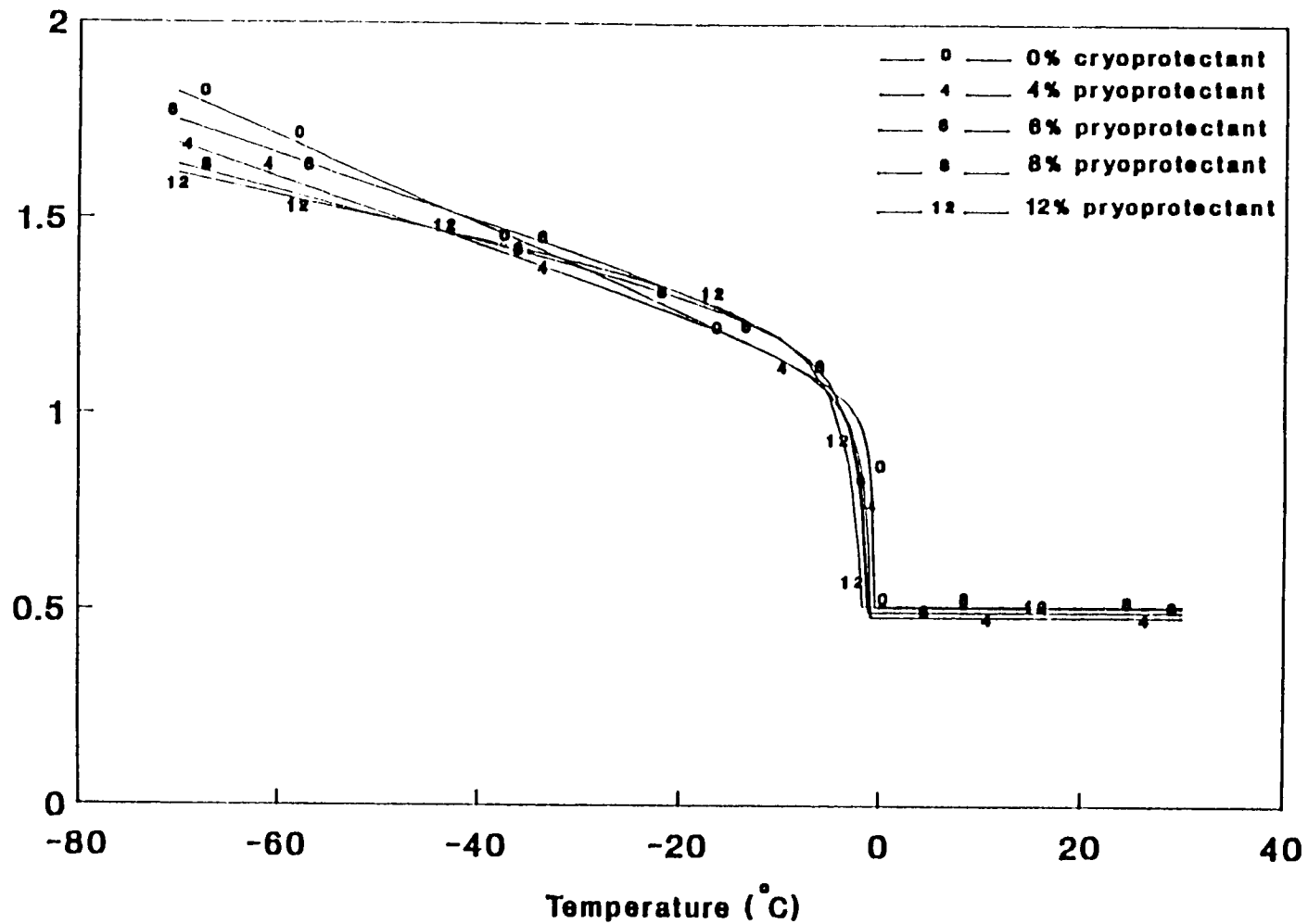


Fig. 3.10. Comparison of predicted k values by the modified model
(The k values at -70° C obtained by extrapolation)

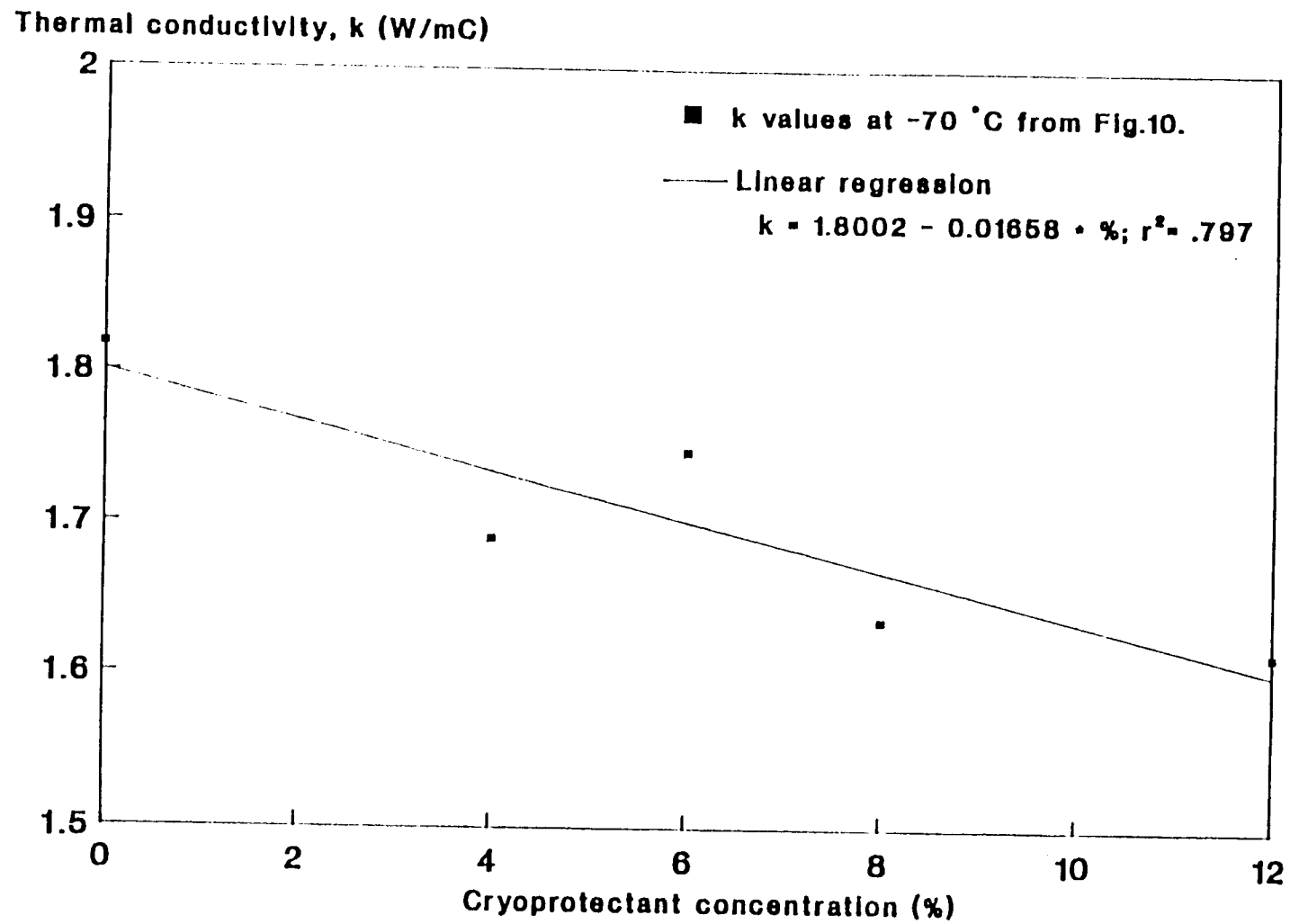


Fig. 3.11. Predicted k values at -70° C vs cryoprotectant concentration

the probe method does not work well for food in a temperature range slightly below T_i . A numerical solution of the partial differential equation may be used to evaluate how the apparent specific heat affects the k measurement and corrects the error, as suggested by Schwartzberg (1988). Another is to use a steady state measurement technique, such as guarded hot plates. Either may do a better job, but it still may not be superior to a prediction by a precise model. Further research in this area is therefore necessary.

CONCLUSIONS

This system works well and appears to be an improvement over other report approaches. The research also indicated that as the probe method is used more and more for foods, the experimental procedure needs to be standardized.

The probe method is not appropriate for determination of thermal conductivity at temperatures slightly below the initial freezing point. The prediction of k values in this temperature range using a precise model is probably more accurate than measurements.

Sample history relating to freezing and thawing, time postmortem under refrigerated conditions, and freezing rate during the measurement do not significantly affect the measured k values.

Thermal conductivity of surimi has a relatively weak dependence upon the cryoprotectant level when the water content of the sample is controlled.

The Schwartzberg model (1977, 1983) and its modification by Succar and Hayakawa (1983) agree well with experimental data.

CHAPTER 4. THERMAL PROPERTIES OF SURIMI ANALYZED USING DSC

ABSTRACT

Thermal properties of surimi made from Alaska pollock (Theragra chalcogramma) were analyzed using differential scanning calorimetry (DSC) in the freezing range. Each dynamically corrected thermogram was used to determine initial freezing point, unfreezable water (bound water), apparent specific heat, enthalpy and unfrozen water weight fraction. When water content was controlled at 80.3% (wet basis), the cryoprotectant concentration had little effect on thermal properties in the unfrozen and fully frozen (-40°C) ranges. However, the initial freezing point and thermal properties just below this point were significantly affected. The study also demonstrated the great potential of DSC for measuring and modeling frozen food thermal properties.

INTRODUCTION

The thermal properties of frozen foods are of interest to food engineers in modeling freezing and frozen storage processes and in designing equipment. Indeed, as modern computer technology develops, the improved accuracy of models describing freezing and frozen storage of foods depends mainly on the accuracy of thermal property data. In recent years, many researchers have successfully developed thermal property models for frozen foods. Most of these models are based on the equation of freezing point depression (Heldman, 1982; Schwartzberg, 1977, 1983; Chen, 1985a, 1985b, 1986). Upon comparing these models with published experimental data, Succar (1985) reported the Schwartzberg model showed best agreement because it allowed use of empirical parameters to improve accuracy. Among those researchers who have investigated thermal property models, few have included measurements; however, a number of them referenced data of Riedel (1956, 1957) (Fennema et al. 1973; Schwartzberg, 1977, 1983; Chen, 1985a). There seem to have two reasons for this disregard of measurements: the accuracy of measured values was seen to be no better than that of predicted values; and measurements of improved precision were extremely difficult at temperatures near the initial freezing point.

Differential scanning calorimetry (DSC) has been widely used in polymer science for a variety of analyses. The advantages of DSC are that it works rapidly and simply, much valuable information can be obtained by a single

thermogram, and a very small sample can yield accurate results (McNaughton and Mortimer, 1975). This technique has been used to analyze thermal properties of frozen food. For example, Duckworth (1971), Ross (1978) and Roos (1986) successfully determined the unfreezable water of foods; and Ramaswamy and Tung (1981) studied apparent specific heat, C_p , of apples. However, these earlier uses of DSC in frozen food research focused on only one or two properties.

In analyzing thermal properties of frozen foods with DSC, many researchers have reported a distorted C_p curve near the initial freezing point, T_i . This limitation has restricted the application of DSC in this field. To study apparent specific heat, Jason and Long (1955) used an adiabatic calorimeter which operated as a differential thermal analyzer (DTA). They reported that a slope of infinity was not found at T_i , nor did the C_p function fall sharply to the expected low values at the temperature just above the unfrozen region. They suspected that a time "lag" was responsible. The distorted C_p curves were also found in the reports of Roos (1986) and Ramaswamy and Tung (1981). In biophysical chemistry, some researchers have extensively investigated the methods of dynamic correction, and several correction methods have been suggested (Randzio and Suurkuusk, 1980; Mayorga and Freire, 1987). Although most of the instruments they modeled were microcalorimeters, the principle of measurement is the same.

This is a report of research in which DSC was used to analyze thermal properties of surimi, an intermediate raw minced fish material which is typically thawed from the frozen state to make seafood analogs. In this study, a number of thermal properties were dealt. The initial freezing point, T_i , is the temperature at which crystallization begins. It is one of the basic parameters of food composition effects in thermal property models; unfreezable water (or bound water), b , is the amount of water remaining unfrozen at -40°C (Fennema, 1985). It is important to the accuracy of thermal property models (Succar, 1985). Unfreezable water is also a composition-dependent variable; latent heat of fusion, H_L , is the heat of phase change; enthalpy, H , is the energy content relative to some low temperature datum, often selected as -40°C (Fennema et al., 1973; Heldman, 1982; Schwartzberg, 1983). Enthalpy data are essential to food engineers not only to support the design of freezers and frozen storage processes, but also to mathematically model the freezing process by a so-called enthalpy formula method (Mannapperuma and Singh, 1988); apparent specific heat, C_p , is the rate of enthalpy change with respect to temperature, dH/dT . It includes both sensible heat and latent heat of fusion in the frozen temperature range. Apparent specific heat is one of the most important thermal properties used in solving the classical non-linear heat conduction equations that describe freezing and frozen storage processes (Schwartzberg, 1977); unfrozen water weight fraction, n_w , is the amount of water remaining unfrozen at a certain temperature. It includes both uncrystallized free water and bound water.

The temperature-dependent model of n_w is the basic equation used to predict the frozen food thermal properties including thermal conductivity, apparent specific heat, enthalpy and density (Heldman, 1982; Schwartzberg, 1983). Published reports use a variety of terms to describe the temperature-dependent water portion of frozen foods. Fennema et al. (1973) used a term "per cent frozen water," defined as the mass percentage of ice with respect to the total amount of initial water; Heldman and Singh (1981) used "unfrozen product fraction," defined as the mass fraction of unfrozen product with respect to the total food sample. In this report, "unfrozen water weight fraction" is a term similar to that used by Schwartzberg (1983), which means the summation of bound water and melted free water divided by the total mass of the sample.

Overall, the objectives of our research were: to demonstrate alternative DSC techniques for analyzing thermal properties of frozen foods; to measure the initial freezing point, bound water, latent heat of fusion, apparent specific heat, enthalpy and unfrozen water weight fraction of surimi at different cryoprotectant concentrations and to investigate the effects of cryoprotectant level on these properties; and to compare existing thermal property models for frozen foods with DSC data and to evaluate possible improvements.

MATERIALS & METHODS

Materials

Surimi samples were made from Alaska pollock (Theragra chalcogramma) obtained in Alaska. Surimi was taken from the production line prior to addition of cryoprotectants and air-shipped with gel-ice to Corvallis, Oregon. The water content of the surimi was 80.3%, measured by drying the samples in a vacuum oven at 105 ° C for 24 hours, with 6 replicates. The surimi was then mixed with cryoprotectants (0, 4, 6, 8 and 12%) consisting of half sucrose and half sorbitol (Lampila, 1988). The water content of the mixture was controlled to 80.3% (wet basis) for all cryoprotectant levels. All samples were stored in a -80 ° C freezer after they were evacuated and sealed in 3 plastic frozen storage bags to prevent moisture loss.

DSC measurement

A DuPont 910 differential scanning calorimeter (DSC) was used with a sample temperature capability of -85 ° C obtained with a two-stage mechanical cooling accessory. To eliminate water condensation in and under the DSC cell, I forced 40 mL/min nitrogen gas through the purging port while 140 mL/min nitrogen gas flushed through the cooling port. The system was calibrated using DuPont calibration software, with indium and distilled water samples used for calibration of heat flow and two temperature points. Surimi samples of 6 to 8 mg (7.23 ± 1.18 mg for 15 scans) were sealed in aluminum pans and weighed on a

Mettler semi-microbalance (Model AE 240) with an accuracy of ± 0.01 mg. Empty aluminum pans were used as references. For each cryoprotectant level, I ran five scans: a baseline, a distilled water standard, and three replicate surimi samples, all scanned from -80°C to 40°C at a heating rate of $2^{\circ}\text{C}/\text{min}$. A sensitivity of 1X was selected for the measurements. Fig. 4.1 shows a typical single thermogram of surimi with 0% cryoprotectant concentration. The instrument was first calibrated so the peak of a distilled water standard occurred at 0°C , as described below.

Initial freezing point

To determine the initial freezing point, I scanned a distilled water sample weighing 6 ± 0.5 mg prior to scanning the three replicate surimi samples for each cryoprotectant level. Peak temperature for the distilled water standard was adjusted to 0°C using the standard DuPont DSC software. The peak temperature of the surimi thermogram then indicated the initial freezing point, T_i , as shown roughly in Fig. 4.1.

Apparent specific heat

Displacement of the thermogram from the baseline (Fig.1) gives a differential sample heating rate (Δq) from which the apparent specific heat can be calculated at each temperature (DuPont Instruments, 1988):

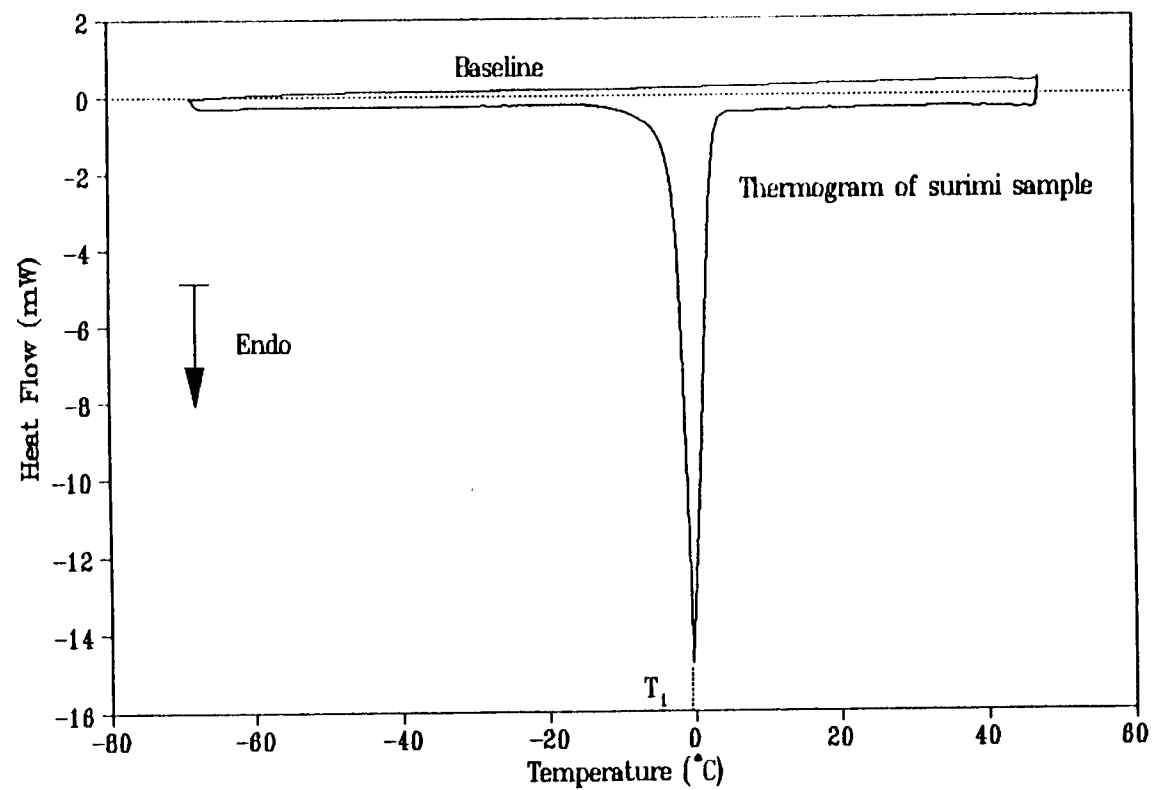


Fig. 4.1. A typical DSC thermogram of surimi sample

$$C_p^* = \frac{E \Delta q}{\beta m} \dots\dots\dots 4.1$$

where E is a "cell calibration constant" (DuPont Instruments, 1988) which takes into account any error relating to enthalpy measurement of the DSC. An average of E values for seven calibrations in this research was 1.033, with a standard deviation of ± 0.050 ($\pm 4.8\%$). In the measurement, a ratio method (O'Neill, 1966) was applied with a distilled water standard in the unfrozen and fully frozen temperature ranges. By comparing apparent specific heat determined using Equation 4.1 with a distilled water standard under the same condition, I ensured a more accurate measurement. The calculation was carried out using the spreadsheet Quattro Pro (Borland International, Inc., Scotts Valley, CA).

Curve BDFG in Fig. 4.2 shows temperature-dependent C_p values of surimi having an 8% cryoprotectant concentration, as determined by Equation 4.1. Because of the relatively slow time response of dynamic calorimetry, the curve was distorted to the right, thus giving C_p values which were an incorrect function of temperature. Randzio and Suurkuusk (1980) described a first-order correction which can be modified to apply to these results:

$$C_p(T) = C_p^*(T) + \tau \frac{dC_p^*(T)}{dt} \dots\dots\dots 4.2$$

The time constant τ describes the delay of the sample response due to the mass of the calorimeter cell and thermal resistance between the cell and its surroundings. After correction, the trace represented by BDF in Fig. 4.2 will shift to that represented by BCE. In this research, τ was evaluated by iteration of the integral by assuming that the enthalpy change (areas under the curve) indicated by BDF and BCE must be the same (Randzio and Suurkuusk, 1980). That is, Area BDFEIB equals Area BCEIB within 1 kJ/kg (approx. $\pm 0.4\%$). Typically, τ was on the order of 1 second (0.94 ± 0.08 second for 15 iterations). Analysis and numerical integration were carried out using Quattro Pro.

Unfreezable water

Unfreezable water, b , was considered as the difference between the total water content of the product and the amount of water detected by the DSC fusion endotherm (Ross, 1978). The heat of fusion can be determined by the area of BCEIB in Fig. 4.2. It indicates the amount of free water that has gone through a phase change between -40°C to T_i .

Unfrozen water weight fraction

On the DSC thermogram (Fig. 4.2), a partial area of the melting peak (area of BCEIB) at any temperature represents the amount of free water melted from -40°C to the temperature of interest. The unfrozen water weight fraction, n_w , was determined by the summation of unfreezable water and melted free

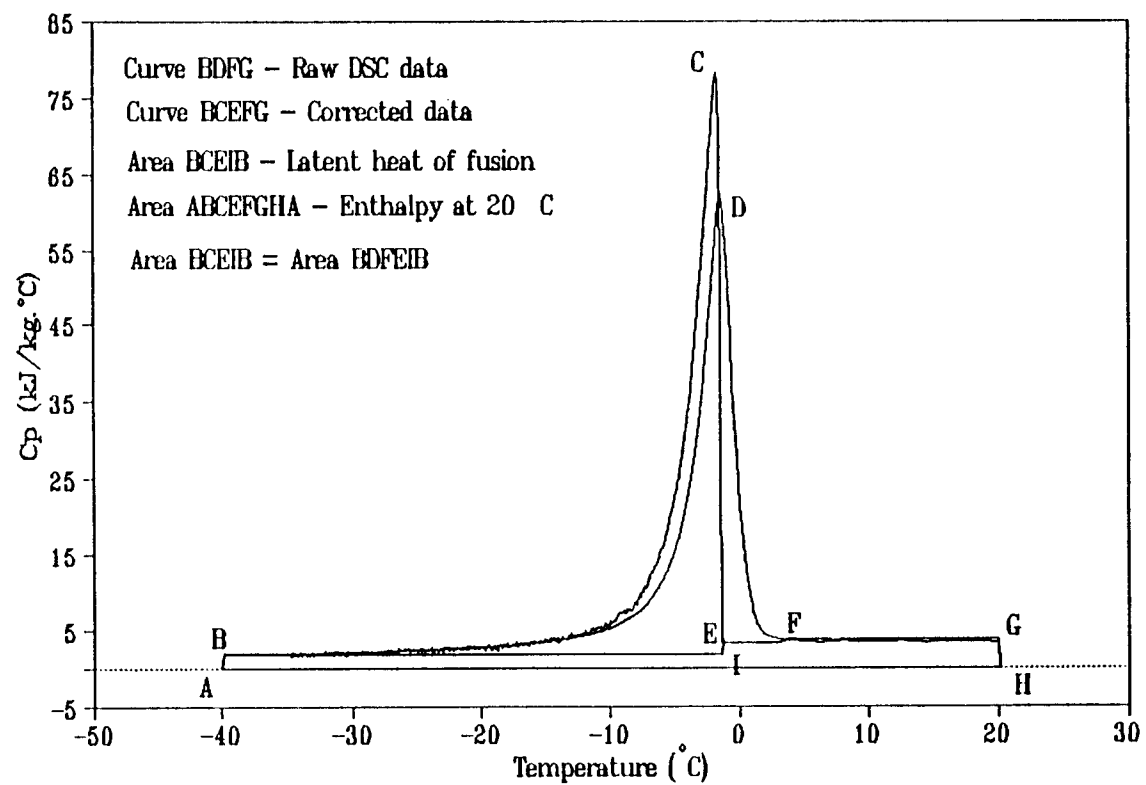


FIG. 4.2. Illustration of the correction and calculation

water divided by the total mass of the sample.

Enthalpy

Enthalpy, H, can be mathematically determined by

$$H = \int_{T_R}^T C_p(T) dT \dots \dots \dots 4.3$$

The temperature datum (T_R), at which $H=0$, was selected as -40°C . An enthalpy value at any temperature was determined as a partial area under the C_p curve. For example, Area ABCEFGHA (Fig. 4.2) represents the H value at 20°C .

RESULTS & DISCUSSION

DSC measurement

Fig. 4.3 shows DSC thermograms (prior to any dynamic correction) for three different cryoprotectant levels; that for distilled water is included for comparison. Peak temperatures shifted toward lower temperatures as

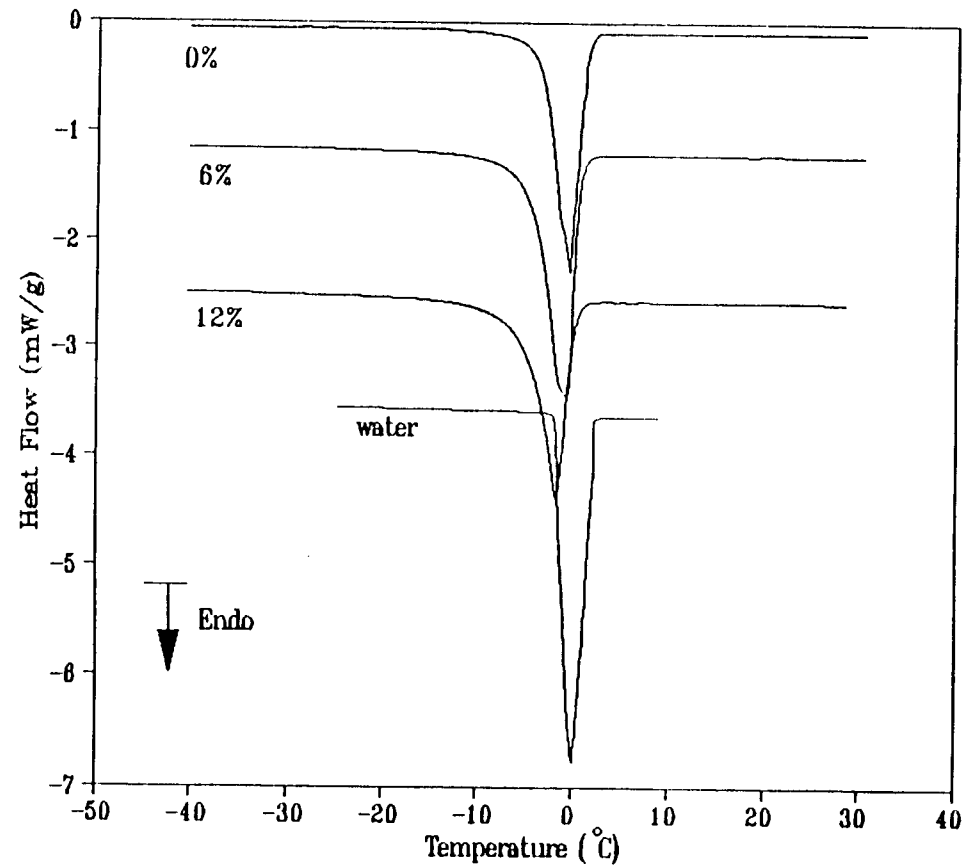


Fig. 4.3. Thermogram of surimi with different cryoprotectant levels

to cryoprotectant concentrations increased. The phase change of surimi occurred over a broader range of temperature as cryoprotectant was added (and protein content was accordingly decreased, since water content was controlled at 80.3%). The temperatures at which the phase change began (the "incipient melting points" defined by Roos, 1986) were about -13°C , -21°C and -28°C for surimi at 0%, 6% and 12% cryoprotectant levels, respectively.

Frequent calibration has been found important with respect to all factors influencing accuracy of DSC measurement, such as mechanical cooling, nitrogen purging, water condensation, inconsistency of sample loading, sample pan position and sample size. For seven calibrations using a distilled water standard, an average value of H_L was 330.2 (compared to 333.22 kJ/kg reported by Heldman and Singh, 1981), with a standard deviation of 10.9 kJ/kg; and the average peak temperature was $0.16 \pm 0.20^{\circ}\text{C}$. These data may also indicate the error involved in DSC measurement.

Initial freezing point

Table 4.1 shows the initial freezing points determined from the peak temperature of the DSC thermograms and from our previous research (Wang and Kolbe, 1990). It can be seen that the T_i values reported here are more scattered and consistently 0.1 to 0.3°C lower than those from our previous research. Scatter was most likely due to the error of DSC in temperature readings. The lower DSC T_i values should be expected; as discussed by

Table 4.1. Initial freezing points

Cryo. conc. %	From DSC thermogram		From time-temp. curve	
	T _i	S.D. ¹	T _i	S.D. ²
	° C	° C	° C	° C
0	-0.22	0.07	-0.35	0.06
4	-1.24	0.15	-0.75	0.04
6	-1.33	0.24	-1.01	0.08
8	-1.49	0.20	-1.16	0.09
12	-1.65	0.02	-1.63	0.04

¹ Evaluated from 3 replicates.

² Evaluated from 4 replicates.

Fennema et al. (1973), the time-temperature curve extrapolation method often results in an erroneously high freezing point. Although each of the two methods had different advantages, the data analyzed by DSC are more favorable because they are not affected by freezing rate and supercooling. There was almost no temperature gradient within the sample, and the system had been frequently calibrated using a distilled water standard.

Apparent specific heat

Table 4.2 gives the dynamic corrected C_p values. For comparison, I include Riedel's data and plot them with C_p of surimi at 0% cryoprotectant level in Fig. 4.4. Good agreement was clearly demonstrated. In the unfrozen and fully frozen temperature ranges, C_p values under different cryoprotectant levels were not statistically different. For example, at 20° C and -40° C, the mean of five C_p values with different cryoprotectant concentrations were $1.64 \pm 5.9\%$ and $3.67 \pm 1.4\%$, respectively.

I should point out here that one disadvantage of the dynamic correction process was that the noise of the signal significantly increased (refer to Fig. 4.2). In Table 4.2, the C_p values in the unfrozen and fully frozen temperature ranges are based on raw DSC data which were determined by using

Table 4.2. Measured apparent specific heat of surimi

Cryoprotectant concentrations											
Temp.	0%		4%		6%		8%		12%		Riedel ¹
° C	C _p kJ/kg.C	S.D. %	C _p kJ/kg.C	S.D. %	C _p kJ/kg.C	S.D. %	C _p kJ/kg.C	S.D. %	C _p kJ/kg.C	S.D. %	Fish muscle kJ/kg.C
-40	1.78	3.7	1.52	6.1	1.60	2.8	1.70	8.8	1.62	3.7	1.84
-35	1.82	5.2	1.54	4.8	1.59	3.4	1.80	8.6	1.69	5.9	---
-30	1.90	4.8	1.60	7.1	1.63	2.0	1.89	8.4	2.03	4.7	2.09
-25	1.98	4.3	1.71	6.6	1.87	2.6	2.22	7.3	2.37	1.4	---
-20	2.14	5.2	1.97	5.8	2.19	3.2	2.58	6.6	2.81	2.6	2.59
-15	2.26	0.2	2.66	4.3	2.84	3.2	3.19	4.3	3.50	3.9	3.07
-10	3.56	0.2	4.49	4.2	4.52	2.6	5.82	4.9	6.78	2.4	4.14
-8	4.67	1.6	6.47	2.7	6.47	10.3	8.55	4.1	10.04	1.1	5.27
-6	6.79	0.4	11.33	9.9	11.09	11.7	15.37	5.6	17.65	2.1	7.73
-4	14.24	6.8	28.96	9.6	27.01	13.7	34.21	3.6	33.45	2.1	15.30
-2	57.77	2.1	81.41	4.1	79.65	12.0	81.74	5.7	59.03	5.3	67.30
T _i	107.87	1.3	99.80	3.7	89.92	11.7	83.21	6.1	63.44	4.0	108.47 ²
10	3.68	2.2	3.59	6.0	3.55	1.5	3.98	11.1	3.57	0.6	3.72
20	3.74	1.8	3.64	6.6	3.66	1.8	3.70	2.7	3.61	1.6	3.72

¹ From Chen (1985a), which were averaged values of cod (80.3% water content) and haddock (83.6% water content) reported by Riedel (1956).

² Temperature for this value was -1° C according to Chen (1985a).

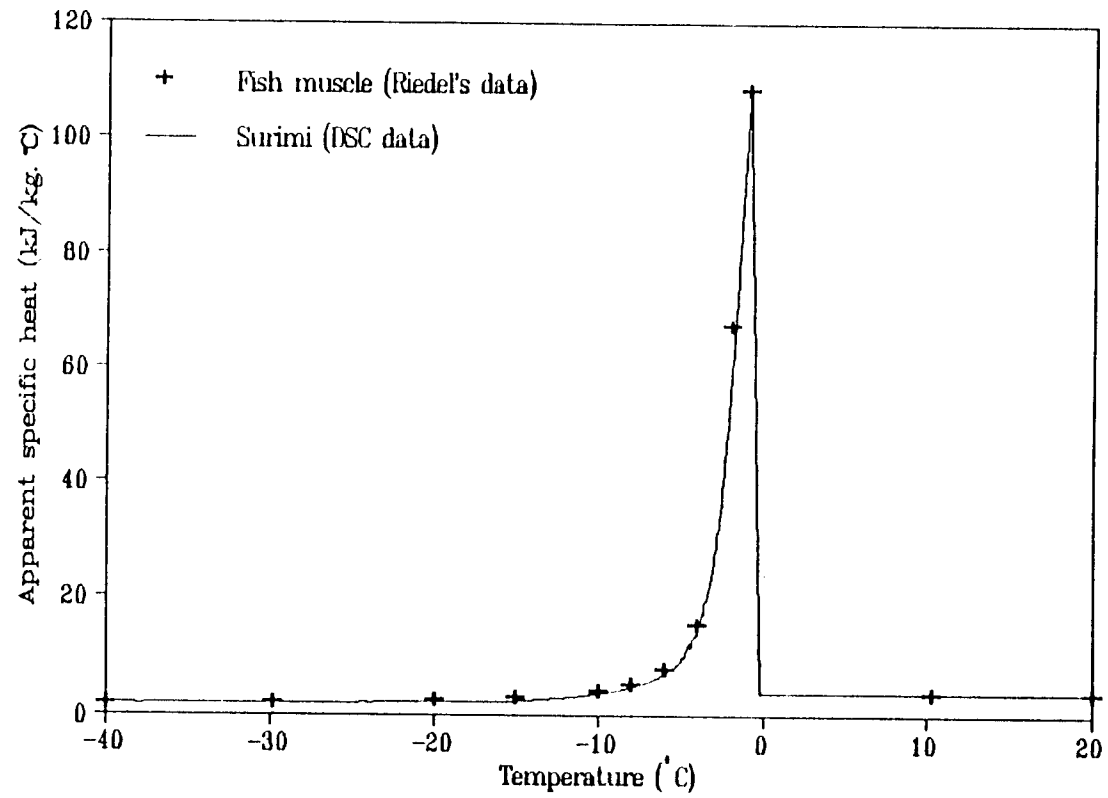


Fig. 4.4. Measured apparent specific heat of surimi with 0% cryoprotectant concentration

the ratio method and which were not influenced by the signal noise. However, in the range of -20°C to T_i , dynamic correction had to be applied and the noise had to be smoothed out. In our research, the smoothing procedure was to use the mean value of surrounding areas. In addition, an overshoot observed as the value of C_p fell to the unfrozen range was smoothed out as noise.

Randzio and Suurkuusk (1980) reported that to obtain a reliable correction, overshoot should be avoided, and the areas under the peaks of raw DSC data and corrected data should be maintained the same. These two criteria depend not only on the quality of DSC raw data but also on correction parameters, which vary with each measurement and with the characteristics of each individual calorimeter. Therefore, improved methods of determining time constants and better smoothing routines may result in further improvement of DSC measurements.

Because distilled water has C_p values similar to those of high-moisture-content foods in the unfrozen and fully frozen temperature range, I used it in this research to correct C_p values at each end of the temperature scale, employing the ratio method of O'Neill (1966). This method, however, could not be used in the temperature range near T_i because the phase change of foods occurs over a broad range of temperature rather than at a single point. It was therefore necessary to develop a special standard material to make the ratio method applicable to frozen foods. Such material should have similar thermal properties and phase transition characteristics. Tylose (a mixture of

methylcellulose and water) has been extensively used as a food model in the study of freezing and may be adequate for that purpose.

Unfreezable water

Table 4.3 gives the values of the latent heat of fusion, H_L , and calculated unfreezable water, b . Ross (1978) suggested that since both unfreezable water and water activity, a_w , were composition-dependent variables, unfreezable water should always be reported with corresponding water activity. The a_w values of surimi samples at different cryoprotectant concentration were calculated according to Raoult's law and are also reported in Table 4.3. In the calculation of a_w , the molecular weight of water, sucrose and sorbitol used were 18.0, 342.3 and 182.2, respectively (Weast and Astle, 1980). The molecular weight of fish protein solute was estimated as 493.8, an effective molecular weight reported by Chen (1985a).

From Table 4.3, it can be seen that b and a_w vary similarly with respect to the cryoprotectant concentration, first falling, then rising, as cryoprotectant concentration increased. This trend agreed with that reported by Hanafusa (1985), in which the unfrozen water at -40°C was in fact the unfreezable water

Table 4.3. Unfreezable water, latent heat of fusion and water activity of surimi

Cryo. conc. %	b <u>g H₂O</u> g solids	H _L <u>kJ</u> kg	a _w
0	0.54	231.6±4.1% ¹	0.9911
4	0.46	237.8±1.3%	0.9892
6	0.42	240.2±2.5%	0.9882
8	0.46	237.7±0.1%	0.9849
12	0.54	231.8±4.3%	0.9853

AVG ² :	0.48±11.1%	235.8±1.7%	0.9877±0.3%

¹ Evaluated from 3 replicates.

² The average and standard deviation of 5 values at different cryoprotectant levels.

I define here). Statistically speaking, however, both b and a_w values were not significantly different at different cryoprotectant concentrations. The reason may be that when the water content was controlled at 80.3% for all cryoprotectant levels, variation between the concentrations of cryoprotectant and fish protein solute in the proposed range were not significant enough to make statistical separation of the b values. I therefore suggest that the average value in Table 4.3 should be used.

Given the various definitions of b found in published reports, the value of $b=0.48$ were obtained agreed with published data. For example, Schwartzberg (1983) reported that Riedel found $b=0.39$ for fish. From data of unfrozen water at -40°C reported by Pham (1987), $b=0.401$ for cod with an 80.3% water content, the same as that of our surimi samples. Comparing with other meat, Roos (1986) reported that $b=0.6$ for reindeer meat with 74.9% water content. Ross (1978) reported that $b=0.6$ for the mixture of ground beef, soy flour, sucrose, NaCl and lard at the ratio of 11:13:8:1.5:1 ($a_w=0.99$), and $b=0.49$ for isoelectric casein with the same water activity.

Enthalpy

Table 4.4 gives the enthalpy values, H , and Fig. 4.5 shows a typical curve. In another current project, I am simulating a surimi block in a plate freezer, using a finite difference enthalpy formula program provided by Mannapperuma

Table 4.4. Measured enthalpy of surimi

Cryoprotectant concentrations											
Temp.	0%		4%		6%		8%		12%		Riedel ¹
° C	H kJ/kg	S.D. %	H kJ/kg	S.D. %	H kJ/kg	S.D. %	H kJ/kg	S.D. %	H kJ/kg	S.D. %	Cod muscle kJ/kg
-40	0.0	0.0	0.0	0.0	0.0	0.0	0.0	0.0	0.0	0.0	0.0
-35	10.0	5.2	8.1	6.2	8.3	7.5	9.3	8.7	8.8	3.3	---
-30	19.1	4.8	15.6	6.5	16.3	5.1	18.6	8.9	18.2	3.7	19.1
-25	28.5	4.3	24.2	6.6	24.8	4.0	28.7	8.6	29.2	3.1	---
-20	39.0	5.2	33.1	6.3	35.1	3.2	40.8	8.1	42.0	2.1	41.9
-15	49.8	0.2	44.5	6.0	47.4	2.4	55.1	7.6	58.2	0.7	56.2
-10	64.0	0.2	59.9	5.7	65.0	2.5	76.1	6.7	83.0	0.8	74.1
-8	72.2	1.6	68.7	5.6	75.7	3.2	89.8	6.4	99.9	1.2	83.6
-6	83.1	0.4	81.2	5.3	92.6	4.6	113.2	6.2	127.4	1.7	96.2
-4	102.7	6.8	104.9	4.9	128.5	6.9	160.3	5.3	177.4	1.9	117.2
-2	162.9	2.1	161.6	3.6	232.2	7.2	273.2	2.7	275.1	1.3	176.2
T _i	272.5	1.3	286.8	2.4	294.1	6.7	305.6	2.0	292.4	1.9	297.4 ²
10	355.4	2.2	341.2	2.7	382.6	7.3	350.8	1.8	340.5	2.1	359.0
20	391.8	1.8	386.2	4.6	418.8	6.7	389.5	2.0	376.9	1.9	395.6

¹ Chen (1985a) cited from Riedel (1956). Water content was the same as that of the surimi samples, 80.3%.

² Temperature for this value was -1° C.

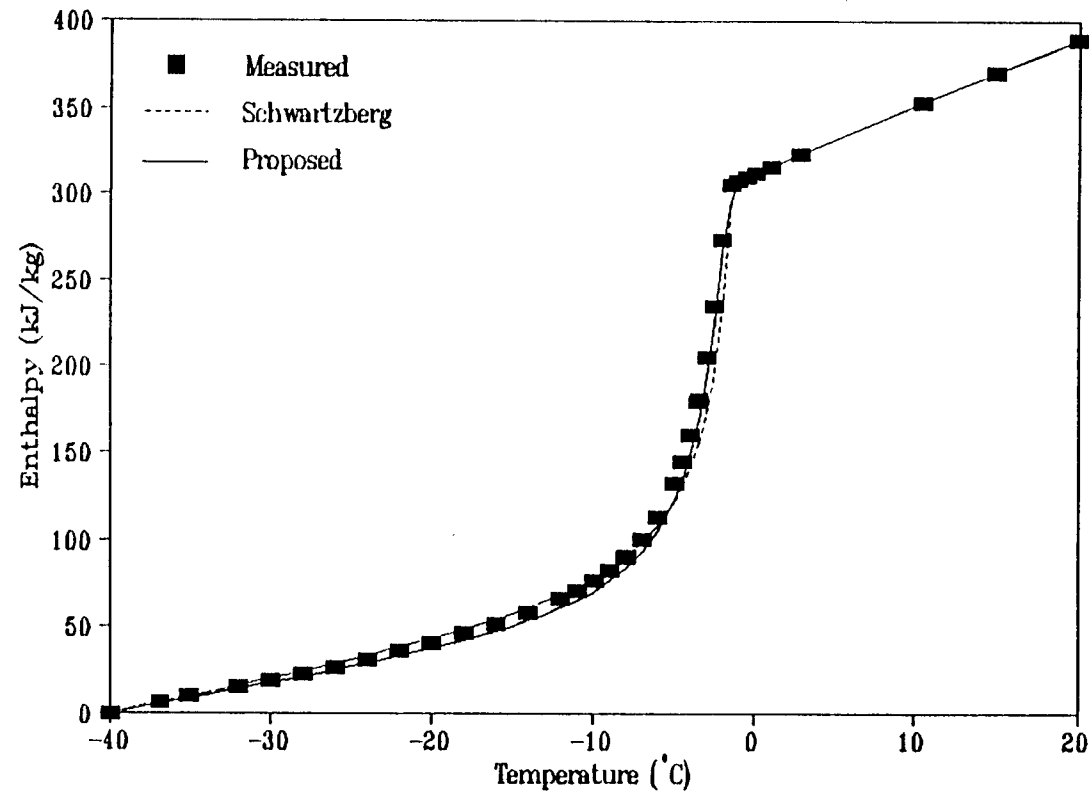


Fig. 4.5. Enthalpy of surimi with 8% cryoprotectant concentration

and Singh (1988). The H values with 8% cryoprotectant concentration were used in the calculation and good agreement with experimental data has been observed.

It should be mentioned here that at 20° C, the H values at different cryoprotectant levels were not statistically different. The average value was 392.6 kJ/kg with a standard deviation of $\pm 4.0\%$. This showed that the cryoprotectant concentration had little effect on H values at that temperature and at a constant water content.

Unfrozen water weight fraction

Table 4.5 reports the unfrozen water weight fraction, n_w , at different cryoprotectant levels and Fig. 4.6 shows a typical n_w curve for surimi with 8% cryoprotectant concentration. In the low temperature range, all values reported here are relatively higher than Riedel's. This disparity was due to the difference in water content and initial freezing point. It was probably also influenced by the different bound water values used (Table 4.3).

Modeling

Schwartzberg's model (1977, 1983) was investigated in this research because of its sound theoretical background, broad potential applications and good agreement with experimental data. Derivation of this model resulted in an

Table 4.5. Measured unfrozen water weight fraction of surimi

Cryoprotectant concentrations											
Temp.	0%		4%		6%		8%		12%		Riedel ¹
° C	n _w	S.D. %	n _w	S.D. %	n _w	S.D. %	n _w	S.D. %	n _w	S.D. %	Haddock (83.6% H ₂ O)
-40	0.106	4.1	0.091	1.3	0.083	2.5	0.091	0.1	0.106	4.3	0.065
-35	0.107	5.2	0.091	6.2	0.083	3.4	0.091	0.5	0.107	0.5	---
-30	0.108	4.8	0.091	6.5	0.084	2.0	0.091	0.8	0.112	1.1	0.067
-25	0.111	4.3	0.092	6.6	0.086	2.7	0.096	0.8	0.121	1.7	---
-20	0.115	5.2	0.096	5.8	0.093	3.2	0.106	1.1	0.135	2.1	0.079
-15	0.121	0.2	0.107	4.3	0.107	2.4	0.124	1.4	0.160	3.2	0.095
-10	0.137	0.2	0.133	5.7	0.136	2.6	0.162	2.0	0.211	4.3	0.111
-8	0.151	1.6	0.155	2.7	0.159	3.2	0.193	2.6	0.252	4.5	0.135
-6	0.174	0.4	0.195	5.3	0.200	4.6	0.253	3.8	0.325	4.8	0.159
-4	0.223	6.8	0.298	4.9	0.296	6.9	0.385	4.2	0.467	4.4	0.202
-2	0.399	2.1	0.591	4.1	0.577	7.2	0.715	1.7	0.752	3.1	0.371
T _i	0.803	1.3	0.803	2.4	0.803	6.7	0.803	0.8	0.803	2.4	0.836 ²

¹ From Riedel (1956) as cited by Fennema et al. (1973).

² Temperature for this value was 0° C according to Fennema et al. (1973).

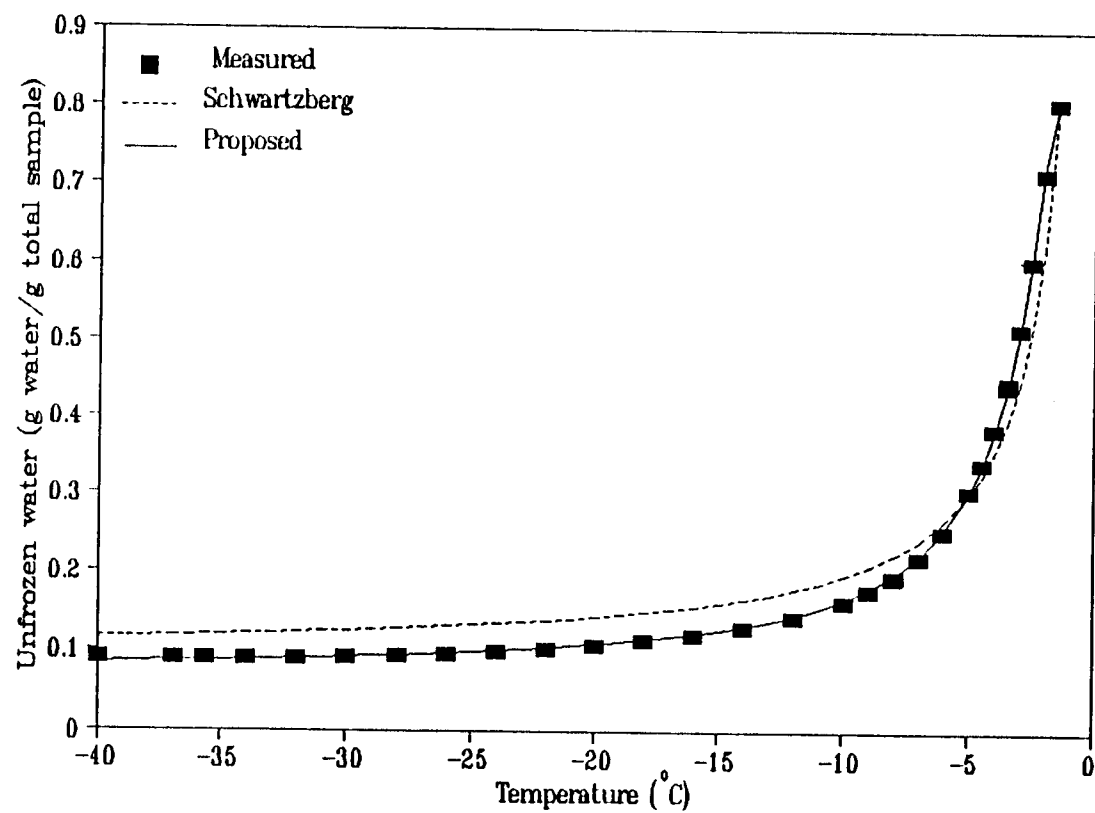


Fig. 4.6. Unfrozen water weight fraction of surimi with 8% cryoprotectant concentration

equation describing unfrozen water weight fraction, n_w , as a function of temperature:

$$\frac{n_w - bn_s}{n_{wo} - bn_s} = \frac{T_o - T_i}{T_o - T} \dots\dots\dots 4.4$$

This equation was the basis for developing the models of C_p , H and thermal conductivity, k . The n_w equation is limited in application due to two assumptions inherent in the freezing point depression equation: ideality and dilution of the solution (Fennema et al., 1973). A variety of published modifications of the C_p , H and k models were in fact attempts to correct the deviation caused by these two restrictions. Since DSC is capable of measuring n_w , it naturally leads to another approach -- correcting the unfrozen water weight fraction model. Comparison of models with data in our study focused on surimi with 8% cryoprotectant concentration, since this level is common in commercial production.

Fig. 4.6 shows measured n_w values compared with the prediction (dotted line) of Equation 4.4. The Schwartzberg model does not appear to fit well, a conclusion which seems unexpected. In the low temperature range, the maximum deviation with respect to experimental data was about 15.7%. First, this deviation may partially reflect the deviation from the assumptions of ideality and dilution. As freezing proceeds to the low temperature range, solutes

become more concentrated, and the assumptions of ideality and dilution are less valid. Second, one can see that Equation 4.4 holds only at the upper ($T=T_i$) limit. When $T=-40^\circ\text{C}$, however, the left-hand side of the equation is zero because of the definition of b , but the right-hand side will equal a non-zero quantity (0.025 assuming $T_i=-1^\circ\text{C}$ and $b=0.46$). The only way to decrease the error is to lower the datum temperature and redefine b . Such an inherent inaccuracy at low temperature may cause a series of model inaccuracies in this temperature range, for example, overestimation of C_p and H , and underestimation of k .

To better model n_w values measured by DSC, I suggest using an equation in the following form:

$$n_w = a' + b'\left(\frac{1}{T}\right) + c'\left(\frac{1}{T}\right)^2 + d'\left(\frac{1}{T}\right)^3 \dots\dots\dots 4.5$$

Using nonlinear regression, the four parameters estimated for different cryoprotectant concentrations are given in Table 4.6. The plot (Fig. 4.6) of the equation proposed here for the surimi with 8% cryoprotectant concentration agreed well with measured data.

Using Equation 4.4, Schwartzberg derived a C_p model as:

$$C = C_f + (n_{wo} - bn_s) \frac{(T_o - T_i) \Delta H_o}{(T_o - T)^2} \dots\dots\dots 4.6$$

Table 4.6. Parameters in Equation 4.5

Cryo. conc.	a'	b'	c'	d'	r ²
0%	0.0878	-0.5448	0.0826	0.0422	0.9976
4%	0.0687	-0.4951	2.0700	1.9347	0.9992
6%	0.0606	-0.5962	1.8294	1.8731	0.9998
8%	0.0627	-0.7574	2.9423	3.6133	0.9997
12%	0.0665	-1.3333	1.7686	3.2827	0.9995

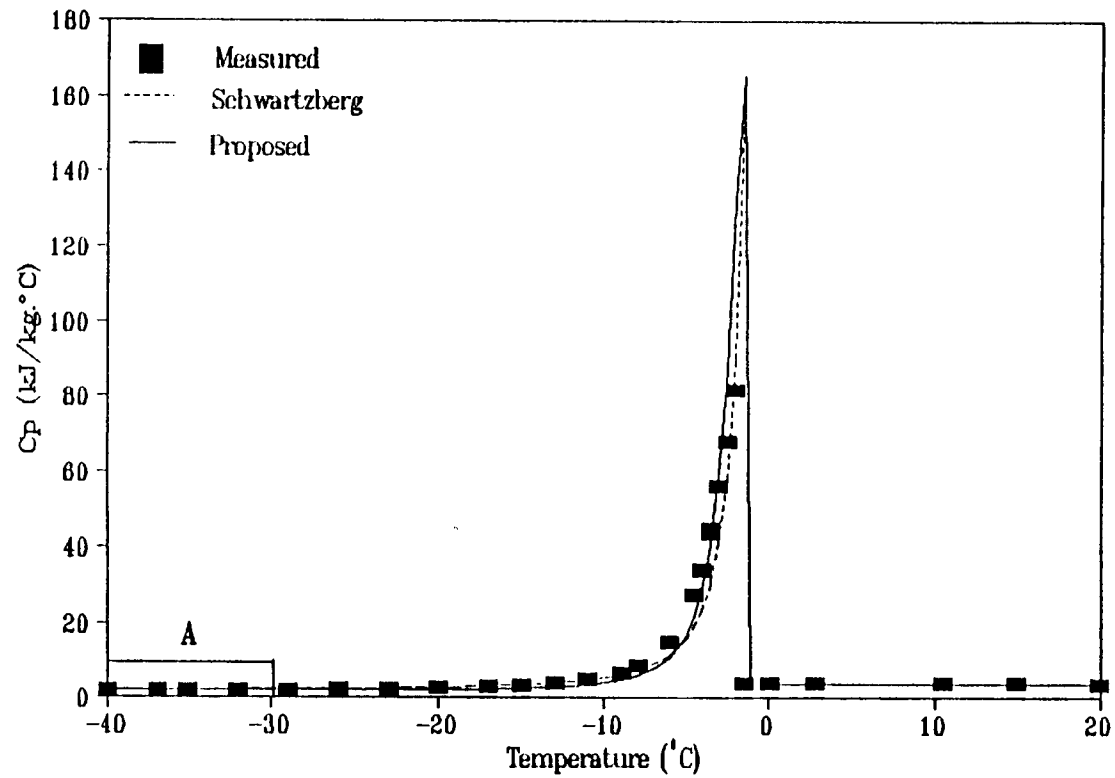


Fig. 4.7. Apparent specific heat of surimi with 8% cryoprotectant concentration

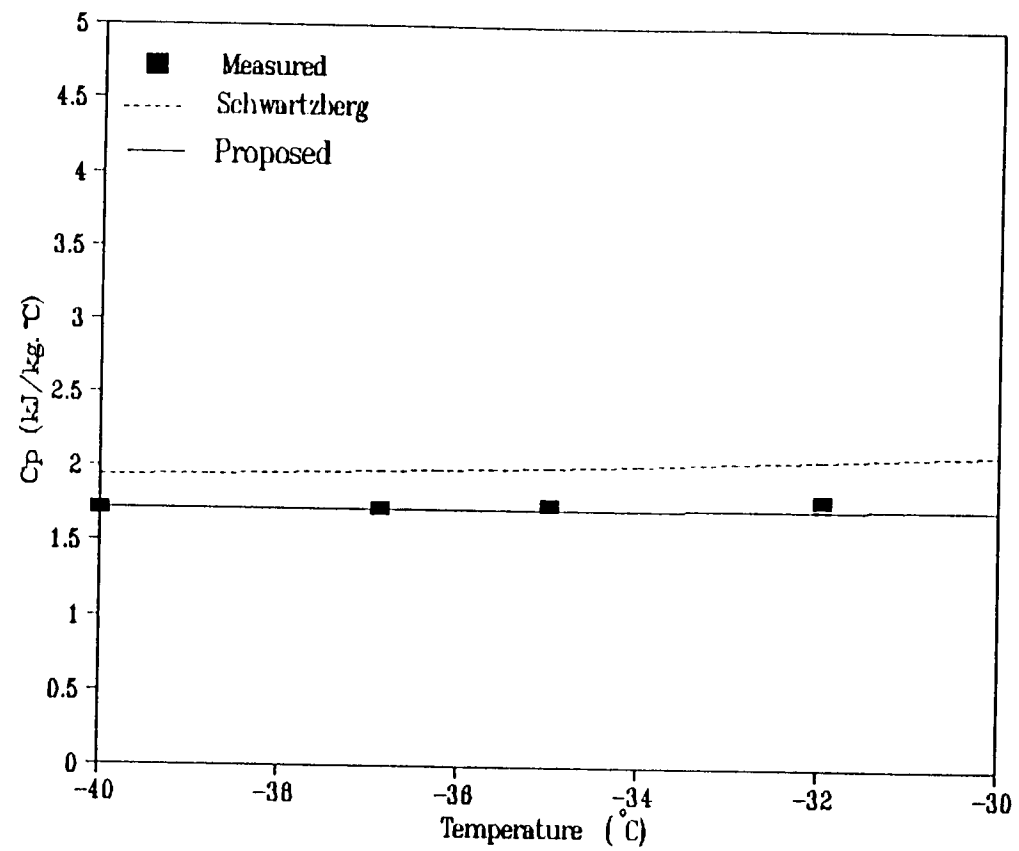


Fig. 4.8. Enlargement of the portion A in the Fig. 4.7

Combining Equations 4.4, 4.5 and 4.6, I obtained a modified model of C_p and plotted it as the "Proposed" curve in Fig. 4.7. Both the models of Schwartzberg and of that proposed in this paper seemed to fit well, although they departed from the experimental data in different temperature ranges. To rescale and compare the models in the lower temperature range, I enlarged portion A, as marked in Fig. 4.7, and shown in Fig. 4.8.

Schwartzberg's H model is in the form:

$$H = (T - T_R) \left[C_f + \frac{(n_{wo} - bn_s) \Delta H_o (T_o - T_f)}{(T_o - T_R) (T_o - T)} \right] \dots \dots \dots 4.7$$

Fig 4.5 illustrates three sets of H values in which one termed as "Proposed" represents the modification of Equation 4.7 by using Equations 4.4 and 4.5. Both models fit well with the experimental data. At the datum temperature, the H value was not overestimated by the Schwartzberg model because the model forces $H=0$ when $T=T_R$.

Although calorimetry data do not directly relate to thermal conductivity k , Equation 4.5 may also be used to improve the accuracy of a k model. Data reported by the authors (Wang and Kolbe, 1990) are compared to three k models (Fig. 4.9). One is the original model of Schwartzberg (1977, 1983). Another is the proposed model derived by inserting Equation 4.5 into the Schwartzberg k model. The third is a non-linear regression model suggested by

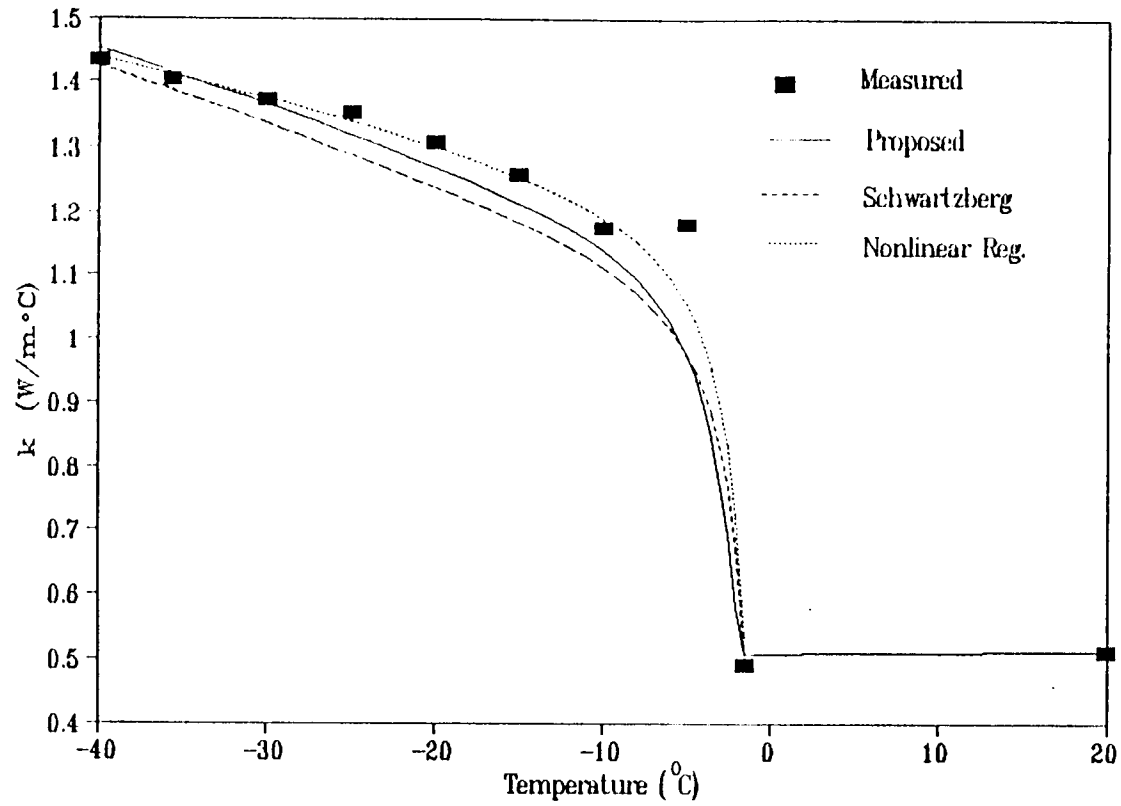


Fig. 4.9. Thermal conductivity of surimi with 8% cryoprotectant concentration

Succar and Hayakawa (1983). Again, underestimation of k values by the Schwartzberg model was obvious from the figure. The proposed model clearly shows the improvement over the Schwartzberg original. One should expect that the proposed model would not fit as well as the one suggested by Succar and Hayakawa (1983), which was associated directly with the experimental data of k , rather than n_w .

From the above discussion, It can be seen that the Schwartzberg model agreed well with experimental data, although further improvement is possible using the variations described. Among several parameters in Equation 4.4, the value of b may warrant further study. Chen (1986) developed a model describing b as a function of temperature and solids concentration. Such a relationship to replace our assumption of a constant b value may influence the goodness of fit, especially in the low temperature range. Nevertheless, this work has demonstrated the potential of developing thermal property models using DSC analysis.

CONCLUSIONS

By applying dynamic correction techniques, I demonstrated that DSC has great potential as a tool for investigating frozen food thermal properties. A single DSC thermogram could be used to obtain initial freezing point, unfreezable water, latent heat of fusion, unfrozen water weight fraction, apparent specific heat and enthalpy. To improve the accuracy of results, further research

needs to be conducted regarding dynamic correction, standard testing materials and standard measurement procedures. When water content was controlled, cryoprotectant level had little effect on the thermal properties in the unfrozen and fully frozen temperature range, but had significant effect on initial freezing point and thermal properties at temperatures slightly lower than T_i . The Schwartzberg model agreed well with experimental data; however, our study demonstrated further improvements by using DSC analysis.

CHAPTER 5. ANALYSIS OF FOOD BLOCK FREEZING USING A PC-BASED FINITE ELEMENT PACKAGE

ABSTRACT

A commercial PC-based finite element package was used to simulate the process of freezing a food block in a plate freezer. The capability of the program to handle temperature-dependent thermal properties and time-dependent boundary conditions enabled the simulation resulting from measured changes in thermal properties, ambient temperatures and overall heat transfer coefficient. Predicted temperature history agreed well with measured data. Sensitivities of important model parameters, which were varied within their experimental error range, were also investigated using a factorial experimental design method. The result showed that in decreasing order of influencing freezing time prediction, attention should be given to apparent specific heat, block thickness, overall heat transfer coefficient, ambient temperature, thermal conductivity, and density.

INTRODUCTION

With modern computers having high speeds and almost unlimited memory, there is little difficulty in accurately and easily simulating food freezing processes using numerical methods. Many researchers have developed their own programs using either finite difference or finite element approaches. Graduate students in this area have frequently put their major effort into developing the programs as a major part of their theses. However, these programs are often limited by an orientation to specific applications, by their awkward input/output formats, or by a difficulty to expand to a different set of conditions.

Many commercial finite element programs are now available, especially those aimed at the aerospace and automotive industries. These packages are powerful, expandable and user-friendly. They can handle a variety of nonlinearities, including temperature-dependent thermal properties, and time- and/or temperature-dependent boundary conditions. They often have very extensive graphics capabilities including immediate display for model geometry, boundary conditions, field contour and interfacing with other graphics software. They allow users to run the package using macros and user files, and to modify the package by using common programming language. Some of them have menu-driven analysis procedures or on-line documentation assistance, which are extremely helpful to new users.

To model freezing of foods, a heat conduction equation can describe the process if it is written with temperature-dependent thermal properties accounting

for the phase change of foods that occurs over a broad range of temperatures. An example is the use of "apparent specific heat" or "effective specific heat," which includes both sensible heat and latent heat of fusion. Application of such models has been well documented in literature (Cleland et al., 1986; Hayakawa et al. 1985; and Hung, 1990). Modeling freezing in a plate freezer may present additional complications due to non-uniform boundary conditions. Because the cooling medium in the freezer plates is a two-phase-flow, the overall heat transfer coefficient and ambient temperature (temperature of the refrigerant) vary with the state of the refrigerant. This may not be so easily handled by many existing freezing programs.

Besides the use of an appropriate program, success in modeling a freezing process also depends on the use of good quality data to define parameters associated with the model. These parameters are temperature-dependent apparent specific heat, thermal conductivity and density; time-dependent overall heat transfer coefficient and ambient temperature; and block thickness. Sensitivities of these parameters have been investigated by many researchers (Cleland and Earle, 1976; Cleland et al., 1982, 1987a, 1987b; Hsieh et al., 1977; and Hayakawa et al. 1983). However, most of their analyses were based on data measured over a very broad range and for a wide variety of food products. In this project, I am interested in how these parameters affect the freezing time prediction when they might vary in the experimental error range.

The objectives of this research were (1) to explore application of PC-based finite element package to model food block freezing in a plate freezer; and (2) to investigate the sensitivities of model parameters affecting the freezing time prediction as they vary in the experimental error range.

THEORETICAL CONSIDERATIONS

Freezing of foods can be modeled by a nonlinear heat conduction equation:

$$\rho(T)C_p(T)\frac{\partial T}{\partial t} - \frac{\partial}{\partial x}\left[k(T)\frac{\partial T}{\partial x}\right] + \frac{\partial}{\partial y}\left[k(T)\frac{\partial T}{\partial y}\right] + \frac{\partial}{\partial z}\left[k(T)\frac{\partial T}{\partial z}\right] \dots\dots\dots 5.1$$

with appropriate initial and boundary conditions. In a plate freezer, a food block can be considered as an infinite slab if one is interested in analyzing the temperature change at the thermal center. The equation thus describes a one-dimensional problem (Fig. 5.1) as:

$$\rho(T)C_p(T)\frac{\partial T}{\partial t} - \frac{\partial}{\partial x}\left[k(T)\frac{\partial T}{\partial x}\right] \dots\dots\dots 5.2$$

The initial temperature (at $t \leq 0$) is:

$$T(t,x) = T_o \dots\dots\dots 5.3$$

When $t > 0$, the boundary condition of the "third kind" becomes:

$$U(T_a - T_s) = -k(T)\frac{\partial T}{\partial x}\bigg|_{x=0} \dots\dots\dots 5.4$$

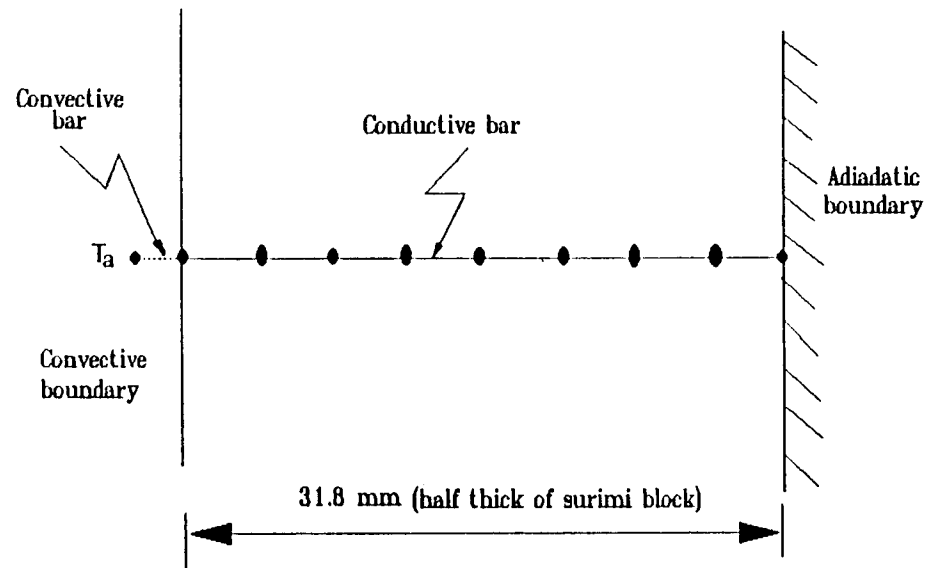


Fig. 5.1. Grid and boundary conditions used in the finite element analysis

Where T_a is ambient temperature. For a plate freezer (Fig. 5.2), T_a will be taken as the temperature of two-phase refrigerant flowing in the freezer plates.

U is an overall heat transfer coefficient defined as:

$$U = \frac{1}{1/h + D/k + \dots} \dots\dots\dots 5.5$$

In this equation, h is the convection heat transfer coefficient, D is thickness of any packaging material, and k is thermal conductivity of the packaging material. Therefore, U is associated not only with convection in the refrigerant passage, but also with effective contact influences between the food block and refrigerant. These include construction of the plates, pressure placed on the plates, air films, packaging materials, surface irregularities, etc. The h value here is in fact a convection coefficient between the refrigerant and freezer plate passage surface and is dominated by the state of the two-phase-flow refrigerant. Flow rates, boiling, and thus h can be expected to be high at the beginning of the process, and to diminish as freezing progresses. As a result, both values of U and T_a should be time-dependent variables throughout the freezing process.

Due to symmetry, the problem can be simplified by taking half the thickness of the food block so that one side has the boundary condition as given in the Equation 5.4 while the other side is adiabatic as:

$$\left. \frac{\partial T}{\partial x} \right|_{x=\frac{L}{2}} = 0 \dots\dots\dots 5.6$$

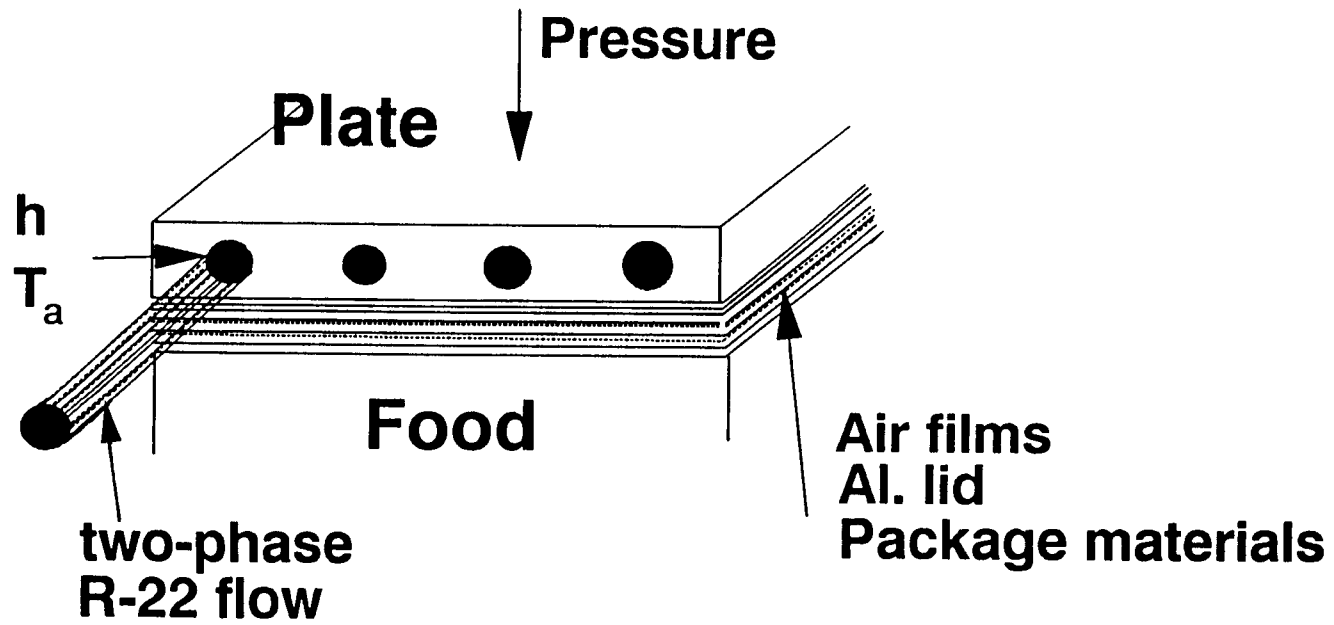


Fig. 5.2. Illustration of boundary conditions

Both finite difference and finite element approaches have been commonly used to model freezing process (Cleland et al., 1986; Hayakawa et al., 1985; Schwartzberg, 1983; and Hung, 1990). However, the finite element approach handles irregular shaped boundaries and complicate boundary conditions more easily than does the finite difference method (Segerlind, 1976). Therefore, a finite element method is often a better choice to handle complex problems (Hung, 1990).

A commercial PC-based finite element package, ANSYS-PC/THERMAL 4.3 (Swanson Analysis Systems, Inc., Houston, PA) was used in our project. Since this was considered as a one-dimensional problem and the half thickness of the food block was only about 31.8 mm ($1\frac{1}{4}$ inch), 10 nodes (9 elements) were used in the analysis. As shown in Fig. 5.1, the first element was "convection link" while the rest of the elements were "conducting bars" (refer to ANSYS, 1988). ANSYS has the capability to simulate a phase change process by defining the phase change temperature and entering the value of latent heat of fusion; however it does not work here because the phase change of foods occurs over a broad range of temperatures. ANSYS allows use of temperature-dependent specific heat, thus the problem can be handled by using the apparent specific heat. A time step optimization feature in the ANSYS program enables shortening computer-run-time. However, this had to be inactivated to avoid calculation having a big time increment near the initial freezing point. A large amount of heat is removed at this temperature and jumping over of it may result

a serious error in the calculation. For a transient problem, the ANSYS program uses an implicit time integration scheme to solve the governing equation. This scheme is unconditionally stable, but a time step needs to be chosen to balance accuracy of the solution with computer-run-time. The finer the time step, the more accurate the solution, but the more iterations and longer computer-run-time is needed. Estimated time step and number of iterations determined in this analysis were 1 min. and 150, respectively, following the procedure given in ANSYS (1988). When a smaller time step was tried, results showed no effect on temperature history, indicating that the proposed time step and iteration were adequate.

In running ANSYS, models of thermal conductivity $k(T)$ and apparent specific heat $C_p(T)$ were taken from Wang and Kolbe (1990a, 1990b) assuming the food product to be surimi with 8% cryoprotectant concentration and 80.3% moisture content. Density values of $\rho(T)$ were evaluated according to Succar and Hayakawa (1983). These temperature-dependent properties were entered in an user file as tables of values. The values were entered every 1° C from -10° C to the initial freezing point, then at a greater interval in the rest of the temperature range. The overall heat transfer coefficient and ambient temperature were also entered in the user file as linear functions of time according to regression analysis of measured data.

EXPERIMENTAL PROCEDURES

Food samples

The food samples used were surimi made from Alaska pollock (Theragra chalcogramma). Samples had cryoprotectant ingredients of 4% sucrose, 4% sorbitol, and 0.03% tripolyphosphate (TTP), and were purchased from UniSea Inc., Seattle, WA. Moisture content of the sample was 78.4% (with 0.09% standard deviation) measured by drying of six replicates in a vacuum oven at 105° C for 24 hours. The surimi blocks were thawed in a 3° C room for 48 hours before the experiment.

Temperature measurement

To verify the model, three experiments were conducted with surimi blocks in a plate freezer (Dole Refrigerating Co., Lewisburg, TN) at the Utilization Research Center, National Marine Fisheries Service, Seattle, WA. Type T, 30 gage thermocouples (Omega Engineering, Inc., Stamford, CT) were threaded through four 18 gage hypodermic needles of different lengths. To ensure the thermocouples placing at desired positions, the hypodermic needles were fixed on an aluminum frame (5/64 inch thick) to serve as a guide. Thermocouple locations are given in Fig. 5.3. Temperatures on the freezer plate surface and on refrigeration suction lines were also measured. All these temperature

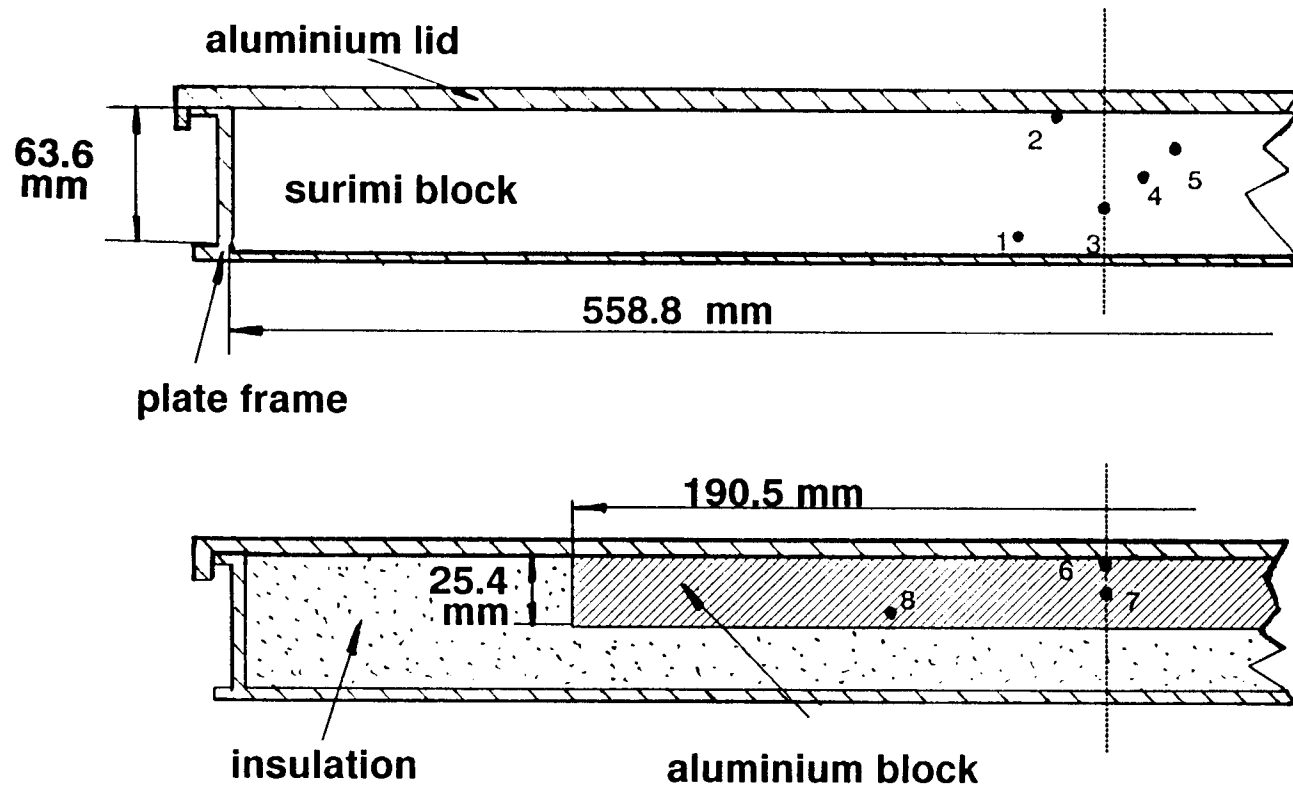


Fig. 5.3. Experiment set-up and thermocouple locations

measurements were programmed and recorded by a Campbell Scientific 21X Datalogger (Campbell Scientific, Inc., Logan, UT) interfaced by using a PC.

Surimi blocks were wrapped in a 1.5 mil polyethylene film. As a result of folding, there were three layers of the film between the block and the freezer plate. To minimize freezer cycling, 8 plates of salt water/thermal mass were frozen with the sample and the differential switch on the plate freezer was adjusted to the minimum. Both pressure and temperature history of R-22 refrigerant circuit, indicated by gages on the freezer, were also manually recorded.

Overall heat transfer coefficient measurement

Cleland et al. (1982) reported that measurement of the overall heat transfer coefficient, U , was more important than that of temperature, although it was also more difficult. Later, to determine U value, they used a piece of metal having known thermal properties in place of food in an immersion freezing operation. They reported that the experimental error was about 9% with 95% confidence (Cleland et al., 1987a, 1987b). Cowell and Namor (1974) used the same method for a plate freezer but they assumed the U value to be a constant. In our project, the U value was estimated using an aluminum block (Fig. 5.3) having dimensions 190.5 x 127.0 x 25.4 mm (7.5 x 5 x 1 inch). To make a valid infinite slab case, the aluminum block was insulated on all faces except that contacting the freezer plate. The block was also wrapped with polyethylene film in the same way as the surimi sample. Three 30 gage thermocouples placed at

locations within the block gave readings that were essentially identical, indicating validity of the lumped parameter model (Welty et al., 1984). In the theory of the lumped parameter model, the U value is determined by plotting the transient response of a mass subjected to a step change in ambient temperature, assuming an exponential response of the lumped-mass. For the plate freezer in this project, however, the lumped-mass model was applied in each time interval. The ambient temperature was also varied with respect to the time intervals according to the measured data.

Sensitivity analysis of model parameters

A factorial experimental design technique (Box et al., 1978) was used to analyze the sensitivity of the model to various parameters. Table 5.1 gives the six factors in two levels that were considered in our analysis. The values in level 1 were taken as "control"; most of them were either measured in the current project (values of U , T_a and L) or taken from previous research (Wang and Kolbe, 1990a, 1990b). In level 2, all variations from the control were assumed to be within the range of experimental error and in the direction which would increase the freezing time. These included -10% for U (Cleland et al., 1987a, 1987b) and $k(T)$ (Wang and Kolbe, 1990a); +10% for $C_p(T)$ (Wang and Kolbe, 1990b); +4% for $\rho(T)$, +2° C for T_a , and +5 mm for L . The later values without references were estimated from authors' experience. According to orthogonal theory, 8 trials were carried out to represent a total of 128 (2^8)

Table 5.1. Factors and levels in the experiment

	U	k(T)	C _p (T)	ρ(T)	T _a	L
	W/m ² K	W/Mk	kJ/kgK	kg/m ³	° C	mm
Level 1	W&K ^a	W&K	W&K	S&H ^b	REC ^c	63.5
Level 2	-10% ^d	-10%	+10%	+4%	+2 ° C ^e	+5 mm

^a W&K indicates data from the current project or from previous research (Wang and Kolbe, 1990a, 1990b).

^b S&H indicates data estimated using the model reported by Succar and Hayakawa (1983).

^c REC indicates recorded refrigerant temperature data which is a function of time. ^d The percentage indicates the amount of adjustment from its corresponding value in Level 1.

^e T_a in Level 2 is also a function of time, 2 ° C higher than its corresponding value in Level 1.

Table 5.2. Layout and results of the sensitivity analysis

Trial No.	U W/m ² K	k(T) W/Mk	C _p (T) kJ/kgk	ρ(T) kg/m ³	T _a ° C	L mm	Freezing Time min.
#1	1 ^a	1	1	1	1	1	120
#2	1	1	1	2	2	2	145
#3	1	2	2	1	2	2	180
#4	1	2	2	2	1	1	142
#5	2	1	2	1	1	2	162
#6	2	1	2	2	2	1	170
#7	2	2	1	1	2	1	142
#8	2	2	1	2	1	2	164
<hr/>							
Main effect: (min.)	12.75	7.75	20.75	4.25	12.25	19.25	
% increase:	10.6%	6.5%	17.3%	3.5%	10.2%	16.0%	

^a The number here, 1 or 2, represents the levels given in Table 1.

experiments in which the experimental factor varied one at a time. The upper part of Table 5.2 gives the detailed experimental layout.

RESULTS AND DISCUSSION

ANSYS analysis

Fig. 5.4 shows a typical ANSYS result which agreed well with measured data. Measured temperature history at thermal center was not available from the experiment, because the tested surimi block was thicker than expected. As a result, the thermocouple designed to measure the temperature at geometric center was 1/4 inch off.

In most freezing analyses reported in literature, both ambient temperature and overall heat transfer coefficient are considered constants. In our project, however, the ambient (refrigerant) temperature, T_a , was not a constant according to our measurement (Fig. 5.5). Furthermore, when using the lumped-mass model to estimate the overall heat transfer coefficient, U , it was found that the semi-logarithmic plot of the metal temperature history was not linear at all (Fig. 5.6). This indicated that the U value was not a constant either. That both the T_a and U values were not constants would directly relate to characteristics of the two-phase-flow of refrigerant in the freezer plates. At beginning, great temperature difference between the food block surface and the refrigerant resulted a great amount of heat being carried away. Thus the rate of refrigerant

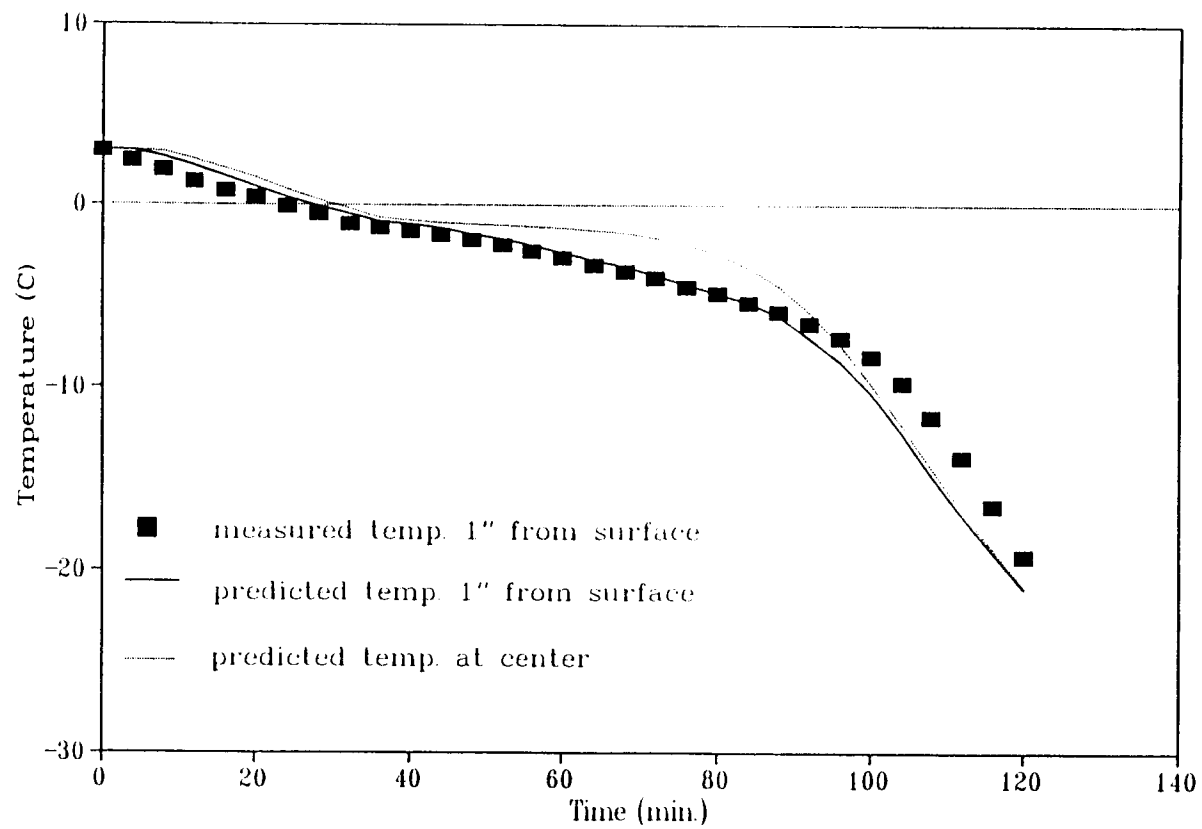


Fig. 5.4. Predicted temperature history compared with experimental data

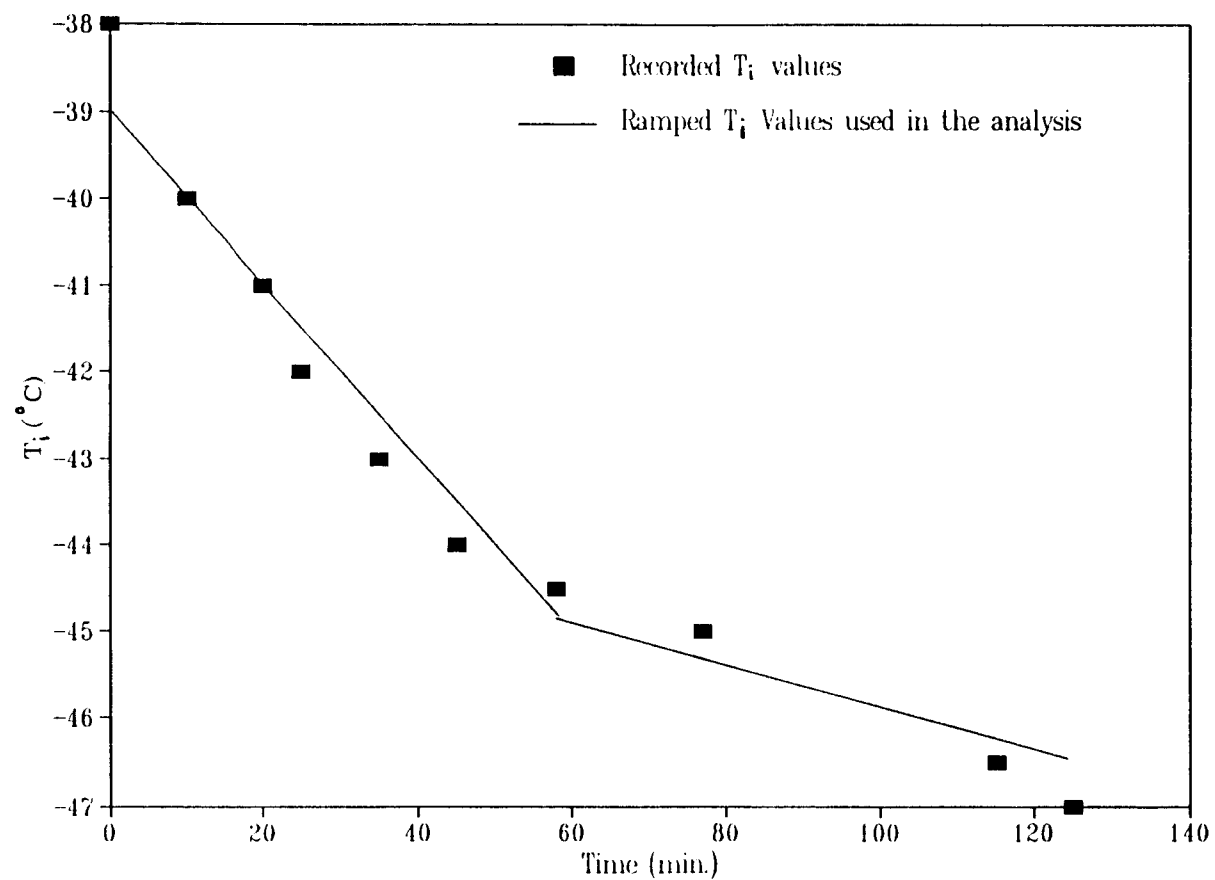


Fig. 5.5. Measured variable ambient temperature

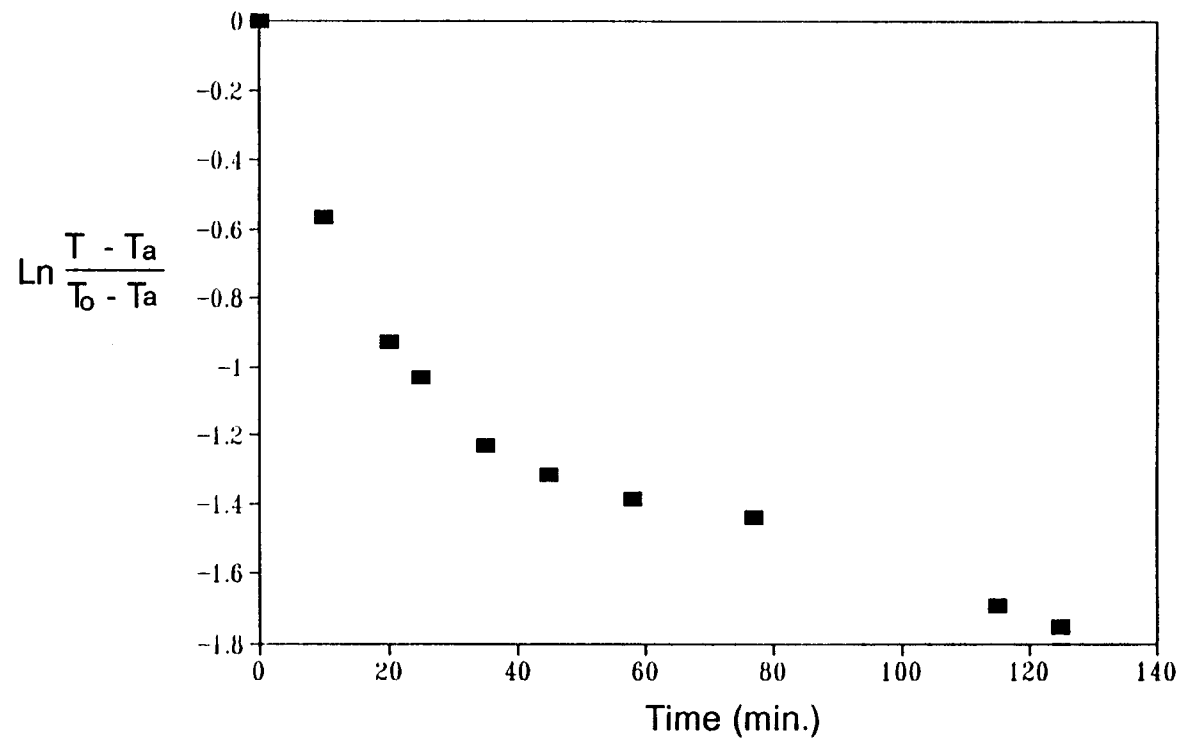


Fig. 5.6. A semi-log plot of time-temperature history of the aluminum block

flow was high and the refrigerant was rapidly boiling; additionally both T_a and the U values were relatively high. Later, after phase change on the food block surface, the temperature difference became smaller, the heat flow rate decreased and the refrigerant boiling slowed down, and the T_a and U values declined accordingly. Fig. 5.7 shows how the U value changed as a function of time.

In running ANSYS, both the T_a and U values were divided into two linear functions of time indicated by the solid lines in Fig. 5.6 and 5.7. The U values were estimated by applying the lumped-mass solution at each time interval, i.e., using the slopes of semi-logarithmic plot between the two adjacent data points. This is in fact only an approximation because the lumped-mass model can only be applied in case of constant U value. The T_a readings taken from the temperature gage on the freezer may have also included some inaccuracy due to the gage itself, sensor location, and load on the freezer. Although developing methodology to measure and model non-constant heat transfer coefficient is beyond the scope of this report, results did demonstrate an important advantage of this commercial PC-based finite element package. That is its ability to easily accommodate variable boundary conditions characteristic of this plate freezer problem.

It should be noted that the thermal properties used in this simulation were taken from models (Wang and Kolbe, 1990a, 1990b) for which the moisture content was controlled at 80.3%. However, the moisture content of the sample used in the plate freezer experiment was 78.4%. Two cases were tried in

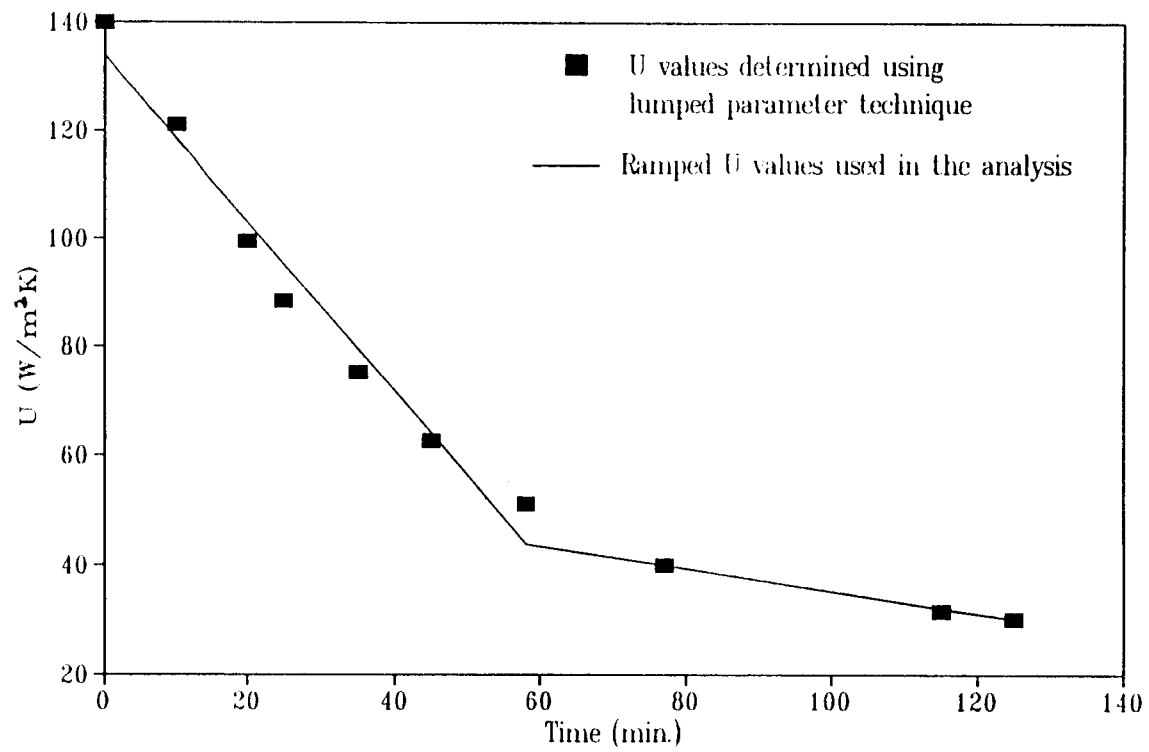


Fig. 5.7. Variable overall heat transfer coefficient used in the ANSYS analysis

running ANSYS. One was to use thermal property models determined from our previous projects for the higher moisture content material. Another was to use the thermal property values adjusted to the 78.4% moisture content applying models developed by Dickerson (1969), Schwartzberg (1983), and Succar and Hayakawa (1983). If freezing time is defined as the time elapsed from 3° C (initial temperature of the surimi block in the experiment) to -20° C at thermal center, the freezing time with adjusted thermal property values was only 6 minutes (5%) less than that shown in Fig. 5.4. Because the "adjusted values" carried many uncertainties (for example, relating to initial freezing point), using previously measured data was more reliable. The 5% difference in freezing time prediction may be considered to be an error due to the inaccurate thermal property data used.

Sensitivity analysis

With the definition of freezing time described before, the freezing time determined from Fig. 5.4 was 120 minutes. This may be taken as a "control" for the convenience of the following discussion.

Table 5.2 gives the result of the factorial experimental design analysis. In the table, each model parameter was taken as a factor and adjusted in the experimental error range to see how it affected the freezing time prediction. The "effect" of a factor means the change in response (in this case, increase of the freezing time) as the values from Level 1 were move to Level 2. The "main

effect" measures the average effect of that factor over all conditions of the other variables (Box et al., 1978). The percentage increase of the freezing time in the table was defined as:

$$\frac{\text{Main effect}}{\text{Control}} \times 100\%$$

Results from the table indicate that the sensitivity of the model to the varied parameters, in the order of from higher to lower, were $C_p(T)$, L , U , T_a , $k(T)$ and $\rho(T)$. It cannot be overemphasized that this result is only applicable in the adjusted range I proposed. For example, the effect of the U value seems a little lower than what one might expect. This may be caused by using only 10% adjustment according to the experimental error reported by Cleland et al. (1987a, 1987b). Some literature has reported a greater uncertainty in estimation of the U values.

CONCLUSIONS

ANSYS worked well to simulate the freezing process for surimi. Its capability of modification, expansion, interfacing, and especially that of permitting temperature-dependent properties and time-dependent boundary conditions has great potential for a variety of food process modeling. This paper has demonstrated that spending time to write an individual program is no longer necessary.

Sensitivity analysis showed that errors in measured parameters affect freezing time prediction in different degrees. The order of highest-to-lowest degree of influence were: apparent specific heat, block thickness, overall heat transfer coefficient, ambient temperature, thermal conductivity and density.

CHAPTER 6. SUMMARY AND RECOMMENDATIONS

In summary, the following conclusions and recommendations can be drawn from this research:

The system developed to measure thermal conductivity for frozen foods works well and appears to be an improvement over other reported approaches. This research also indicated that as the probe method is used more and more for foods, the experimental procedure needs to be standardized. The probe method is not appropriate for determining thermal conductivity at temperatures slightly below the initial freezing point. The prediction of k values in this temperature range using a precise model is probably more accurate than measurements. Sample history relating to freezing and thawing, time postmortem under refrigerated conditions, and freezing rate during measurement, do not significantly affect the measured thermal conductivity values.

By applying dynamic correction techniques, this research demonstrated that DSC has great potential as a tool for investigating frozen food thermal properties. A single DSC thermogram can be used to determine many important thermophysical properties of frozen foods, including initial freezing point, unfreezable water, latent heat of fusion, unfrozen water weight fraction, apparent specific heat and enthalpy. To improve the accuracy of results, further research needs to be conducted, to apply dynamic correction techniques, and to develop standardized testing materials and measurement procedures.

When water content is controlled, thermophysical properties of surimi have a relatively weak dependence upon the cryoprotectant level in the unfrozen and fully frozen temperature ranges. However, cryoprotectant levels have a significant effect on initial freezing point (T_i) and on properties at temperatures slightly lower than T_i .

The Schwartzberg model for thermal properties of frozen foods agreed well with experimental data; however, this study demonstrated further improvements by using DSC analysis.

ANSYS worked well to simulate the freezing process for surimi. Its capability of modification, expansion, interfacing, and especially that of permitting temperature-dependent properties and time-dependent boundary conditions has great potential for a variety of food process modeling. This thesis has demonstrated that spending time to write an individual program is no longer necessary. Sensitivity analysis showed that errors in measured parameters affect freezing time prediction in different degrees. The order of highest-to-lowest degree of influence were: apparent specific heat, block thickness, overall heat transfer coefficient, ambient temperature, thermal conductivity and density.

BIBLIOGRAPHY

- Ansari, F. A., V. Charan and H. K. Varma. 1985. Measurement of thermophysical properties and analysis of heat transfer during freezing of slab-shaped food commodities. Intl. J. Refrig., 8(2):85.
- ANSYS. 1988. ANSYS-PC/TH4.3 Reference Manual. Swanson Analysis System, Inc., Houston, PA.
- ASTM (American Society for Testing Materials). 1976. Steady-state thermal transmission properties by means of guarded hot plate. ASTM Designation: C 177-76.
- Batty, J. C. and S. L. Folkman. 1983. Food Engineering Fundamentals. John Wiley & Sons. New York, N.Y.
- Bonacina, C. and Comini, G. 1973. On the solution of the non-linear heat conduction equations by numerical methods. Intl. J. Heat Mass Transfer. 16:581.
- Boose, J. R. and R. A. Keppeler. 1967. Thermal properties of frozen sucrose solutions. ASAE Paper No. 67-885. Presentation at ASAE winter meeting, Detroit, MI.
- Box, G. E. P., Hunter, W. G. and Hunter J. S. 1978. Statistics for Experimenters, An Introduction to Design, Data Analysis, and Model Building. John Wiley & Sons, New York.

- Burros, B. C. 1986. Thermal analysis and food chemistry. *American Laboratory*, 18(1):20.
- Charm, S. E. 1963. A method for experimentally evaluating heat-transfer coefficients in freezers and thermal conductivity of frozen foods. *Food Tech.* 17(10):93.
- Charm, S. E., Brand, D. H. and Baker, D. W. 1972. A simple method for estimating freezing & thawing times of cylinders & slabs. *J. ASHRAE*, 11:39.
- Chavarria, V. M. and Heldman, D. R. 1984. Measurement of convective heat transfer coefficients during food freezing processes. *J. Food Sci.*, 49:810.
- Chen, C. S. 1985a. Thermodynamic analysis of the freezing and thawing of foods: Enthalpy and apparent specific heat. *J. Food Sci.* 50:1158.
- Chen, C. S. 1985b. Thermodynamic analysis of the freezing and thawing of foods: Ice content and mollier diagram. *J. Food Sci.*, 50:1163.
- Chen, C. S. 1986. Effective molecular weight of aqueous solutions and liquid foods calculated from the freezing point depression. *J. Food Sci.*, 51:1537.
- Cleland, D. J., Cleland, A. C. and Earle, R. L. 1986. Prediction of freezing and thawing times for foods - a review. *Intl. J. Refrig.*, 9:192.
- Cleland, D. J., Cleland, A. C., Earle, R. L. and Byrne, S. J. 1987a. Experimental data for freezing and thawing of multi-dimensional objects. *Int. J. Refrig.*, 10:22.

- Cleland, D. J., Cleland, A. C., Earle, R. L. and Byrne, S. J. 1987b. Prediction of freezing and thawing times for multi-dimensional shapes by numerical methods. *Intl. J. Refrig.*, 10:32.
- Cleland, A. C. and Earle, R. L. 1977. A comparison of analytical and numerical method of predicting the freezing times of foods. *J. Food Sci.*, 42(5):1390.
- Cleland, A. C. and Earle, R. L. 1976. A comparison of freezing calculations including modification to take into account initial superheat. *Bull. I.I.R. Annexe-1*:369.
- Cleland, A. C. and Earle, R. L. 1976. A new method for prediction of surface heat transfer coefficients in freezing. In proceedings of the International Institute of Refrigeration meeting Towards an Ideal Refrigerated food chain. Melbourne, Australia. pp.361.
- Cleland, J. C. and Earle, R. L. 1984. Assessment of freezing prediction methods. *J. Food Sci.* 49:1034.
- Cleland, J. C. and Earle, R. L. 1982. Freezing time prediction for foods--a simplified procedure. *Intl. J. Refrig.*, 5(3):134.
- Cleland, J. C. and Earle, R. L. 1984. Freezing time predictions for different final product temperatures. *J. Food Sci.*, 49:1230.
- Cleland, A. C., Earle, R. L. and Cleland, D. J. 1982. The effect of freezing rate on the accuracy of numerical freezing calculations. *Intl. J. Refrig.*, 5:294.
- Cleland, J. C. and Earle, R. L. 1979. Prediction of freezing times for foods in rectangular packages. *J. Food Sci.*, 44:964.

- Comini, G. and Bonacina, C. 1974. Application of computer codes to phase-change problems in food engineering. In Proceedings of the International Institute of Refrigeration meeting Current Studies on the Thermophysical Properties of Foodstuffs. Bressanone, Italy.
- Cowell, N. D. and Namor, M. S. S. 1974. Heat transfer coefficients in plate freezing: the effect of packaging materials. In Proceedings of the International Institute of Refrigeration meeting Current Studies on the Thermophysical Properties of Foodstuffs, Bressanone, Italy.
- Disney, R. W. 1954. The specific heat of some cereal grains. *Cereal Chem.*, 31:229.
- Dickerson, R. W. 1969. Thermal properties of foods. In the Freezing Preservation of Foods. D. K. Tressler, W. B. VanArsdel and M. J. Copley (Eds). AVI Publishing Co., Westport, CT.
- Duckworth, R. B. 1971. Differential thermal analysis of frozen food systems. The determination of unfrozen water. *J. Food Tech.* 6:317.
- DuPont Instruments. 1988. Differential Scanning Calorimeter 910 Operator's Manual. DuPont Company, Wilmington, DE.
- Fennema, O. R. 1985. Food Chemistry. 2nd ed. Marcel Dekker, Inc., New York.
- Fennema, O. R., Powrie, W. D. and Marth, E. H. 1973. Low-temperature preservation of foods and living matter. Marcel Dekker, Inc., New York.

- Hanafusa, N. 1985. The interaction water and protein with cryoprotectant. IIF-IIR-Commission C1:59, Tokyo, Japan.
- Haswell, G. A. 1954. A note on the specific heat of rice, oats, and their products. *Cereal Chem.* 31:341.
- Hayakawa, K., Nonino, C. and Succar, J. 1983 Two dimensional conduction in food undergoing freezing: development of computerized model. *J. Food Sci.*, 48:1849.
- Hayakawa, K., Nonino, C. and Succar, J. 1983. Two dimensional heat conduction in food undergoing freezing: predicting freezing time of rectangular or finitely cylindrical food. *J. Food Sci.*, 48:1841.
- Hayakawa, K, Scott, K. R. and Succar, J. 1985. Theoretical and semitheoretical methods for estimating freezing or thawing time. *ASHRAE Trans.*, 91(2b):353.
- Heldman, D. R. 1983. Factors influencing food freezing rates. *Food Tech.*, 2:103.
- Heldman, D. R. 1974. Predicting the relationship between unfrozen water fraction and temperature during food freezing using freezing point depression. *Trans. of ASAE*, 17:63.
- Heldman, D. R. 1982. Food properties during freezing. *Food Techn.*, 36(2):92.
- Heldman, D. R. and Gorby, D. P. 1975. Prediction of thermal conductivity in frozen foods. *Trans. of ASAE*, 18:740.

- Heldman, D. R. and Singh, R. P. 1981. Food Processing Engineering. 2nd Ed. AVI Publishing Co., Westport, CT.
- Heldman, D. R. and Singh, R. P. 1986. Thermal properties of frozen foods. In Physical and Chemical Properties of Food. Ed. by Okos, M. R. American Society of Agricultural Engineers, St. Joseph, MI.
- Heldman, D. R. and Steffe, J. F. 1985. Educational use of computer models for food freezing process. *Food Techn.*, 39(4):87.
- Hsieh, R. C., Lerew, L. E. and Heldman, D. R. 1977. Prediction of freezing times for foods as influenced by product properties. *J. Food Process Eng.*, 1:183.
- Hwang, M. P. and Hayakawa, K. 1979. A specific heat calorimeter for foods. *J. Food Sci.*, 44(2):435.
- Ingersoll, I. R., Zobel, O. J. and Ingersoll, A. C. 1954. Heat Conduction with Engineering and Geological Applications. McGraw Hill Book Co., New York.
- Jason, A. C. and Long, R. A. K. 1955. The specific heat and thermal conductivity of fish muscle. *Proc. IX, Int'l Congress of Refrigeration*, Vol. 2:160.
- Jul, M. 1984. The Quality of Frozen Foods. Academic Press, London.
- Kreith, F. 1963. Principles of Heat Transfer. International Textbook Co. Scranton.

- Lamplila, L. E. 1988. Private communications. Virginia Seafood Agricultural Experiment Station, Hampton, VA.
- Lee, C. M. 1986. Surimi manufacturing and fabrication of surimi-based products. *Food Tech.*, 40(3):115.
- Lentz, C. P. 1961. Thermal conductivity of meats, fats, gelatin gels, and ice. *Food Tech.*, 15:243.
- Long, R. A. K. 1955. Some thermodynamic properties of fish and their effect on the rate of freezing. *J. Sci. Food Agric.*, 6:621.
- Lund, D. B. 1983. Application of differential scanning calorimetry in foods. In Physical Properties of Foods. M. Peleg and E. B. Bagley (Eds). AVI Publishing Co., Westport, CT.
- Mannapperuma, J. D. and Singh, R. P. 1988. Prediction of freezing and thawing times of foods using a numerical method based on enthalpy formulation. *J. Food Sci.*, 53:626.
- Mayorga, O. L. and Freire, E. 1987. Dynamic analysis of differential scanning calorimetry data. *Biophys. Chem.*, 27:87.
- Maxwell, J. C. 1904. A treatise on electricity and magnetism. 3rd Ed. Clarendon Press. Oxford.
- McNaughton, J. L. and Mortimer, C. T. 1975. Differential scanning calorimetry. In *Physical Chemistry series two*, Vol. 10, Thermochemistry and Thermodynamics. H. A. Skinner (Ed). Butterworths, London.

- Meffert, H. F. 1983. History, aims, results and future of thermophysical properties work with in COST 90. In Physical Properties of Foods. R. Jowett et al., (Eds). Applied Science Publishers. London.
- Miles, C. A., Vanbeek, G. and Veerkamp, G. H. 1983. Calculation of thermophysical properties of foods. In Physical Properties of Foods. R. Jowett et al., (Eds). Applied Science Publishers. London.
- Mohsenin, N. N. 1980. Thermal Properties of Foods and Agricultural Materials. Gondon and Breach Science Publishers. New York, N.Y.
- Murakami, E. G. and Okos, M. R. 1988. PC-based thermal property probe apparatus. ASAE paper No. 86-6525; presented at the 1988 ASAE winter meeting, Chicago, IL.
- Murakami, E. G., Choi, Y. and Okos, M. R. 1985. An interactive computer program for predicting thermal properties. ASAE paper No. 85-6511; presented at the 1985 ASAE Winter meeting, Chicago, IL.
- Nagaoka, J., Takaji, S. and Hohani, S. 1955. Experiments on the freezing of fish in an air blast freezer. Proc. 9th Int. Cong. Refrig., 4:105.
- Nix, G. H., Lowery, G. W., Vachon, R. I. and Tanger, G. E. 1967. Direct determination of thermal diffusivity and conductivity with a refined line-source technique. Presented as paper 67-314 at the AIAA Thermophysical Specialist Conference in New Orleans.
- Ohlsson, T. 1983. The measurement of thermophysical properties. In Physical Properties of Foods. R. Jowett et al., (Eds). Applied Science Publishers.

London.

O'Neill, M. J. 1966. Measurement of specific heat functions by differential scanning calorimetry. *Analytical Chem.*, 38:1331.

Pham, Q. T. 1985. A fast, unconditional stable finite difference scheme for heat conduction with phase change. *Intl. J. Mass Transfer.* 28(11):2079.

Pham, Q. T. 1987. Calculation of bound water in frozen food. *J. Food Sci.* 52:210.

Poppendiek, H. F., Randall, R. Breeden, J. A., Chambers, J. E., and Murphy, J. R. 1966. Thermal conductivity measurements and predictions for biological fluids and tissue. *Cryobiology.* 3(4):318.

Purwadaria, H. K. and Heldman, D. R. 1983. A finite element model for prediction of freezing rate in food products with anomalous shapes. *Trans. of ASAE*, 25:827.

Ramaswamy, H. S. and Tung, M. A. 1981. Thermophysical properties of apples in relation to freezing. *J. Food Sci.*, 46:724.

Randzio, S. L. and Suurkuusk, J. 1980. Interpretation of calorimetric thermograms and their dynamic corrections. In Biological Microcalorimetry. A. E. Beezer (Ed.). Academic Press, New York, NY.

Riedel, L. 1956. Calorimetric investigations of the freezing of fish meat. *Kaeltetechnik*, 8:311.

Riedel, L. 1957. Calorimetric investigations of the meat freezing process. *Kaeltetechnik*, 9:38.

- Reid, D. 1988. Private communication. Department of Food Science, Univ. of California, Davis, CA.
- Roos, Y. H. 1986. Phase transition and unfreezable water content of carrots, reindeer meat and white bread studied using differential scanning calorimetry. *J. Food Sci.*, 51(3):684.
- Ross, K. D. 1978. Differential scanning calorimetry of nonfreezable water in solute-macromolecule-water system. *J. Food Sci.*, 43:1812.
- Sastry, S. K. and Datta, A. K. 1984. Thermal properties of frozen peas, clams and ice cream. *Can. Inst. of Food Sci. and Tech. J.*, 17(4):242.
- Sastry, S. K. 1984. Freezing time prediction: an enthalpy based approach. *J. Food Sci.*, 49(4):1121.
- Sastry, S. K. 1987. Private communications. Department of Agricultural Engineering, Ohio State University, Columbus, OH.
- Sastry, S. K., Beelman, R. B. and Speroni, J. J. 1985. A three dimensional finite element model for thermally induced changes in foods. *J. Food Sci.* 50:1293.
- Scott, E. P. and Heldman, D. R. 1984. Prediction of frozen food quality during fluctuation temperature storage. ASAE Paper No. 84-6520. Presented at the ASAE winter meeting in Chicago, IL.
- Schwartzberg, H. G. 1976. Effective heat capacities for the freezing and thawing of food. *J. Food Sci.*, 41:152.
- Schwartzberg, H. G., Rosenau, J. R. and Haight, J. R. 1977. The prediction of

freezing and thawing temperature vs. time behavior through the use of effective heat capacity equation. pp. 311-317, Proceedings of the International Institute of Refrigeration Meeting Freezing, Frozen Storage, and Freezer Drying. Karlsruhe, Germany.

Schwartzberg, H. G. 1977. Effective heat capacities for the freezing and thawing of foods. Proceedings of the International Institute of Refrigeration meeting Freezing, Frozen Storage, and Freezer Drying. Karlsruhe, Germany.

Schwartzberg, H. G. 1983. Mathematical analysis of the freezing and thawing of foods -- A Compilation of Readings and Problems in Food Engineering. Univ. of Mass., Unpublished.

Schwartzberg, H. G. 1988. Private communication. Department of Food & Agricultural Engineering, Univ. of Massachusetts, Amherst, MA.

Singh, R. P. 1983. Numerical techniques. In Computer-aided Techniques in Food Technology. I. Saguy (Ed). Marcel Dekker, Inc., New York, N.Y.

Singh, R. P. and Heldman, D. R. 1984. Introduction to Food Engineering. Academic Press, Inc., Orlando.

Sonu, S. C. 1986. Surimi. NOAA (National Oceanic and Atmospheric Administration). NOAA-TM-NMFS-SWR-013.

Succar, J. 1985. Estimation of thermophysical properties of food at freezing temperatures. ASHRAE Trans., 91(2b): 312.

- Succar, J and Hayakawa, K. 1983. Parametric analysis for predicting freezing time of infinitely slab-shaped food. J. Food Sci., 49:468.
- Succar, J. and Hayakawa, K. I. 1983. Empirical formulae for predicting thermal physical properties of food at freezing or defrosting temperatures. Lebensm.-Wiss. u. -Technol., 16:326.
- Sweat, V. E. 1976. A Miniature thermal conductivity probe for Foods. ASME-AlChe Heat Transfer Conference, St. Louis, MO.
- Sweat, V. E. 1972. Effects of Temperature and Time Postmortem on the Thermal Conductivity of Chicken Meat. Ph.D Thesis. Purdue University.
- Sweat, V. E. 1975. Experimental values of thermal conductivity of selected fruits and vegetables. J. Food Sci., 39:1080.
- Sweat, V. E. 1975. Modeling the thermal conductivity of meats. Trans. of ASAE, 18(3):564.
- Sweat, V. E. 1987. Private communications. Department of Agricultural Engineering, Texas A&M University.
- Sweat, V. E. 1985. Thermal conductivity of food: present state of the data. ASHRAE Trans., 91(2B):299.
- Sweat, V. E. 1983. Thermal properties of foods. In Engineering Properties of Foods, M. A. Rao and S. S. Rizvi (Eds). Marcel Dekker, Inc., New York.
- Sweat, V. E. and Haugh, C. C. 1972. A thermal conductivity probe for small food samples. Trans. of ASAE, 17(1):56.

- Underwood, W. M. and McTaggart, R. B. 1960. The conductivity of several plastics, measured by an unsteady state method. Heat Transfer (Storrs). Chem. Engr. Progress Symposium Series. 56(30):262.
- Wang, D. Q. and Kolbe, E. 1987. Measurement and prediction of freezing times of vacuum canned pacific shrimp. Intl. J. Refrig., 10(1):18.
- Wang, D. Q. and Kolbe, E. 1990a. Thermal conductivity of surimi -- measurement and modeling. J. Food Sci., 55(5):1217.
- Wang, D. Q. and Kolbe, E. 1990b. Thermal properties of surimi analyzed using DSC. J. Food Sci., in press.
- Wang, D. Q. and Kolbe, E. 1990C. Analysis of food block freezing using a PC-based finite element package. J. Food Engineering, in review.
- Weast, R. C. and Astle, M. J. 1980. CRC Handbook of Chemistry and Physics. CRC Press. Inc., Boca Roton, FL.
- Welty, J. R., Wicks, C. E., and Wilson, R. E. 1984. Fundamentals of momentum, heat, and mass transfer. 3rd. ed. John Wiley & Sons, Inc. New York.